IMPACT OF TWIN SCREW GRANULATION ON THE COMPACTABILITY OF PHARMACEUTICAL MATERIALS

Tarja Hietala
University of Helsinki
Division of Pharmaceutical
Chemistry and Technology
Industrial Pharmacy

December 2016

HELSINGIN YLIOPISTO
HELSINGFORS UNIVERSITET
UNIVERSITY OF HELSINKI

Tiedekunta/Osasto Fakultet/Sektion – Faculty	Osasto/Sektion– Department
Farmasian tiedekunta	Farmaseuttisen kemian ja teknologian osasto

Tekijä/Författare – Author
Tarja Hietala

Työn nimi / Arbetets titel – Title

Kaksoisruuvirakeistuksen vaikutus farmaseuttisten apuaineiden puristuvuuteen

Oppiaine /Läroämne – Subject

Teollisuusfarmasia

Työn laji/Arbetets art – Level	Aika/Datum – Month and year	Sivumäärä/ Sidoantal – Number of pages
Pro gradu	Joulukuu 2016	126

Tiivistelmä/Referat – Abstract

Kaksoisruuvirakeistus on herättänyt huomattavan määrän kiinnostusta jatkuvatoimisena märkärakeistusmenetelmänä lääketeollisuudessa ja se onkin eniten tutkittu kyseisistä rakeistusprosesseista. Vaikka useissa kuivarakeistus- ja erätoimisissa märkärakeistustutkimuksissa on todettu rakeistuksen vaikuttavan materiaalien puristuvuuteen ja tablettien lujuuteen, on silti epäselvää, kuinka jatkuvatoiminen rakeistus vaikuttaa näihin ominaisuuksiin.

Tämän pro gradu -työn tavoitteena oli tutkia jatkuvatoimisen kaksoisruuvirakeistuksen vaikutusta yleisesti käytettyjen farmaseuttisten apuaineiden puristuvuuteen. Lisäksi haluttiin selvittää, kuinka sideaine vaikuttaa materiaalien puristuvuuskäyttäytymiseen. Tarkoituksena oli myös arvioida, kuinka kaksi puristuvuuden heikkenemistä selittävää mallia (UCC-malli ja huokoisuusmalli) soveltuvat kuvaamaan kaksoisruuvirakeistuksen jälkeen tapahtuvaa puristuvuuden muutosta ja mahdollista tablettien lujuuden heikkenemistä käytetyillä materiaaleilla. Aikaisemmin näitä malleja on sovellettu ainoastaan kuivarakeistukseen ja erätoimiseen märkärakeistukseen.

Tutkimuksessa käytettiin full factorial -koeasetelmaa, jossa muuttujia (sideaine, sideaineen lisäystapa ja massaa työstävien elementtien lukumäärä) vaihdeltiin kahdella tasolla. Täyteaineena formulaatioissa käytettiin joko mikrokiteistä selluloosaa (MCC), mannitolia tai vedetöntä dikalsiumfosfaattia (DCPA), sideaineena polyvinyylipyrrolidonia (PVP) tai hydroksipropyyliselluloosaa (HPC) ja liukuaineena magnesiumstearaattia, joka lisättiin rakeisiin ennen tabletointia. Lisäksi full factorial -koeasetelmasta toistettiin yksi rakeistus (PVP, kuiva sideaine, neljä massaa työstävää elementtiä) jokaiselle tutkittavalle täyteaineelle. Yhteensä rakeistettiin 27 erää. Rakeistuksen jälkeen rakeet kuivattiin ja jauhettiin sekä tabletoitiin. Lisäksi kaikki formulaatiot suorapuristettiin, jotta kaksoisruuvirakeistuksen aiheuttamat mahdolliset muutokset aineiden puristuvuudessa ja tablettien lujuuksissa voitiin havaita. Vastemuuttujina tutkimuksessa selvitettiin rakeistuksen vääntömomentti sekä rakeiden kaatotiheys ja partikkelikokojakauma. Lisäksi määritettiin tablettien lujuus ja huokoisuus ja näiden avulla materiaalien puristuvuus.

Mikrokiteisen selluloosan puristuvuus huononi kaksoisruuvirakeistuksen jälkeen hornifikaation (engl. hornification) vuoksi. Mannitolin puristuvuus taas parani rakeistuksessa muodostuneiden huokoisten rakeiden ansiosta. DCPA:n puristuvuus muuttui vain vähän johtuen oletettavasti rakeiden hajoamisesta tabletoinnin aikana. Sideaineen havaittiin vaikuttavan materiaalien puristuvuuteen siten, että PVP:n käyttö sai aikaan lujempia tabletteja verrattuna vähemmän hydrofiiliseen HPC:hen. Sideaineen lisäystapa ei kuitenkaan aiheuttanut suurta muutosta tablettien lujuudessa.

UCC-malli kuvasi hyvin mikrokiteisen selluloosan puristuvuuden laskua ja tablettien lujuuden heikkenemistä. Täten mallia voidaan käyttää tablettien lujuuksien arvioinnissa, kun mikrokiteistä selluloosaa rakeistetaan kaksoisruuvirakeistimella. Lisäksi mallin avulla voidaan pienten esikokeiden perusteella suunnitella, millä rakeistusolosuhteilla saavutetaan tietty tabletin lujuus. Näin voidaan vähentää esikokeisiin käytettyjä resursseja. Mallia ei voitu soveltaa mannitoliin ja DCPA:han, sillä niiden UCC-mallin mukainen puristuvuus parani kaksoisruuvirakeistuksen jälkeen.

Huokoisuusmallia ei voitu käyttää kuvamaan muutosta mannitoliin puristuvuudessa, sillä sen puristuvuus parani.Huokoisuusmallia voitiin kuitenkin soveltaa mikrokiteiseen selluloosaan ja DCPA:han, sillä niiden puristuvuus heikkeni rakeistuksen jälkeen. Huokoisuusmalli kuvasi mikrokiteisen selluloosan puristuvuuden heikkenemistä kuitenkin vain osittain, sillä tutkimuksessa ei saatu riittävästi tablettien lujuusarvoja, koska tabletit olivat liian heikkoja. Huokoisuusmalli kuvasi hyvin DCPA-tablettien lujuuden heikkenemistä tablettien huokoisuuksilla, jotka saavutetaan kun käytetään teollisuudessa yleensä käytettyjä puristuspaineita.

Tulosten yhteenvetona voidaan todeta, että kaksoisruuvirakeistus voi vaikuttaa merkittävästi tablettien lujuuteen ja että formulaation puristuvuus voi joko parantua tai heiketä riippuen käytetyistä materiaaleista. Lisäksi voidaan suositella sideaineen lisäämistä rakeistukseen jauheseoksessa sideaineliuoksen sijaan, sillä sideaineen lisäystavalla oli vain pieni vaikutus tablettien lujuuteen. Näin ollen vältytään aikaavievältä sideaineen liuotukselta ja mahdollistetaan kaksoisruuvirakeistuksen käyttäminen tablettien jatkuvatoimisessa tuotannossa.

Avainsanat – Nyckelord – Keywords

Twin screw granulation, continuous granulation, tensile strength, compactability, tabletability, Unified Compaction Curve model

Säilytyspaikka – Förvaringställe – Where deposited

Farmaseuttisen kemian ja teknologian osaston kirjasto, Helsingin yliopisto

Muita tietoja – Övriga uppgifter – Additional information

Ohjaaja AstraZenecalla: Gavin Reynolds

HELSINGIN YLIOPISTO
HELSINGFORS UNIVERSITET
UNIVERSITY OF HELSINKI

Tiedekunta/Osasto Fakultet/Sektion – Faculty	Osasto/Sektion– Department
Faculty of Pharmacy	Division of Pharmaceutical Chemistry and Technology

Tekijä/Författare – Author
Tarja Hietala

Työn nimi / Arbetets titel – Title

Impact of twin screw granulation on the compactability of pharmaceutical materials

Oppiaine /Läroämne – Subject

Industrial pharmacy

Työn laji/Arbetets art – Level	Aika/Datum – Month and year	Sivumäärä/ Sidoantal – Number of pages
Master's thesis	December 2016	126

Tiivistelmä/Referat – Abstract

Twin screw granulation (TSG) has gained considerable interest as a continuous wet granulation method in the pharmaceutical industry and has been studied the most. However, there is still lack of understanding how continuous granulation affects the material compaction behavior even though it has been noticed in several dry and batch wet granulation studies that the granulation process has an influence on the final tablet strength. Thus, studies on the material compactability and tabletability after continuous wet granulation are relevant for the overall understanding of twin screw granulation process and its effect on material behavior in tableting.

Hence, the main objective of this study was to investigate the influence of continuous twin screw granulation on the compactability and tabletability of commonly used excipients. Additionally, the impact of binder on the compaction behavior of materials was examined. Furthermore, the suitability of two "loss in compressibility" models i.e. the Unified Compaction Curve (UCC) model and a porosity model to predict the loss in tablet strength after twin screw granulation and for the materials used was assessed. Earlier, the models have been applied to dry and batch wet granulations only.

Full factorial design of three variables (binder type, binder addition method and the number of kneading elements) with two levels was conducted for the ConsiGma1 twin screw granulation of formulations containing microcrystalline cellulose (MCC), mannitol or anhydrous dicalcium phosphate (DCPA) as the main excipient and polyvinylpyrrolidone (PVP) or hydroxypropyl cellulose (HPC) as binder. Magnesium stearate was added as lubricant after granulation prior to tableting. In addition to the full factorial design, granulation with PVP, dry binder addition and four kneading elements was repeated for each main excipient. In total this made 27 experiments. The granules were dried and milled after granulation and all the batches were tableted. Additionally, all the formulations were direct compressed in order to be able to detect the change in compactability and tabletability after granulation.

Torque of the granulation was determined as well as bulk density and particle size distribution of the granules. Additionally, the tensile strength and porosity of the tablets were analysed. Tabletability and compactability were determined based on the compaction pressure and the obtained tensile strength and porosity values of the tablets. Furthermore, parameters (P_{WG}, T_{WG} and ε_{WG}) describing the loss in compressibility models were calculated.

MCC experienced loss in compactability and tabletability after twin screw granulation due to hornification effect. On the other hand, the compaction behavior of mannitol improved due to the formation of porous granules. The compactability of DCPA decreased and the tabletability increased. However, the change was only moderate presumably due to brittle nature of DCPA. Additionally, the binder type had an effect of the compaction behavior of the materials, PVP producing stronger tablets compared with the less hydrophilic HPC. However, the binder addition method played only a small role in modifying the compaction behavior.

The UCC model was applicable to MCC as loss in tabletability was detected. Thus, the model can be used to predict tablet tensile strength when MCC is granulated with twin screw granulator. Additionally, the UCC model can be used to design the granulation process to achieve a target tensile strength based on small scale preliminary studies thus reducing the resources needed for case-studies. However, the UCC model was not feasible to mannitol and DCPA because they experienced improvement in tabletability after twin screw granulation. The porosity model was applicable to MCC and DCPA but not to mannitol as it showed improvement in compactability. The porosity model described the loss in compactability of MCC only moderately due to lack of tensile strength data points and the linearity of the tensile strength-porosity relationship. However, the model described well the loss in compactability of DCPA at tablet porosities achieved with compaction pressures used in industry.

As a conclusion, the results demonstrate that twin screw granulation can have a significant impact on the final tablet strength and that the compaction behavior of the formulation can change either way depending on the used materials. Furthermore, the small influence of the binder addition method on the tablet strength indicates that the time consuming binder dissolving process step can be excluded from the tablet production chain enabling continuous manufacturing with twin screw granulation.

Avainsanat – Nyckelord – Keywords

Twin screw granulation, continuous granulation, tensile strength, compactability, tabletability, Unified Compaction Curve model

Säilytyspaikka – Förvaringställe – Where deposited

Library of the division of Pharmaceutical Chemistry and Technology, University of Helsinki

Muita tietoja – Övriga uppgifter – Additional information

Supervisor in AstraZeneca: Gavin Reynolds

TABLE OF CONTENTS

APPENDICES

1. INTRODUCTION

Tablets are the most common solid dosage form used in the pharmaceutical industry for several reasons including cost-effective manufacturing process, good stability and ease of handling and administration. Although tablets are convenient to handle they must have sufficient strength to resist breakage and remain intact during their life cycle from production to distribution and administration. Good compactability and tabletability (Chapter 3.3) of a material are important for a successful tableting process and subsequent tablet strength. However, in several studies it has been observed that the granulation process affects the material compaction behavior (Chapter 3.3) (Krycer et al. 1982; Staniforth J. 1988; Westermarck et al. 1998; Shi et al. 2011a; 2011b; Nguyen et al. 2013).

Pharmaceutical industry has faced increasing pressure to reduce costs due to the competition raised from generics production (Vervaet and Remon 2010). This has evoked a shift towards continuous manufacturing in which material is continuously processed and discharged. Continuous processing has several advantages including reduced processing time, space and costs, increased quality control and less scale-up problems compared to conventional batch processing. Among the available continuous wet granulation techniques, twin screw granulation is the most promising one and has been studied the most.

However, there is still lack of understanding how continuous granulation affects the material compaction behavior even though several studies on the influence of dry and batch wet granulation on material compactability and tabletability have been conducted (Bultmann 2002; Freitag and Kleinebudde 2003; Badawy et al. 2006; Shi et al. 2011b). Thus, studies on the material compaction behavior after continuous wet granulation are relevant for the overall understanding of twin screw granulation (TSG) process and its effect on final tablet strength. Additionally, the knowledge of material behavior in tableting after twin screw granulation aids designing formulations for continuous wet granulation processing routes.

One useful method in gaining understanding about the loss of tabletability of the material due to granulation is the Unified Compaction Curve (UCC) model which enables the determination of the pressure imparted on the material during granulation process (Farber et al. 2008). This pressure is connected to compaction behavior and tablet strength. Consequently, the model can be used to estimate the final tablet strength for different granulation conditions.

Thereby, the main objective of the current study was to investigate the effect of continuous twin screw granulation on the compactability and tabletability of commonly used excipients. Additionally, the influence of binder in changing the compactability behavior of materials was examined. Furthermore, the suitability of two "loss in compressibility" models i.e. the UCC model and a porosity model to predict the loss in tablet strength for twin screw granulated tablets and the materials used was assessed.

2. GRANULATION

Some formulations can be tableted by direct compaction but poorly flowing mixtures must be granulated beforehand. Thus, the primary objective of granulation is to enhance the powder flow by agglomerating primary particles to form granules with larger particle size. Additionally, other reasons for the granulation of powders are to increase bulk density of the material, reduce dust formation during handling, minimize segregation of the mixed powder and improve uniform distribution of the drug in the solid dosage form.

The main granulation processes are dry and wet granulation. Granulation can also be carried out by melt extrusion however this will not be discussed here. In the dry granulation process, the powder blend is compacted in a heavy-duty tableting press into a tablet (slugging) or between two counter-rotating rolls to form a ribbon (roller compaction). The resulting product is milled to form granules. In the wet granulation process, the primary particles of the powder blend are granulated with a liquid binder. Subsequently, the granules are dried and milled. Several granulators can be used to

carry out wet granulation such as extrusion systems, high-shear, fluidized-bed and rotor granulators.

Furthermore, granulation can be performed as a batch wise or as a continuous process. In pharmaceutical industry granulation has traditionally been a batch process (Leuenberger 2001; Plumb 2005; Vervaet and Remon 2005). This is due to unique regulatory standards and small production scale of pharmaceuticals relative to other industries. The continuous process has been considered suitable only for larger production volumes therefore batch process has been preferred. However, nowadays it has been realised that the continuous process is suited for production from small to large scale and is now seen as an interesting choice for batch processing with the benefit of improved process control as well as reduced scale-up and costs. Additionally, the regulatory aspect has changed to encourage the use of continuous processing in pharmaceutical industry by emphasizing the importance of quality-by-design (QbD) and process analytical technologies (PAT) (Bush 2005; Plumb 2005). Continuous granulation can be conducted for example by roller compaction or high shear, fluid bed and extrusion granulation. Because the wet granulation with twin screw extruder was the main focus of this study, the continuous twin screw granulation will be discussed in more detail in the following chapters (2.1, 2.2 and 2.3).

2.1 Twin screw granulation

Twin screw extrusion is commonly used as a continuous extrusion process in the polymer, food and chemical industries (Owolabi et al. 2008; Vervaet and Remon 2010). However, during the last decade twin screw granulation has gained considerable interest as a continuous wet granulation method in the pharmaceutical industry (Vervaet and Remon 2005; Thompson 2014). The first to utilize a twin screw extruder for the wet granulation of paracetamol were Gamlen and Eardley (1986) in 1986. Later, Lindberg et al. (1987; 1988a; 1988b) prepared effervescent paracetamol products using a similar extruder. The conventional twin screw extruder includes a die plate at the end of the barrel to produce the extrudates. However, in the patent of continuous twin screw granulation belonged to Ghebre-Sellasie et al. (2002), the granulator does not have a die plate at its outlet end. Accordingly, Keleb et al. (2004b) used twin screw granulator

without the die plate to prove that efficient wet granulation without the need for subsequent wet sieving step is possible.

2.1.1 Advantages and possible drawbacks of twin screw granulation

TSG has several advantages over current batch wet granulation methods including lower production costs, wider range of output capacity and smaller but more flexible equipment design (Gamlen and Eardley 1986; Keleb et al. 2004a; Shah 2005; Vervaet and Remon 2005; Thompson and Sun 2010; Vervaet and Remon 2010). Additionally, the flow space inside the barrel is confined providing controlled and reproducible shear history for the material moving between the screws and the barrel resulting in high product consistency (Keleb et al. 2004a; Shah 2005). Moreover, due to a short material residence time the changes are reflected almost instantaneously when process parameters are adjusted (Gamlen and Eardley 1986).

Less scale-up problems are encountered with TSG as an ideal continuous granulator can produce a small development batch and a production scale batch with similar process settings by extending the granulation time thus minimizing the costs generated from expensive, material and time-consuming scale-up studies (Vervaet and Remon 2005; Shah 2005; Vervaet and Remon 2010). Furthermore, real-time monitoring of the continuous granulation process and in-line analysis increase quality control improving product uniformity and additionally enables the real-time release of the product instead of batch release based on end-product testing. Furthermore, improved quality control enhances process efficiency and reduces the amount of waste as less material is rejected or reprocessed (Vervaet and Remon 2005; Vervaet and Remon 2010).

Keleb et al. (2002; 2004a) compared wet extrusion and high shear granulation and observed that lower water concentration was needed in extrusion. In addition, better product properties and higher consistency was achieved with extrusion as the granules showed lower friability and higher yield together with higher tensile strength and faster dissolution of tablets compared to products obtained from high shear granulation.

There are some disadvantages related to continuous granulation such as more complicated cleaning process and material waste during the time over which the equilibrium state is reached (Vervaet and Remon 2005; Thompson and Sun 2010). Additionally, in continuous processing the batch cannot be defined in a traditional way. Instead the processed material is indentified by time i.e. the amount of material produced during a specific time interval (Vervaet and Remon 2005; 2010; Thompson and Sun 2010). However, these minor drawbacks are compensated with the several advantages discussed earlier.

2.1.2 Equipment and process

A twin screw granulator consists of powder hopper and a feeder, two screws and a barrel with temperature control jacket and inlets for a liquid supply as well as a fluid bed dryer unit(s). During the twin screw granulation process (Figure 1) powder is added in the hopper and a feeder transports the powder into the barrel. The powder can be preblended or added as unmixed but in the latter case sufficient mixing in the granulator must be ensured (Van Melkebeke et al. 2008). The loss-in-weight feeders such as a screw feeder are usually used for the powder feeding.

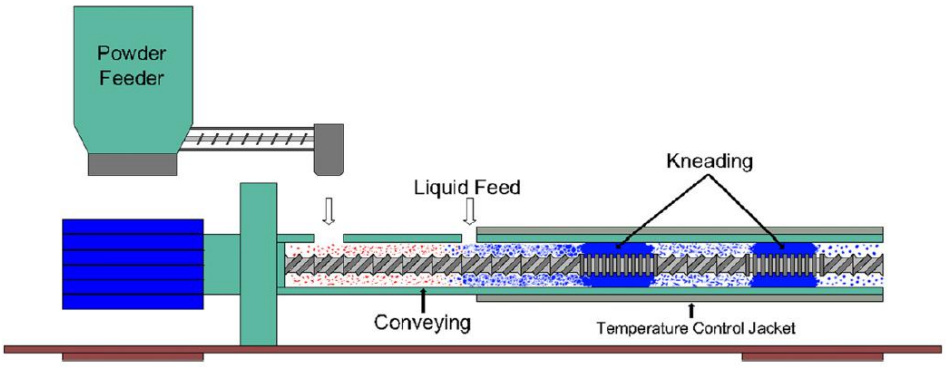

Figure 1. A Schematic diagram of twin screw granulation process (Seem et al. 2015).

As the powder is fed inside the granulator the screws (Figure 2) continuously and consistently mix, wet and agglomerate the material transported inside a barrel. The screws inside the barrel rotate either in the same direction (co-rotating screws) or in the opposite directions (counter-rotating screws) and are constructed from different screw

elements on the screw rod resulting in variety of screw configurations. There are three main screw element types which are conveying, kneading and comb mixing elements (Djuric 2008; Thompson and Sun 2010). Additionally, the use of tooth-mixing-elements, screw mixing elements and cutters has been studied (Vercruysse et al. 2015).

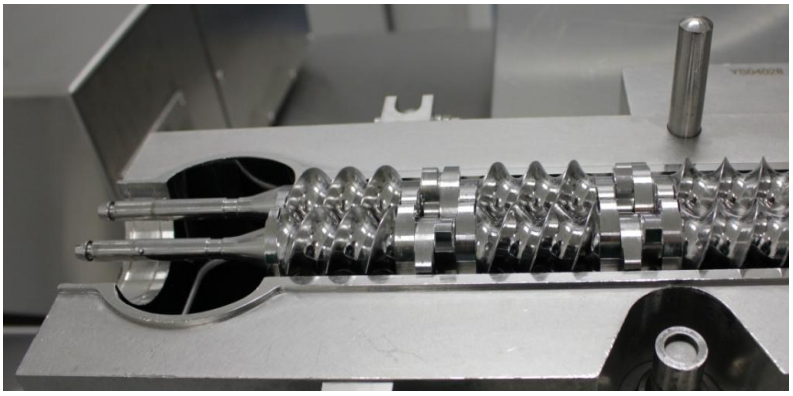

Figure 2. Two co-rotating screws.

The conveying elements (Figure 3) transport the material forward from the barrel inlet and between mixing zones producing only low shear forces (Lindberg 1988; Thompson and Sun 2010). The granulation liquid is added through inlets with a liquid pump before the first mixing zone. The mixing zones consist of kneading or comb mixing elements. The kneading blocks are composed of kneading disks as in Figure 3. The disks can be aligned at 30º, 60º or 90º angle and produce forwarding (F) or reversing (R) flow (Djuric 2008).

Figure 3. A conveying element and kneading disks.

The kneading blocks impart high shear forces during mixing and compaction of the material to form granules (Thompson and Sun 2010). The mixing in kneading blocks can be either distributive or dispersive depending on the size and direction of the angle and the width of the kneading disks (Van Melkebeke et al. 2008). Distributive mixing spreads the components without breaking them but dispersive mixing breaks the granules or alters their morphology to sheared and/or elongated. Additionally, the kneading elements break large granules and distribute liquid. The comb mixer elements are built up of rings with angular cuts to produce distributive mixing and to allow for the material to flow through the element (Thompson and Sun 2010). After a short residence time the processed material is discharged from the barrel by the conveying elements and dried in the fluid bed dryer unit(s).

2.2 Mechanisms of granule formation in twin screw granulation

In wet twin screw granulation three processes take place simultaneously in the granulator barrel that is wetting and nucleation, consolidation and growth, and attrition and breakage (Seem et al. 2015). Dhenge et al. (2012a) studied the progression of granule formation in the different sections of screw configuration (Figure 4) of a twin screw granulator.

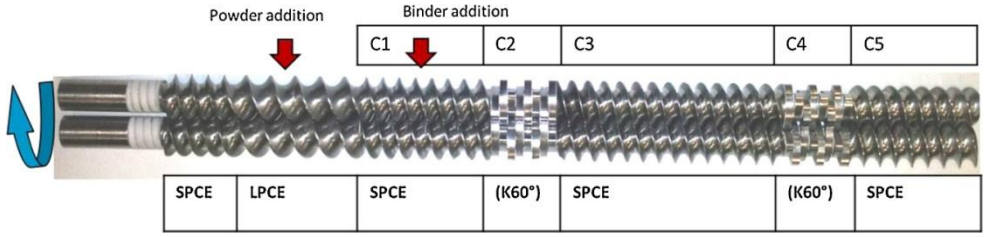

Figure 4. Sections C1 to C5 in the screw configuration (SPCE Short pitch conveying element L = D, LPCE Long pitch conveying element L = 2D). (Dhenge et al. 2012a)

The authors noticed that the nucleation occurred in compartment 1 (C1) consisting of four conveying elements as the binder solution was injected on that compartment (Dhenge et al. 2012a). Compartment 2 (C2) had eight kneading disks (L=D/4) at orientation of 60º which caused the consolidation and breakage of the granules.

Coalescence and breakage took place in the compartment 3 (C3) having seven conveying elements. Compartment 4 (C4) was a kneading block similar to C2 with eight kneading disks. Coalescence and consolidation occurred in C4 and the granule size increased. Finally, the granule size decreased by breakage in compartment 5 (C5) that had four conveying elements.

Furthermore, it was observed that the granule growth in kneading elements was due to continuous breakage and coalescence in contrast to conveying elements where growth occurred mostly by layering (Dhenge et al. 2012a). Additionally, El Hagrasy et al. (2013) proposed two rate processes that took place in the kneading section depending on the offset angle of the kneading disks. Breakage and layering occurred in a 90º configuration whereas shear elongation, breakage and layering were dominant at a reverse angle of 30º. The other offset angles (30ºF, 60ºF and 60ºR) demonstrated a combination of the two rate processes. In the following sections the granulation rate processes discussed above are explained in more detail.

2.2.1 Wetting and nucleation

Wetting and nucleation (Figure 5) is the stage in wet granulation where the binder solution is brought into contact with the dry powder surface to form the initial nuclei (Ennis and Litster 1997; Iveson et al. 2001).

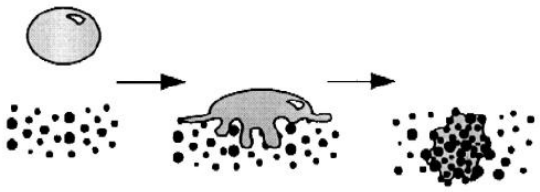

Figure 5. Wetting and nucleation (Ennis and Litster 1997).

Schæfer and Mathiesen (1996) have proposed two mechanisms (Figure 6) for nuclei formation based on the relative droplet size. Distribution occurs when the drop size is small compared to particle size. The liquid coats the surface of the primary particles

which subsequently will form agglomerates by coalescence. Immersion takes place when the solid particles are small compared to the drop size. In this case the particles will immerse into the binder droplets. In twin screw granulation the nuclei are formed by the immersion mechanism as the binder is pumped into the barrel resulting in large drops compared to the powder size (Dhenge et al. 2012a; 2012b; El Hagrasy et al. 2013).

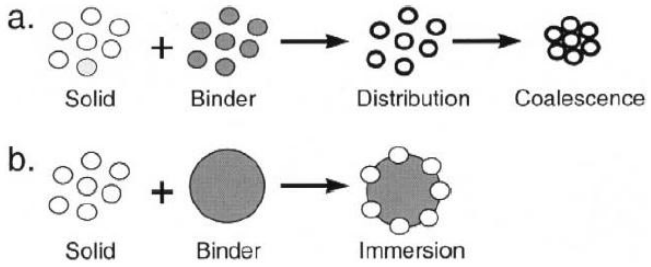

Figure 6. The nuclei formation mechanisms (Schæfer and Mathiesen 1996).

The dispersion of the binder solution throughout the powder bed is critical to uniform nuclei formation (Ennis and Litster 1997; Ennis 2010). Poor wetting can produce ungranulated powder with few large nuclei and over-wetted masses resulting in wide nuclei distribution. Subsequently, this can lead to broad granule size distribution. The wetting can be characterised for example by the contact angle between the liquid and the powder and by the rate the drop penetrates the powder bed (Ennis and Litster 1997). Both the rate and extent of powder wetting are important for good liquid distribution (Ennis and Litster 1997; Ennis 2010). They can be enhanced by decreasing the contact angle and increasing the surface tension of the binder solution. Additionally, the rate of binder spreading and penetration can be improved by decreasing the viscosity of the binder solution by lowering the binder concentration or increasing the temperature.

2.2.2 Coalescence and consolidation

As the granules collide during granulation, the granules will adhere together if the forces between the particles are strong enough to resist the rebound and breakup forces (Ennis 2010). The granule growth can occur through coalescence (Figure 7) of two or

more granules or by the layering of powder onto the surface of previously formed granules (Ennis and Litster 1997).

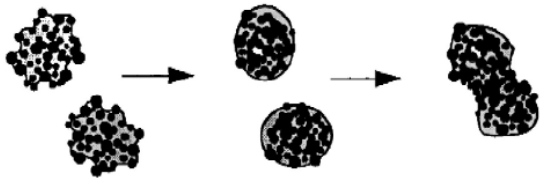

Figure 7. Consolidation and coalescence (Ennis and Litster 1997).

The mechanical forces from the granulator cause consolidation of the granules by compaction. This leads to decrease in granule porosity and increase in liquid pore saturation (Iveson et al. 2001; Ennis 2010). Figure 8 represents the four stages of liquid saturation.

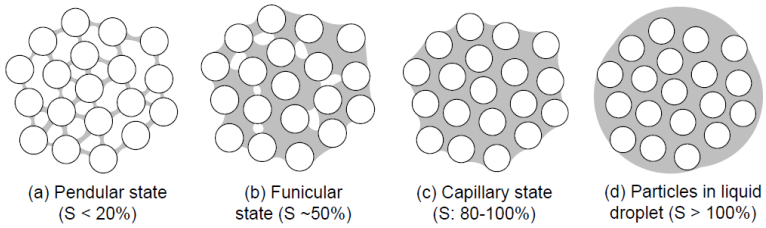

Figure 8. Liquid saturation stages of granules (Capes 1980).

In the pendular state the particles are linked together with liquid bridges. When the liquid fills all the voids the capillary state is reached. The transition from pendular to capillary stage occurs via funicular stage where some voids still exist. If additional liquid is added the mixture forms unfavourable granulated slurry where the particles are distributed inside the liquid drop. Sufficient amount of liquid in the granules is important for the formation of strong wet granules and for the reduction in the amount of ungranulated powder.

The liquid bridges formed in wet granulation are only temporary but they enable the formation of solid bridges in drying. In addition to the liquid and solid bridges, a number of different bonding mechanisms in the granule formation can exist including adhesion and cohesion, intermolecular forces and molecular interlocking.

Illustrative regime maps for batch wet granulation can be found from the literature for example one by Iveson and Litster (1998) for high shear and drum granulation. The regime map predicts the granule growth behavior based on the liquid content (Maximum pore saturation, S_{max}) and the extent of deformation (Stokes deformation number, De) of the granules during impact. In contrast to batch wet granulation, twin screw granulation is continuous, open end process and thus granule growth is dependent on the binding properties of the liquid rather than on the rate processes (Dhenge et al. 2012b). The binding ability of the liquid depends on the liquid-to-solid (L/S) ratio, determined as the ratio of granulation liquid to solid powder, and the viscosity of the binder solution (Dhenge et al. 2012b; Kumar et al. 2014a). Additionally, the free volume in the barrel of twin screw granulator is smaller than in high shear or fluid bed granulation (Dhenge et al. 2012b). Hence, the stresses experienced by the material are suggested to be higher and in form of shear forces rather than impact forces.

Based on these observations, Dhenge et al. (2012b; 2013) developed granule growth regime maps for twin screw granulation with and without kneading elements. The former is discussed here as the screw configuration usually includes kneading elements. The regime map for screw configuration with kneading elements is presented in Figure 9. According to the regime map, the granule growth behavior of a system is a function of deformation value (β) of the granules and the combined influence of L/S ratio and binder viscosity (Dhenge et al. 2012b).

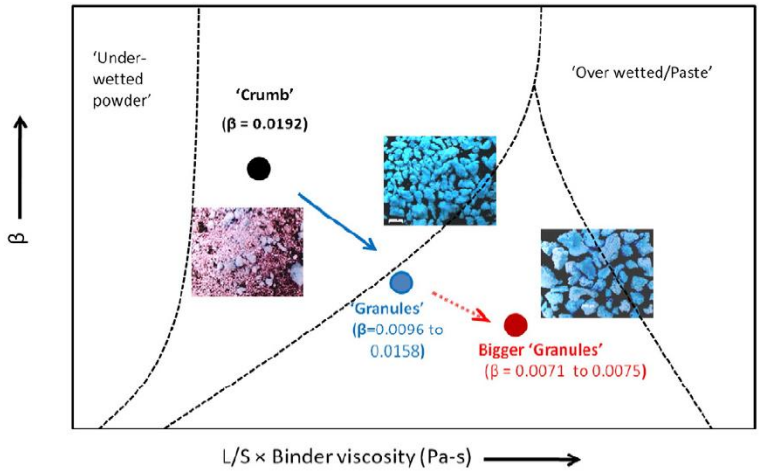

Figure 9. Granule growth regime map for continuous twin screw granulation (Dhenge et al. 2012b)

Due to the significance of the shear stresses acting on the material for granule formation the Stokes deformation number used in the regime map by Iveson and Litster (1998) has been changed to deformation value (β) which is determined by the ratio of the shear stresses (σ) acting on the material to the granule strength (τ) (Dhenge et al. 2012b). The shear stresses (σ) experienced by the powder or granules are determined as the ratio of torque (T) to the volume (V) of the material in the barrel.

There are four different categories of granule formation in the regime map: under-wetted powder, crumb, granules and over-wetted material (Dhenge et al. 2012b). Under-wetted powder refers to ungranulated or poorly granulated material caused by insufficient amount of granulation liquid. Crumb i.e. small or poorly granulated granules are formed due to small increase in liquid amount or binder viscosity. Consolidated, stable and strong granules are formed upon further addition of granulation liquid. If the L/S ratio or binder viscosity increases in excess the granules may turn into over wetted material or paste. High deformation values can change the growth behavior from granule to crumb at intermediate L/S x viscosity values as the weaker system is unable to resist the shearing forces caused by the screws. The regime map boundaries may differ between different granulation conditions e.g. screw configurations and formulations used.

2.2.3 Attrition and breakage

During wet granulation the granules may reduce in size by breakage (Figure 10) into fragments (Ennis and Litster 1997). Additionally, granules may break by attrition or fracture during drying or subsequent handling. Attrition generates fine particles as pieces of the granule surface are separated in consequence of friction and collisions to other granules. The formation of the fine dust due to attrition is undesirable. In contrast, the granule fragments formed in breakage during granulation may coalescence again with other granules to induce further growth. Breakage is an important rate process in granulation as it removes lumps and redistributes liquid as well as creates wet surfaces for the coalescence of fragments and layering of fines (Sayin et al. 2015a). In twin screw wet granulation breakage takes place mainly in the kneading sections and other mixing elements but also in the conveying elements at some extent (El Hagrasy and Litster 2013; Sayin et al. 2015a; 2015b).

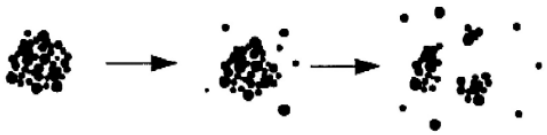

Figure 10. Attrition and breakage (Ennis and Litster 1997).

2.3 Influence of formulation and process variables of twin screw granulation on granule and tablet properties

Owing to the flexibility of twin screw granulator design discussed in previous chapters there are several process parameters that can be changed including screw speed, powder feed rate, L/S ratio, the location of the liquid and powder feed inlets, screw configuration and barrel temperature. The impact of binder, screw configuration and some other factors on granulation process and product properties are discussed in more detail in the following chapters.

2.3.1 Effect of the binder

2.3.1.1 Effect of the binder type

In a study by Tan et al. (2011) the effect of different binders on the strength of acetaminophen tablets was studied. Hydroxypropylcellulose (Klucel EXF) produced the strongest and polymethacrylate (Eudragit E PO) the weakest tablets. On the other hand, tablets from the granules with polyvinylpyrrolidone (Kollidon K30) were not produced due to the stickiness of the formulation in the feeder and lack of steady powder addition in the granulation. However, tablets produced from high shear granules with polyvinylpyrrolidone in the same study had intermediate tensile strengths compared with hydroxypropyl cellulose and polymethacrylate.

2.3.1.2 Effect of the binder addition method

El Hagrasy et al. (2013) compared the effect of binder addition in dry and liquid form on granule properties. It was observed that the granule size distributions were similar but the amount of the fines decreased and the granule size distribution got narrower as the amount of the binder in the liquid phase increased. This was attributed to the enhanced distribution of the binder and thus improved binding efficiency when the binder was dissolved in the granulating liquid. Secondly, the hydroxypropylmethyl cellulose (HPMC) used as the binder forms a gel when dissolved in the water and due to the short residence time in the granulator the authors theorized that probably some of the binder remained insolubilised when added as a dry powder thus resulting in smaller granules.

Similarly, Vercruysse et al. (2012) concluded that the wet binder was more effective in twin screw granulation because of the short residence time of the material in the barrel. In addition to change in the amount of fines and span of the distribution the granule porosity decreased when the percent of the binder in liquid form increased (El Hagrasy et al. 2013). In contrast, Keleb et al. (2002) could not find significant differences in granule properties between the two addition methods. However, the tablet disintegration time was slightly affected but again there was no change in tablet tensile strength.

2.3.1.3 Effect of the binder concentration

In addition to the binder addition method, the binder concentration (dry or wet) and viscosity of the binder solution have an impact on product properties. The influence of increase in binder solution concentration is a combination of the higher amount of binder i.e. improved binding properties and the higher viscosity of the liquid. Dhenge et al. (2012b) used the word “thickening” to describe the change in material consistency with higher binder concentration and viscosity which causes higher frictional resistance to flow and increase in the cohesiveness of the material resulting in higher torque and a longer residence time. The increase in the residence time leads to enhanced mixing and liquid distribution together with increased compaction and consolidation of the granules.

A series of studies were conducted by Keleb at al. (2002; 2004a; 2004b) who investigated the influence of binder concentrations on granule and tablet properties. The tablet tensile strength and disintegration time increased significantly as the aqueous or dry binder concentration increased. The fraction of fines decreased and that of over-sized granules (>1400 um) increased with higher amounts of binder due to enhanced binding properties of PVP (Keleb et al. 2004a; 2004b). Similar observation was made by Thompson and Sun (2010) who noticed increase in coarse granules (>1180um) and reduction in fines with higher aqueous binder concentration.

Dhenge et al. (2012b) observed that the median granule size (d50) increased and the size distribution became mono-modal with higher hydroxypropyl cellulose (HPC) concentration and viscosity. The larger average granule size was attributed to the increased stickiness of the wet material which enabled enhanced binding of the particles producing higher number and strength of the viscous bridges. The stronger bonds reduced the breakage of the granules resulting in increased granule size (Dhenge et al. 2012b; Yu et al. 2014; Saleh et al. 2015). Additionally, the greater number and strength of the liquid bonds resulting from the increased stickiness and longer residence time led to densified and stronger granules as the binder viscosity increased (Dhenge et al. 2012a; 2012b). Furthermore, the increase in binder viscosity produced more spherical granules with improved flow properties as the elongation decreased.

Dhenge et al. (2013) studied the effect of viscosity of the granulation liquid on granule properties using conveying screws only. It was found that the porosity decreased with higher viscosities as in granulation with kneading elements. However, the granule size decreased with higher viscosities. The authors suggested that the reduction in mean granule size was due to the insufficient liquid distribution of the viscous binder by the low shear forces produced in the conveying elements resulting in some large binder-rich granules and higher fraction of very small granules or ungranulated material. For the same reason the small granules were weaker and the large granules stronger compared with the granules produced with low viscosity binder (Dhenge et al. 2013; Saleh et al. 2015).

2.3.2 Effect of the screw configuration

The are several factors that can be changed in the screw configuration including the element type and the arrangement of the elements, the length of the element as well as the offset angle of the mixing disks.

2.3.2.1 Effect of the element type

Djuric and Kleinebudde (2008) investigated the impact of different screw elements on twin screw granulation process. Screw configurations with conveying, combing mixer and kneading elements were used. Conveying elements produced the most porous and friable granules that resulted in the strongest tablets whereas kneading elements produced the densest and least friable granules and tablets with the lowest tensile strengths. This was due to higher resistance of the granules towards deformation in compaction process. Additionally, the formed tablets had higher intergranular porosity which resulted in weaker tablets because the breakage happened first at the site of the large pores. Combing mixer elements led to granules with a median porosity, friability and compactability. Similar results on the porosity and friability of the granules were observed in another study by Djuric and Kleinebudde (2010) where anhydrous dicalcium phosphate was used for continuous wet granulation. However, despite the different porosities of the granules the tensile strength values of the tablets were comparable.

The granule size was also affected by the element type (Djuric and Kleinebudde 2010; Thompson and Sun 2010). Kneading elements produced less small particles (300–500 μm) and fines (<300 μm) and more oversized granules compared with conveying elements. This was due to the squeezing and retaining effect of the kneading block causing improved liquid distribution and higher saturation resulting in larger granules (Djuric and Kleinebudde 2010). However, in the study by Saleh et al. (2015) both the amount of fines and large sized granules decreased thus resulting in narrower size distribution when kneading elements were included in the screw design. The granule size distributions for kneading and comb mixer elements were similar except the comb mixer produced more fines than the kneading element (Djuric and Kleinebudde 2010; Thompson and Sun 2010).

Thompson and Sun (Thompson and Sun 2010) studied the shape of the granules produced with different element types. The conveying element produced oblong granules and the comb mixing element round to oblong particles. The kneading element formed platelike and elongated granules due to the compression in the region where the kneading disks intermesh.

2.3.2.2 Effect of the length of the kneading section

The length of the kneading section i.e. the number of the kneading elements/disks affects the granule size, porosity and strength as well as the torque inside the barrel (Djuric and Kleinebudde 2008; Vercruysse et al. 2012; Yu et al. 2014). Vercruysse et al. (2012) noticed that more kneading elements in the screw design increased the torque as the kneading elements resisted the flow of the material causing higher friction inside the barrel. Additionally, the mixing of the powder with the granulation liquid was more efficient when the number of kneading elements increased resulting in less fines (<150 μm) and increased proportion of oversized granules (>1400 μm) (Vercruysse et al. 2012; El Hagrasy and Litster 2013). Similarly, Yu et al. (2014) observed that the liquid distribution was improved with a longer kneading section. However, the size of the granules decreased with higher number of kneading elements contrary to the findings by Vercruysse et al. (2012).This was attributed to increased mechanical agitation which fractured the granules resulting in smaller median granule size (Yu et al. 2014).

Furthermore, the enhanced liquid distribution and densification of the material with higher number of kneading elements produced less porous and stronger agglomerates (Djuric and Kleinebudde 2008; Vercruysse et al. 2012). Moreover, the bulk density increased with a longer kneading element section because of the better packing of coarser and more irregular-shaped granules (Vercruysse et al. 2012). The tablet strength was also affected by the number of kneading elements as the denser granules had lower deformability during compression resulting in weaker tablets.

2.3.2.3 Effect of the offset angle

Djuric and Kleinebudde (2008) investigated the influence of kneading element offset angle (60ºF, 30ºF, 90º, 30ºR) on granule properties. The authors found that the most friable and porous granules were produced with a forwarding angle of 60º. The least friable and the densest granules were formed with a nonforwarding angle of 90º and with a reversing angle of 30º. A forwarding angle of 30º produced granules with median friability and porosity. According to Van Melkebeke et al. (2008), only the yield and granule friability were affected by the offset angle (60ºF, 30ºF, 90ºF). The forwarding angle of 90º produced the lowest yield and the strongest granules. The granule porosities were comparable and the compressibility of the granules was not affected by the offset angle. According to Vercruysse et al. (2012), the angle (30ºF, 60ºF, 90ºF) of kneading elements did not have significant effect on granule size distribution. Additionally, in a study by Thompson and Sun (2010) the authors showed that the size distribution was only affected by the offset angle when the fill level of the barrel was high (70%).

2.3.3 Other variables

Screw speed and powder feed rate are the main variables to influence the fill level of the barrel. High powder feed rate increases the fill level and high screw speed decreases it (Thompson and Sun 2010; Vercruysse et al. 2012). Fill level affects the residence time and the degree of compaction and granule densification (Thompson and Sun 2010; Dhenge et al. 2012a; Kumar et al. 2014b). Higher fill level leads to denser granules and to a shorter residence time due to higher throughput force created by the material

entering the barrel which pushes the material forward. The L/S ratio is affected by the powder and liquid feed rates (Kumar et al. 2014a). The L/S ratio has an influence on the size, shape and porosity of the granules (Dhenge et al. 2012a; 2012b; El Hagrasy et al. 2013). With higher L/S ratios the granules become larger, denser and more rounded.

3. TABLET FORMATION AND COMPACTION BEHAVIOR

3.1 Tablet formation

The formation of a tablet of defined geometry due to powder compression is called compaction. The powder compression i.e. the reduction in volume of the powder due to applied force, takes place when two punches, the upper and the lower punch, apply force on to the powder in a die. The tablet formation is a part of a tableting process that also includes preceding die filling and subsequent tablet ejection once the tablet has been formed. During the powder compression material can undergo elastic deformation, plastic deformation and fragmentation or a combination of these. In elastic deformation particles change their shape temporarily and in plastic deformation the change is permanent. During fragmentation, on the other hand, the particles fracture into smaller pieces. As the particles are brought close to each other during compression the particle-particle bonds are formed which hold the material together to form a tablet. The main bonding types are weak forces such as van der Waals, electrostatic and hydrogen bonding, solid bridges and mechanical interlocking. The compaction and the bonding mechanisms of granules are similar to powders. However, in addition to elastic and plastic deformation and fragmentation the granules can reduce their intragranular porosity by densification as well as broke down by erosion or attrition from the granule surface during compression.

3.2 Tablet strength

Tablet must possess sufficient mechanical strength to resist fracturing and attrition during handling from production to administration. The mechanical strength of a tablet is referred to as the crushing strength of a tablet which is equal to the diametral

compression force that fractures the tablet i.e. the breaking force (Seitz and Flessland 1965; Brook and Marshall 1968). The same diametral compression test that is used to measure the breaking force can be used to determine the tensile strength of a tablet if the tablet fails along its diameter parallel to the compression load forming a single tensile failure. For a round flat-faced tablet the tensile strength, which is independent of tablet shape and dimensions, can be calculated from the thickness and the breaking force of a tablet with the Hertz equation (Eq. 1) as follows:

$$\sigma = \frac{2F}{\pi \mathrm{Dt}}, \tag{1}$$

where F is the breaking force, D is the tablet diameter and t is the thickness of the tablet (Fell and Newton 1970). There are also additional equations in the literature for elongated and convex tablets however they will not be considered further here (Pitt and Heasley 2013; Shang et al. 2013).

As the tablet strength arises from the bonds between the particles the factors that affect the bond formation at the contact sites and the strength of the bonds have been considered significant for the tablet strength. The factors affecting the tablet strength can be divided into three groups that are material and formulation factors, processing factors and environmental factors. Material and formulation factors include the compression behavior of the materials. Plastic deformation and fragmentation are considered strength-producing compression mechanisms whereas elastic deformation, which may cause capping or lamination of the tablets, is considered as disruptive mechanism. Additionally, the particle size and shape can affect the tablet strength as in some cases a smaller particle size and more irregular shape increase the tablet strength of materials that fragment to a limited degree during compression. Furthermore, for plastic materials a long lubricant mixing time can reduce the tablet strength due to the formation of a hydrophobic surface that interferes particle bonding. Moreover, binder can have an impact on the tablet strength by increasing the deformation of granules and the strength of the intergranular contact bonds.

The processing factors for example the choice of the granulation and tablet machines and the operation conditions can affect the tablet strength. The granulation process will control the physical properties of the granules including the shape, porosity and strength, which will affect the compression properties of the granules and bond formation during tableting thus having an impact on the tablet strength. Increased porosity, decreased compression shear strength and increased irregularity will result in stronger tablets. Additionally, the formation of large intergranular areas of contact and small pores promote high tablet strength.

3.3 Compaction behavior

The compaction behavior of a material can be described with three different relationships that are compactability, tabletability and compressibility. The compactability may be defined as the ability of a material to form a tablet of specific tensile strength during densification and is represented by a plot of tablet strength as a function of tablet porosity. The tabletability describes the capacity of a material to be compacted into a tablet of specific tensile strength under compaction (tablet strength versus compaction pressure). And finally, the compressibility refers to the ability of material to decrease in volume under compaction pressure (tablet porosity as a function of compaction pressure). These relationships can be used to describe the change in the compaction behavior of a material after granulation discussed later in the text.

4. CHARACTERISTICS AND THE CHANGE IN COMPACTION BEHAVIOR OF THE MATERIALS

Several studies have reported a reduction in tablet strength after dry or wet granulation of the powder prior to tableting (Kochhar et al. 1995; Bultmann 2002; Freitag and Kleinebudde 2003; Shi et al. 2011a; 2011b; Nguyen et al. 2013). This reduction has been described as a “loss of compactability” and “reduction in crushing strength” and has been attributed to several reasons. According to Kochhar et al. (1995) the decrease in the compaction behavior was due to the reduction in the “working potential” or due

to the “work hardening” which describes the increase in resistance to irreversible deformation of a material.

In the work by Bultmann (2002), multiple compaction of MCC in a roller compactor was investigated. The decrease in the crushing strength of tablets was speculated to be due to reduced binding potential i.e. the loss in the ability of the material to form bonds. Moreover, four different magnesium carbonates were dry granulated in the study by Freitag and Kleinebudde (2003). A reduction in the tablet strength compared to tablets made of ungranulated powder was noticed. The reduction was related to higher relative tap density of the compacted material and consequently reduced densification of the granules during tableting. Therefore, the authors concluded that using a starting material with a low relative tap density would allow a high degree of densification even after granulation and eventually result in higher tablet strength.

On the other hand, some materials for example mannitol have been noticed to improve in the compactability after granulation (Krycer et al. 1982; Westermarck et al. 1998). This has been attributed to the better deformability of porous granules compared to primary particles. In the following chapters the characteristics and the change in compaction behavior after granulation of the materials (MCC, mannitol and DCPA) used in the current study are discussed in more detail.

4.1 Microcrystalline cellulose

Microcrystalline cellulose (MCC) is a white powder that consists of porous particles (Rowe et al. 2012). It is used as binder and diluent in dry and wet granulation as well as in direct compaction. MCC is practically insoluble in water but hygroscopic in nature and swells in contact with water. MCC powder is soft and ductile and its plastic deformation under pressure is well documented (David and Augsburger 1977; McKenna and McCafferty 1982; Mashadi and Newton 1987; Roberts and Rowe 1987a; 1987b). The glucose units are attached to each other by beta-(1, 4)-glucoside bonds and hydrogen bonds are formed between the cellulose chains. In the interaction with water, the hydrogen bonds are broken and water is attached between the cellulose chains as described in the next chapter.

4.1.1 Water sorption and swelling of MCC

In the interaction of water and cellulose, the water molecules break the cellulose-cellulose bonds and attach to the hydroxyl groups of cellulose chains by new hydrogen bonds (Khan and Pilpel 1987). Consequently, the microfibrils swell which causes the formation of new pores as the volume of the particles increase (Khan et al. 1988). According to Khan and Pilpel (1987) the hydrogen bonding between cellulose and water molecules takes place in three steps. First, each water molecule is attached to two 6-OH groups between the cellulose chains (Figure 11a). When the moisture content rises to 3 wt% the water molecules are bonded by one hydrogen bond (Figure 11b). As more water is added and the moisture content increases to 6 wt% all the 6-OH groups are hydrogen-bonded thus the extra water molecules form a bulk water phase by weak hydrogen bonds (Figure 11c).

4.1.2 Compactability of MCC

It has been observed that the compatibility of MCC is reduced in wet granulation (Westermarck et al. 1999; Badawy et al. 2006; Shi et al. 2011b). Many reports have tried to explain the reasons behind the phenomenon. Hornification is one of the mostly used explanations. When cellulose is wet granulated and dried most of the formed pores collapse during drying. This phenomenon is called “hornification” and it was first introduced to the papermaking field by Jayme G (Jayme 1944; Minor 1994). Originally, hornification was defined as the decrease in water retention value (WRV) but commonly it describes the physical and chemical changes of pulp fibers during drying i.e. formation of additional hydrogen bonds between microfibrils and shrinkage of the cellulose fibers (Jayme 1944; Smook 1990; Weise 1998). The hydrogen bonds are not broken during rewetting and consequently the original swollen state cannot be achieved completely with water addition (Kleinebudde 1994; Minor 1994). In pharmaceutical manufacturing the increased hydrogen bonding has been called “quasi-hornification” (Chatrath 1992) to describe the increase in the granule density and the loss of compactability of MCC upon wet granulation (Chatrath 1992; Habib et al. 1999).

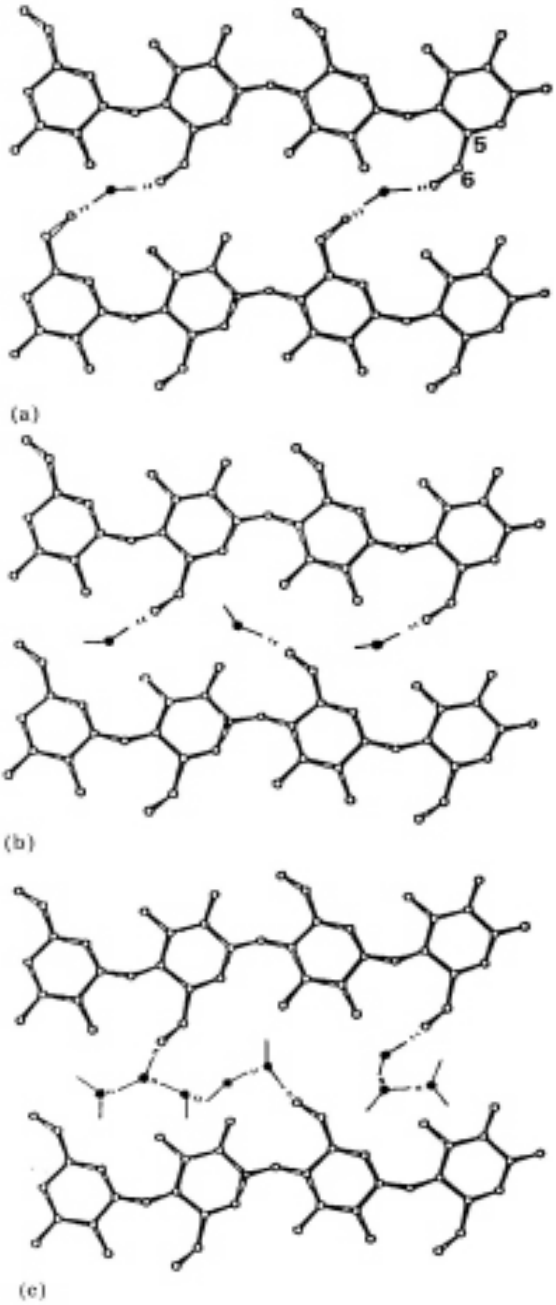

Figure 11. Hydrogen bonding between cellulose and water upon moisture absorption (Khan and Pilpel 1987).

Hydrogen bonding in MCC was observed to increase after wet granulation and drying in a study by Buckton et al. (1999). The authors suggested that this change altered the physical structure of cellulose and caused the change in the enthalpy of water sorption. However, Millili et al. (1996) observed that there were no substantial changes in the number of hydrogen bonds after wet granulation and extrusion of MCC. Thus, they

introduced the concept of autohesion to the pharmaceutical industry to describe the densification of MCC (Millili et al. 1990). Autohesion describes the solid-solid diffusion of free polymer chain ends across the polymer interface to form a stable link. A form of autohesion was described by Kleinebudde (1997) who proposed that MCC particles are broken by the shear forces present in extrusion and that the smaller particles form hydrogen bonds at the amorphous ends of the crystallites resulting in a solid structure of a gel during extrusion/spheronization and subsequent drying.

A sponge model has also been introduced to describe the features of MCC in granulation and extrusion/spheronization (Fielden et al. 1988; Ek and Newton 1998). In the model cellulose acts like a sponge and holds water within and between the fibers until it is compressed during extrusion when the water is squeezed out and acts like a lubricant in the extrusion process. Kleinebudde et al. (2000) studied the effect of the degree of polymerization on the behavior of MCC in extrusion/spheronization process. They concluded that the gel model is more suitable for cellulose with a lower degree of polymerization i.e. MCC and the sponge model is more applicable for powder cellulose which has a higher degree of polymerization.

In a study of high shear granulation of MCC the crystallite size was noticed to decrease and the solid region in the granules to increase with a longer granulation time and higher water level (Suzuki et al. 2001). Thereby, it was proposed that the shear forces of the impeller caused the breakage of the MCC fibrils into smaller particles which formed a network of a continuous solid phase thus hardening the MCC granules.

According to Johansson et al. (1995), the porosity of MCC pellets control the degree of deformation in compaction. Hence, the dense MCC pellets or granules that have low degree of deformation will have weak intergranular bonds due to long separation distance resulting in weaker tablets. Additionally, Staniforth et al. (1988) observed decrease in compactability and lower interparticle bonding of MCC granules compared with powder samples. The authors suggested that in the compaction of granules the degree of plastic deformation was low since most of the force was utilized for breaking

up the granules and not enough energy was used for deformation at particle interfaces to create contact areas for strong interparticle bonding thereby resulting in weaker tablets.

In several studies (Shi et al. 2010; 2011a; 2011b; Nguyen et al. 2013), the loss of MCC tabletability and compactability was observed after high-shear batch granulation. It was found that an increase in the water content or wet massing time led to deteriorated tablet strength due to the decrease in the bonding area. This was caused by surface smoothing and granule rounding. Additionally, lower granule porosity reduced the tablet strength due to higher granule hardness and lower deformability (Shi et al. 2011a; 2011b; Nguyen et al. 2013). The MCC particles were considered as porous and rough agglomerates of the smaller primary particles thus the loss in compactability and tabletability of MCC after batch wet granulation was attributed to the same reasons as the differences between separate granulation batches (Shi et al. 2011a).

Moreover, from the compactability data it was seen that at the same tablet density the tablet strength varied between different granulation batches (Shi et al. 2011a; Nguyen et al. 2013). According to Shi et al. (2011a), this was due to a different pore shape and/or pore size distribution among the tablets. However, Nguyen et al. (2013) attributed this to the different strength of the contact bonds and not to the different pore shape and size. Additionally, this was believed to indicate that the strength rather than the number of the contact bonds determines the tablet strength. Moreover, when a sufficient amount of liquid was incorporated in the granulation the granule strength increased resulting in weaker tablets. Thus, it was suggested that the strength of the hydrogen bonds have an impact on the final tablet strength.

Many explanations have been proposed to explain the characteristics of microcrystalline cellulose in processing with water. However, it seems that additional hydrogen bonding and a formation of a network of some kind are the reasons for the densification and hardening of MCC granules leading to decreased deformability. Subsequently, the low degree of deformability leads to a long separation distance and smaller contact area causing reduced strength and extent of interparticle bonding. Moreover, particle rounding decreases the bond formation by mechanical inter-locking. Consequently,

MCC experiences loss in compactability and results in weaker tablets after wet granulation and subsequent drying.

4.2 Mannitol

Mannitol is a hexahydric alcohol (Figure 12) and isomeric with sorbitol (Rowe et al. 2012). It is a white, crystalline powder that is used as filler in tablet formulations. It is freely soluble in water (1 part in 5.5 parts of water in 20ºC) but non-hygroscopic as its moisture content remains below 1% at 75% relative humidity.

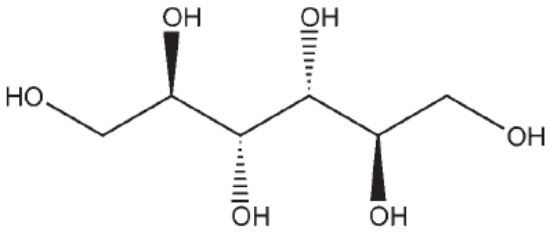

Figure 12. Structure of mannitol (Rowe et al. 2012).

Mannitol is a ductile powder that deforms plastically under pressure (Roberts and Rowe 1987b; Bassam et al. 1990). It has also a degree of brittle character (Bassam et al. 1990). Mannitol has hydroxyl groups in its structure thus it forms hydrogen bonds in tableting (Juppo 1995). Moreover, electrostatic forces, van der Waals attractions and mechanical interlocking constitute the intermolecular bonding mechanisms in tablets. Mannitol powder is cohesive and has poor flowability hence it is often granulated before compression.

In wet granulation, small mannitol particles dissolve in the granulation liquid and recrystallise onto the surface of larger particles (Juppo and Yliruusi 1994). Additionally, the recrystallised mannitol or binder particles form solid bridges that attach the small mannitol particles together. In compression, mannitol granules deform plastically and also fragment under pressure (Juppo et al. 1995). Mechanical interlocking between the granules may also take place due to the fibrous surface structure of mannitol granules.

In addition to better flowability, mannitol granules have also better compactability compared with the powder. Krycer et al. (1982) noticed that tablets compressed from mannitol granules were stronger compared with tablets made from mannitol crystals. According to the authors the high porosity of mannitol granules enables high interparticulate friction during consolidation thus increasing the bonding between particles compared with the tableting of the crystals. Consistent with the results from Krycer et al. (1982), Westermarck et al. (1998) found that the wet granulation improved the compactability of mannitol as granule tablets had higher breaking forces than tablets made from ungranulated powder. This was attributed to the greater extent of deformation of the porous granules together with fragmentation under pressure which caused large area available for bonding. Furthermore, the granules had higher specific surface area compared to powder. According to Juppo et al. (1995), the good compressibility of mannitol granules is due to the plastic deformation of porous granules which brings surfaces near causing strong adhesion between particles. This deformation, together with fragmentation and mechanical interlocking of the granules, produces a strong tablet.

Furthermore, in a study by Vanhoorne et al. (2016) the authors found that tablets produced from δ-mannitol after twin screw granulation were stronger than direct compacted tablets or tablets compacted from granules manufactured using β-mannitol. This was attributed to a moisture induced polymorphic transition of δ-mannitol to β-mannitol during granulation. The polymorphic change resulted in a specific structure of aggregates of small needle-shaped primary particles and high specific surface area. This unique granule morphology led to increased plastic deformability and hence better tabletability.

Juppo and Yliruusi (1994) observed that mannitol granules have a high porosity percentage which is due to the fibrous network including a high number of small pores formed by the needle-like particles. They also noticed that the porosity of the granules increased with the increasing amount of binder solution. This was attributed to the greater size and amount of larger fibrouslike granules (Juppo et al. 1992; Juppo and Yliruusi 1994).

In such manner, the wet granulation of mannitol powder can be considered as increasing the amount of liquid from zero to a higher level thus increasing the number of porous granules compared to the mannitol powder. Based on the studies and observations discussed it seems that the high porosity and the better deformability of mannitol granules compared with the dense mannitol crystals is the main reason for the improved compactability of mannitol after granulation.

4.3 Anhydrous dicalcium phosphate

Anhydrous dicalcium phosphate (DCPA) (Figure 13) is an abrasive, white powder or crystalline solid that occurs as triclinic crystals (Rowe et al. 2012). It is practically insoluble in water and nonhygroscopic. The moisture content is typically 0.1-0.2% and the moisture is adsorbed only onto the surface. DCPA is a brittle material that goes through particle fragmentation during compression (Rue and Rees 1978; Duberg and Nyström 1982; Roberts and Rowe 1985; Bassam et al. 1990).

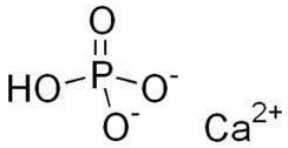

Figure 13. Structure of anhydrous dicalcium phosphate (Rowe et al. 2012).

As described earlier, Djuric and Kleinebudde (2010) found that anhydrous dicalcium phosphate tablets had comparable tensile strengths regardless of the different porosities of the twin screw granulated agglomerates. Thus, it was concluded that with a brittle material the tablet tensile strength is more dependent on the formation of new binding surfaces during fragmentation than on granule porosity. Furthermore, it was speculated that as an insoluble material the strength of DCPA tablets is less dependent on granule porosity compared with water-soluble materials. Additionally, in a study by Djuric et al. (2009), two different twin screw granulators were compared by granulating dicalcium phosphate anhydrate. Despite of the different granule porosities produced by the

different granulators the tensile strength values were similar. Further discussion on the underlying reasons was not presented.

In a study by Souihi et al. (2013) the tensile strengths of DCPA tablets decreased (0.8 MPa) and that of DCPD tablets improved (0.8 MPa) only slightly. The similarity in the tablet strengths compared with direct compacted tablets was attributed to the brittle nature of dicalcium phosphate providing fragmentation during compaction and thus minimizing the propensity of the material for changes in compactability.

Wu and Sun (2007) used brittle fracturing materials including anhydrous dicalcium phosphate in roller compaction to study the effect of size enlargement on the loss of tabletability. It was found that the tabletability of brittle materials was relatively insensitive to changes in granule size. This was attributed to the extensive fragmentation of brittle materials, which reduced the granule size thus minimizing the differences in particle size. Moreover, it was suggested that the larger granules underwent more extensive fragmentation than the smaller particles, which compensated the possible loss in tensile strength caused by the lower surface area.

However, DCPA showed slightly different tensile strengths above 140 MPa between the three granule sizes used i.e. the smallest granules showing the highest tablet strengths (Wu and Sun 2007). It was speculated that the robustness towards the changes in particle size is dependent on the mechanical properties of the material and tableting condition thus DCPA could not minimize all the differences in the granule size due to the compaction parameters used in the study. Nonetheless, the effect of granule size on the tabletability of brittle materials was significantly smaller than with plastic MCC (Sun and Himmelspach 2006). Below 140 MPa the tabletability curves were superimposable for all the used brittle materials (Wu and Sun 2007). The authors emphasized that the curves on either side of the critical pressure point had different slopes, which indicated that the bonding and/or deformation mechanisms had been changed.

Overall, the tabletability of brittle materials was less sensitive to variations in granule properties including size and porosity compared to plastic excipients (Wu and Sun 2007). Hence, the authors suggested that the incorporation of a brittle excipient into a plastic formulation would provide more robust tabletability performance and a better batch-to-batch consistency. Similarly, Osei-Yeboah et al. (2014) observed better tabletability after high shear granulation for a formulation containing increasing concentrations of a brittle excipient (DCPA). This confirmed the hypothesis that a brittle material in an otherwise plastic formulation provides the fragmentation of large granules during compaction thus increasing the bonding area and resulting in stronger tablets.

All in all, it appears that the similarity in compactability and tabletability of DCPA powder and granules is due to the insoluble nature and extensive fragmentation of the material thus providing new surfaces for particle bonding in compaction and minimizing the differences in primary particle and granule properties resulting in comparable tablet strengths.

5. UNIFIED COMPACTION CURVE MODEL

The unified compaction curve (UCC) model was developed by Farber and co-workers (2008) to describe the connection between roller-compaction (RC) conditions and the tablet tensile strength. The model assumes that a tensile strength is generated during the plastic deformation of primary particles i.e. the phenomenon is irreversible and no elastic deformation takes place. Hence, the unified compaction curve model is only applicable to formulations, the major component of which is excipient that goes through plastic deformation under pressure. Additionally, the influence of granule morphology and packing on the tablet strength is not considered as it is assumed that the influence is minimal at pressures used for a tablet compaction (200-300 MPa).

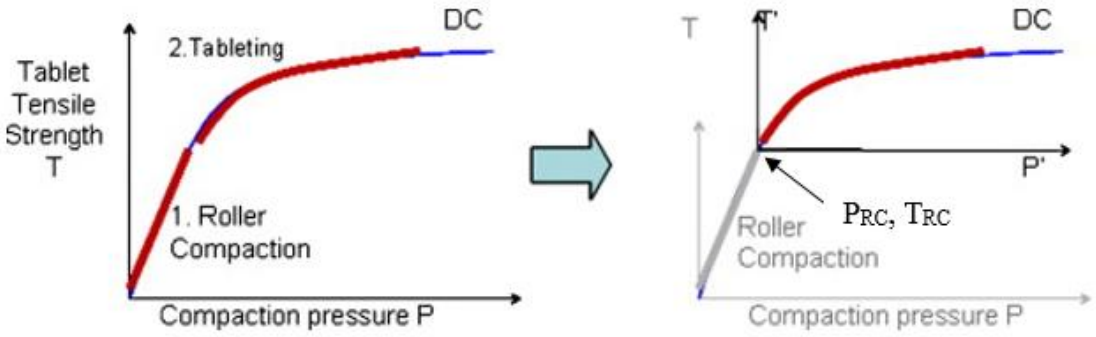

Figure 14. Relationship between DC, RC and tableting in unified compaction curve model (Farber et al. 2008).

According to the model, material experiences compaction pressure during roller compaction and as a consequence ribbons will have a tensile strength (Farber et al. 2008). However, as the ribbons are milled the tensile strength is destroyed but the compaction state of primary particles remains thus resisting further densification. Consequently, tablets compressed from RC granules are usually weaker than tablets compressed from ungranulated blend i.e. the direct compacted tablets. Hence, the final tablet strength depends on the primary particle compaction during both roller compaction and tableting.

The fundamental idea of the UCC model is that once the cumulative compaction aspect is taken into account, the direct compaction (DC) and the roller compaction curves should follow the same curve i.e. the unified compaction curve, which can be seen in Figure 14 (Farber et al. 2008). As a consequence, the DC curve can be considered as a reference curve for roller-compacted tablets. The compaction curve for RC tablets can be attained by moving the origin to P_{RC} (compressive pressure of the rolls) and T_{RC} (tensile strength of the ribbon) along the master curve as seen in right part of Figure 14. The new origin (P_{RC}, T_{RC}) demonstrates the reduction in tablet strength and the second portion of the master curve indicates the tensile strength that can be achieved for RC tablets. As a consequence, the UCC model enables the prediction of the final tablet tensile strength, which can be achieved for roller-compacted tablets, from the roller compaction pressure (P_{RC}). With instrumented rolls, only the DC compaction curve would need to be measured as the P_{RC} is known. This could be done at early stage in the

development and reduce the number of experiments needed to determine suitable RC conditions, for example $P_{RC,}$ to produce tablets that would meet the tablet strength specifications.

Farber and co-workers (2008) studied formulations containing microcrystalline cellulose (MCC), lactose monohydrate, 3% of croscarmellose sodium and 1% of magnesium stearate. Formulations contained at least 50% (w/w) of MCC and the ratio of MCC to lactose was varied. The tensile strength of the tablets made from the formulations by direct compaction as well as roller compaction and tableting were determined. The calculations used to apply the UCC model are explained in the following chapter.

5.1 Calculations

Farber et al. (2008) used Leuenberger´s (1982) equation (Eq. 2) as a starting point for the calculations necessary for the UCC model. Equation 2 demonstrates the relationship between tensile strength (T) and compaction pressure (P):

$$T = T_{max}(1 - e^{-\gamma\rho P}), \quad (2)$$

where ρ is the relative density of the tablet meaning the ratio of compact density to theoretical density, T_{max} is the maximum tensile strength that a formulation can obtain from direct compaction i.e. the tensile strength of DC tablets and γ is the compactability of the formulation. Farber et al. (2008) simplified Equation 2 to yield Equation 3 because ρ is constant with compaction pressures above 200 MPa and γ is also constant, thus

$$T = T_{max}(1 - e^{-bP}), \quad (3)$$

where b = ργ is the material-dependent exponent parameter. Equation 3 is used to determine T_{max} and b from DC compaction curve data. Equation 3 also describes the compaction curve of granules. When RC granules are compressed into tablets the tensile strength that can be obtained is

$$T' = T - T_{RC}, \tag{4}$$

where T is the tensile strength of the DC tablets and T_{RC} is the ribbon tensile strength. Correspondingly, compaction pressure of the RC tablets is

$$P' = P - P_{RC}, \tag{5}$$

where P is the pressure used to compress DC blend and P_{RC} the stress that the rolls generate during roller compaction. Thus, Equation 3 can be presented as Equation 6.

$$T' + T_{RC} = T_{max}\left(1 - e^{-b(P'+P_{RC})}\right) \tag{6}$$

Furthermore, Equation 6 can be simplified to Equation 8 using Equation 7 as follows

$$T_{RC} = T_{max}(1 - e^{-bP_{RC}}), \tag{7}$$

$$T' = T_{max}\left(e^{-bP_{RC}} - e^{-b(P'+P_{RC})}\right) \tag{8}$$

To utilize the UCC model, the tensile strengths of DC tablets were first measured and the direct compaction data fitted to Leuenberger´s (1982) compaction model (Eq. 3) to determine T_{max} and b values (Farber et al. 2008). This was done by minimizing the LSES (Least Sum of the Errors Squared) (Eq. 9) by using the "goal-seek" function in Excel spreadsheet and by varying the b and T_{max} values.

$$LSES = \sum_{1}^{i} (Exp_i - Calc_i)^2 \tag{9}$$

Subsequently, Equation 8 was fitted to the roller compaction data using the LSES and the "goal-seek" function by varying P_{RC} (Farber et al. 2008). The values of T_{max} and b were kept constant for a given formulation. The attained values of P_{RC} were used to calculate the values of T_{RC} with Equation 7. The authors obtained unified compaction

curves for the tested formulations by re-plotting the RC data by superimposing (P´ + P_{RC}) and (T´ + T_{RC}) data points on the DC curves. The obtained data points lie on the DC master curve as seen from the Figure 15, thus demonstrating the cumulative compaction approach to be valid.

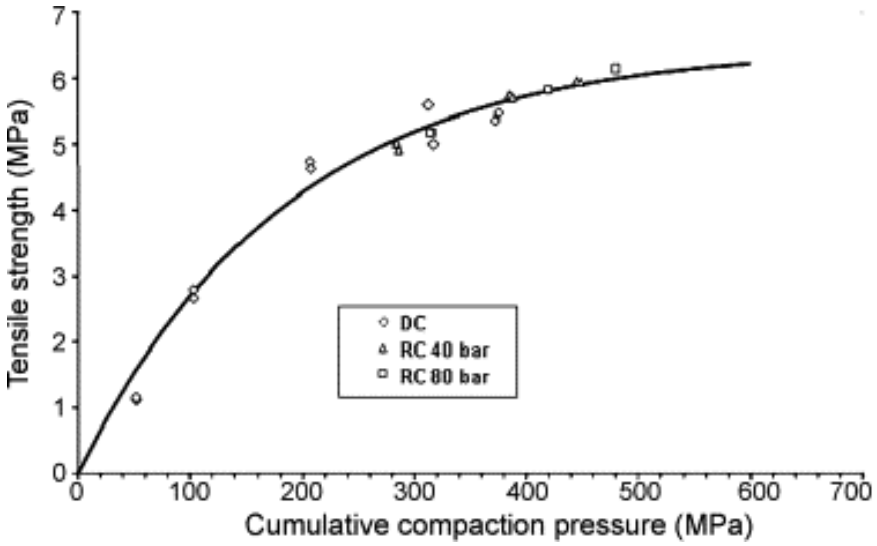

Figure 15. Unified compaction curve (MCC:lactose ratio of 3:1). Solid line represents the fit of Equation 3 to DC data. (Farber et al. 2008)

The UCC model was applicable to formulations containing at least 50% of plastically deforming MCC (Farber et al. 2008). The authors demonstrated that the UCC model is also suitable to be used with DC grade starch. Thus, it was deduced that the model applies to formulations containing a sufficient amount of plastically deforming materials.

5.2 Application of the UCC model to wet granulation with high-shear mixer

Nguyen et al. (2013) studied the effects of the liquid level and wet massing time of wet granulation on the tablet tensile strength. Additionally, the levels of binder flow rate and impeller speed were varied. The formulation consisted of 50% (w/w) of microcrystalline cellulose (PH101), 50% (w/w) of lactose and a 5% (w/v) PVP binder solution. The authors noticed that changing the wet granulation conditions by increasing the liquid level or wet massing time decreased the tablet strength.

To apply the UCC model to wet granulation with high-shear mixer for the first time, Nguyen et al. (2013) combined Equations 4 and 8 to get Equation 10, which they used as a starting point.

$$T = T_{RC} + T_{max}\left(e^{-bP_{RC}} - e^{-b(P'+P_{RC})}\right) \quad (10)$$

In the equation T is the final tablet tensile strength and P' is any tableting compaction pressure (Farber et al. 2008). To create the unified compaction curve for wet granulation the authors introduced Equation 11

$$T = T_{WG} + T_{max}\left(e^{-bP_{WG}} - e^{-b(P'+P_{WG})}\right), \quad (11)$$

where T_{WG} is the tensile strength of the granules produced by wet granulation and P_{WG} is the compaction pressure the powder and granules experience during wet granulation (Nguyen et al. 2013).

The tablet hardness data collected by Nguyen et al. (2013) were converted into tensile strengths and used as a basis for the UCC model. The DC data were fitted to Leuenberger´s (1982) compaction model (Eq. 3) to collect the values of T_{max} and b corresponding to the procedure used by Faber et al. (2008) (Chapter 5.1). Similarly, the P_{WG} and T_{WG} values were obtained in the same way as P_{RC} and T_{RC}. The unified compaction curves for wet granulation were obtained by fitting the data of liquid level and wet massing time effects to Equation 11. New origins ($P' + P_{WG}$ and $T' + T_{WG}$) for the wet granulation compaction curves were formed, thus enabling the curves to be moved along the DC reference curve. As a consequence, DC and wet granulation compaction data could be shown in a single master curve.

The compaction curves for wet granulated tablets were moved upwards and to the right when the liquid level or wet massing time was increased indicating that the tablets produced were weaker compared with the DC tablets (Nguyen et al. 2013). The wet massing time had a stronger effect on the tablet strength than the liquid level. This was considered to be due to the observation that the tensile strength of a tablet for this

formulation was controlled mainly by the number of impeller revolutions that took place during wet granulation. Consequently, the number of impeller revolutions increased as the wet massing time extended. The reduction in tablet strength was attributed to the densification and surface smoothing of the granules due to the pressure applied by the impeller hence decreasing the contact area and mechanical inter-locking between the granules. Furthermore, as the granules got denser the deformability decreased and thus led to weaker tablets.

As the compaction pressure exceeded 500 MPa the UCC model underestimated the tablet strength for both the liquid level and wet massing time curves (Nguyen et al. 2013). However, the tablet compaction pressures used in industry are much lower (200-300 MPa) (Farber et al. 2008). Thus, the UCC model is relevant describing the reduction in tablet strength for varying wet granulation and tableting conditions (Nguyen et al. 2013). Additionally, the model enables the prediction of the compaction pressure the formulation experiences during wet granulation i.e. the pressure imparted by the impeller (P_{WG}), which can be linked back to the compaction behavior and the tensile strength of a tablet. Furthermore, matrix graphs can be generated from process conditions and P_{WG} results attained from small batch of experiments (Nguyen 2014). The matrix graphs can be used as a quality-by-design framework to estimate the tablet strength for given conditions or to determine the granulation operating parameters to achieve a specific tensile strength. Therefore, the UCC model can help to optimize the wet granulation process and thus reduce the resources and costs used to conduct case-studies.

Limitations of the UCC model are the requirement for sufficient amount of plastically deforming material, possible errors in data fitting, demand for the experimental data to fit well the compactability and unified compaction curves and the assumption that the tablet density is consistent at typical compaction pressures.

5.3 Other studies on the UCC model

The UCC model was assessed in a roller-compaction study by Mosig and Kleinebudde (2013). Magnesium carbonate and MCC were used as a brittle and a plastic material,

respectively. In accordance to Farber et al. (2008), it was found that the model is not applicable to brittle fracturing materials (Mosig and Kleinebudde 2013). The compaction curves for magnesium carbonate did not follow the master curve but had a linear profile instead. For MCC the data fitted well the master curve when roller compaction pressures above 200 MPa were used. However, the compaction curve did not conform to the master curve with tableting pressures higher than 10 kN/cm. This was attributed to the ability of the granule to preserve its morphology when tableting with higher pressures.

Another study on high shear granulation and UCC model was conducted by Dave and Dudhat (2013). The authors used formulation of MCC, lactose and PVP (49/49/2% w/w) in wet granulation. The grade of MCC was changed between Avicel PH101 (50 μm) and PH200 (180 μm) to investigate the influence of particle size on tablet strength. It was observed that MCC PH101 had better tabletability compared with MCC PH200 due to its lower particle size and higher cohesiveness but that it did not follow the UCC model contrary to PH200. However, the reasons for the deviation of MCC PH101 from the UCC model were not discussed even though the model was based on the same material.

5.4 Porosity model

Gavi and Reynolds (2014) modified the UCC model to link the tablet porosity to the tensile strength. They used the Ryshkewitch–Duckworth equation (Eq. 12) (Wu et al. 2006) as a starting point and developed an equation (Eq. 13) that can be used to calculate the tensile strength as a function of ribbon (ε_R) and tablet (ε_T) porosities, using two parameters: the tensile strength at zero porosity (T_0) and the bonding capacity (k_b).

$$T = T_0 e^{-k_b \varepsilon} \tag{12}$$

$$T = T_0 e^{-k_b \varepsilon_T} - T_0 e^{-k_b \varepsilon_R} \tag{13}$$

6. AIMS OF THE STUDY

There have been some studies on continuous twin screw granulation considering the influence of raw material properties, formulation, process conditions and parameters on the tablet tensile strength (Keleb et al. 2002; 2004a; Djuric and Kleinebudde 2008; Van Melkebeke et al. 2008; Djuric et al. 2009; Djuric and Kleinebudde 2010; Tan et al. 2011; Vercruysse et al. 2012; Lee et al. 2013; Fonteyne et al. 2014; Vanhoorne et al. 2016; Häkkinen 2016). However, among these studies DC tablets were produced in few (Häkkinen 2016; Vanhoorne et al. 2016) and it seems that there is insufficiency of studies made on twin screw granulator, reported in the literature, where the direct compacted tablets have been compared with tablets made from granules. Consequently, based on the comprehensive literature review done, it appears that there is still lack of knowledge about the contribution of continuous wet granulation on the change of compaction behavior of powders. Hence, the main objective of this study was to understand the change in compactability and tabletability of pharmaceutical materials after twin screw granulation. The aim was to produce variety of granules and tablets of three common pharmaceutical excipients (microcrystalline cellulose, mannitol and anhydrous dicalcium phosphate) and to compare the compaction behavior of the granules with ungranulated powder. Additionally, the contribution of binder (type and addition method) in modifying the compactability and tabletability of granules was investigated. Furthermore, the feasibility of two "loss in compressibility" models to continuous twin screw granulation and for the materials used was evaluated. Earlier the models have been applied to dry and batch wet granulations only.

7. PRELIMINARY STUDIES

Preliminary studies were conducted in order to find a suitable L/S ratio for each main excipient and the binder solution concentration to be used for the granulation of mannitol and DCPA.

7.1 Liquid-to-solid ratio

In the report in general the liquid levels are referred to as liquid-to-solid (L/S) ratios but when regarding liquid level in granulation with binder solution the liquid levels are referred to as water-to-solid (W/S) ratios in order to be able to calculate the right binder solution feed rate and achieve the correct percentages of materials in the granulation.

The aim of the preliminary liquid level studies was to find a L/S ratio that is suitable for producing granules with twin screw granulator. Variety of L/S ratios with purified water were used for the granulation of the blends of main excipient and PVP. The amount of the binder was 5.05% (w/w) and the main excipient 94.95% (w/w). Table 1 shows the masses of the materials. Blends of mannitol with PVP and MCC with PVP were mixed in Muller blender (Muller blender FTMF 200 MG10, Muller, Switzerland) and DCPA with PVP in Pharmatech blender (Pharmatech blender, LD1533, Pharmatech Ltd., England). Mixing time was 10 minutes and mixing speed 13 rpm.

Table 1. Masses of the materials in the blends used for preliminary studies.

Blend	Mass of main excipient (g)	Mass of binder (g)	In total (g)
MCC_PVP	3000.0	159.6	3159.6
Mannitol_PVP	3000.0	159.6	3159.6
DCPA_PVP	3000.0	159.6	3159.6

Granules were produced using a powder feed rate of 15 kg/h, screw speed of 500 rpm, barrel temperature of 25ºC and four kneading elements. Peristaltic pump (Peristaltic pump 1, Flexicon, Denmark) was used with wide tubes (3.2 mm) for MCC and with thin tubes (1.6 mm) for mannitol and DCPA. The inner diameter of the two nozzles used was 0.8 mm. Granulator was run for 30-60 seconds before collecting the granule samples. The produced granules were weighed (~25-100 g) before wet sieving with a 1 mm sieve (Endecotts Ltd., England) and the percentage of the granules larger than 1 mm was recorded for each L/S ratio (Table 2). A visual observation was performed to detect oversized granules.

For mannitol, L/S ratio of 0.20 was observed to be too high as granules were not produced and the powder turned into a paste like material. With L/S ratio of 0.15 and 0.12 some of the granules were oversized even though with L/S ratio of 0.12 the amount of the large granules decreased. With L/S ratio of 0.10 there were still lot of large granules but with L/S ratio of 0.06 a high amount of fines remained ungranulated. Thus, based on the preliminary tests, 0.09 was chosen as the L/S ratio to be used with mannitol in order to make the compaction of the granules successful.

Table 2. L/S ratios and the corresponding amounts of the granules larger than 1 mm.

Material	L/S ratio	Amount of Granules > 1mm (%)
MCC	0.80	54
	1.00	57
	1.10	61
	1.20	69
Mannitol	0.06	31
	0.10	60
	0.12	70
	0.15	75
	0.20	-
DCPA	0.20	22
	0.22	42
	0.23	43
	0.25	49
	0.30	82

For MCC, some of the granules were quite large with L/S ratio of 1.2 and with L/S ratios of 0.8 and 1.0 there were more fines. With L/S ratio of 1.1 the biggest granules seemed a bit smaller than with L/S ratio of 1.2 and in order to get enough granules larger than 1 mm for porosity analysis, L/S ratio of 1.1 was chosen for MCC formulations.

The DCPA granules stuck together (Figure 16) and formed agglomerates with L/S ratios of 0.30 and 0.25. With L/S ratios of 0.22 and 0.23 the granules did not stick together but

some of the granules seemed quite big. With L/S ratio of 0.20 there were lot of fines but in order to avoid from producing too large granules and to make tableting easier the L/S ratio of 0.20 was chosen for DCPA granulation.

Figure 16. DCPA/PVP granules produced with L/S ratios of 0.20, 0.22, 0.23, 0.25 and 0.30 from the left.

7.2 Flowability of the binder solution

The objective was to add binder in the granulation either as dry in the powder blend or as wet i.e. dissolved in the granulation liquid. However, L/S ratios of mannitol and DCPA were rather low so it was not practical to add total amount of the binder in the granulation liquid. Hence, the flowability of the binder solution through the tubes was tested by preparing liquid binders from HPC and purified water with three different concentrations. The aim was to find the highest concentration of the binder solution that could be pumped through the tubes. Table 3 shows the concentrations and the corresponding amounts of water and HPC.

Table 3. Composition of the binder solutions for flowability testing.

Binder solution concentration (w/w) %	Mass of water (g)	Mass of HPC (g)
10.0	300.0	33.3
12.5	300.0	42.9
15.0	300.0	52.9

The liquid binders were prepared by adding the binder in purified water in small sections and continuously mixing with a magnet and a magnetic stirrer (RCT BASIC, IKA, USA). Mixing was continued until the binder was dissolved in the liquid. Only the binder solution of 10% (w/w) concentration could be pumped through the tubes. Therefore, 10% (w/w) was chosen as the concentration of the binder solutions to be used in the granulation of mannitol and DCPA.

8. MATERIALS AND METHODS

This chapter will explain the experimental part of the study including the characterisation of the granules and tablets. Figure 17 represents a flowchart of the experiments.

8.1 Design of experiments

Microcrystalline cellulose (MCC), mannitol and anhydrous dicalcium phosphate (DCPA) were chosen as the excipients to be studied based on their different compressibility properties. Polyvinylpyrrolidone (PVP) and hydroxypropyl cellulose (HPC) were used as binders and magnesium stearate as lubricant in tableting. Table 4 represents the grades and manufacturers of the materials.

Table 4. Grades and manufacturers of the materials.

Excipient Name	Grade	Manufacturer
Microcrystalline Cellulose	Avicel PH101	FMC Biopolymer
β-mannitol	Pearlitol 160C	Roquette
Calcium Phosphate Dibasic Anhydrous	Calipharm A	Univar Innophos
Hydroxypropyl cellulose	HPC Klucel EXF	Ashland
Povidone	Kollidon 30	BASF
Magnesium Stearate	MgSt MF-2-V	Peter Greven

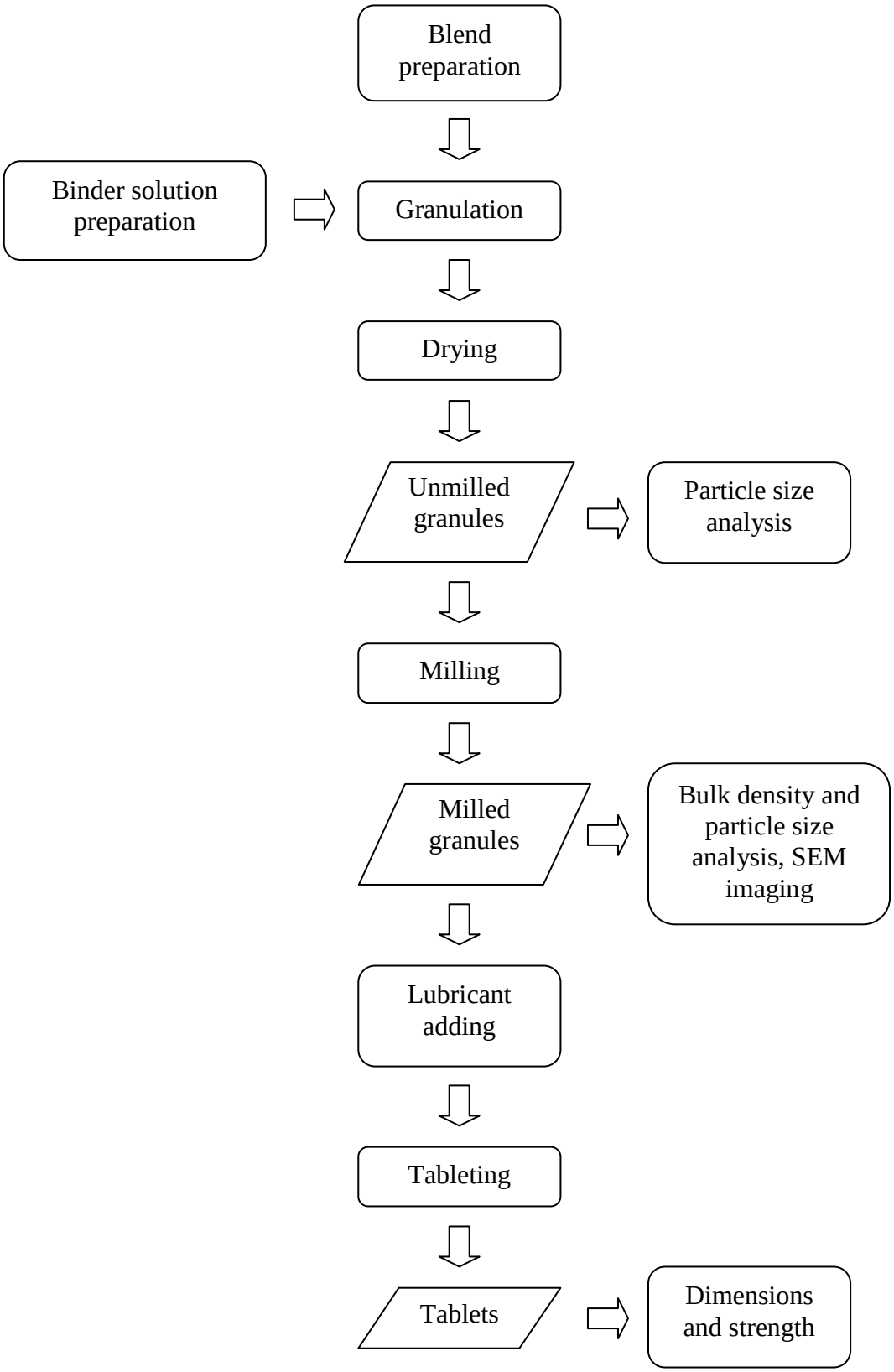

Figure 17. Flowchart of the experiments.

Table 5 represents the chosen variables of the experiments and their levels. The number of kneading elements in the screw configuration was chosen as the process variable with the intention of producing variety of granules. It has been noticed that the number of kneading elements has a great impact on granule properties increasing the size, density and strength of the granules as the number increases (Vercruysse et al. 2012; Beer et al. 2014). Additionally, the number of kneading elements has an influence on tablet strength i.e. the strength decreases due to higher density of the granules as the number of kneading elements increases (Vercruysse et al. 2012). Four and eight kneading elements per screw were selected and they were divided into two separate blocks as recommended (Thompson and Sun 2010).

Table 5. Variables of the experiments and the used levels.

Parameter	Levels
Binder type	PVP and HPC
Binder addition method	Dry powder and dissolved in the granulation liquid
Number of kneading elements	4 and 8

The binder type and addition method were selected as the formulation variables. It has been observed that the binder type can affect the tablet strength and that the binder addition method has an influence on the granule porosity and size distribution decreasing the amount of fines and porosity with the increasing amount of binder in the liquid phase (Tan et al. 2011; El Hagrasy et al. 2013; Stoyanov et al. 2014a; 2014b). PVP and HPC were selected as the binders in order to see if the binder type makes a difference in the compaction behavior after granulation.

Full factorial design of the three variables with two levels was performed for all the three main excipients. Additionally, one granulation run (PVP, dry binder, 4 kneading elements) was repeated for each main excipient. In total this made 27 experiments. Table 6 represents the design of experiments.

Table 6. Full factorial 3^2 design of experiments.

Binder type	Binder addition method	Number of kneading elements
PVP	Dry	4
PVP	Dry	8
HPC	Dry	4
HPC	Dry	8
PVP	Wet	4
PVP	Wet	8
HPC	Wet	4
HPC	Wet	8
PVP	Dry	4

8.2 Preparation and tableting of the direct compaction blends

Six direct compaction (DC) blends consisting of 94% of main excipient that is MCC, mannitol or DCPA, 5% of HPC or PVP as a binder and 1% of magnesium stearate as a lubricant were prepared. Mannitol was sieved before weighing by using a 1 mm sieve (Endecotts Ltd., England). The masses of the materials in the direct compaction formulations are shown in APPENDIX 1. Additionally, batch numbers, expire dates and mean particle sizes of the materials are listed in APPENDIX 2.

Main excipient and the binder were mixed in the Turbula blender (T2F, Willy A. Bachofen - WAB, Switzerland) with fill level of 40-60%. The Turbula blender utilizes rotational and translational movement together with inversional motion causing rhythmically pulsing mixing. The mixing time was 10 minutes and speed 33 rpm. Magnesium stearate was sieved (850 µm, Endecotts Ltd., England) and added in the middle of the main excipient-binder blend before mixing the lubricant with Turbula. The mixing time was 2 minutes and the speed 33 rpm.

The blends were conditioned in an environmental chamber (7392, Vindon Scientific Limited, England) that keeps the chosen conditions in the cabinet in order to stabilize the blends before tableting. The conditioning took place in 25°C and 40% relative humidity (RH) overnight. The moisture content was measured by loss on drying (LOD)

(HB43 Halogen, Mettler-Toledo, Switzerland) after conditioning before the blends were compacted. The sample weight was approximately 1.5 g, temperature 90ºC and the time of measure 15 minutes. The moisture analyser consists of a balance and a halogen heating part and it uses the thermogavimetric method i.e. it measures the weight of the sample at the beginning of the analysis and during the drying as the moisture vaporizes. Subsequently, the moisture content of the sample is shown as a percentage of the starting weight once the analysis has been completed.

Styl`One tablet press (Styl`One Evolution Single Station Tablet Press, Romaco Kilian, Germany) was used to produce compacts of the blends with variety of compaction forces. The punches used were 10 mm in diameter, round and flat faced. The speed used was 25% of full speed (~35 mm/s) and the target mass was set up to be 400 mg. 8-12 forces were used between 3 kN to 45 kN and 8-10 tablets were produced for each force.

8.3 Preparation of the blends for granulation

The blends used for granulation with purified water consisted of 94.95% (94/99) of main excipient (MCC, mannitol or DCPA) and 5.05% (5/99) of binder (HPC or PVP) in order to achieve the right relative amounts of main excipient, binder and lubricant (94/5/1%) when adding the magnesium stearate after granulation. Mannitol was sieved with a 1 mm sieve before use. APPENDIX 3 represents the masses of the materials used for the blends.

Mannitol blends used for granulation with 10% (w/w) binder solution consisted of 95.91% of mannitol and 4.09% of binder (20% of the total amount of the binder was in liquid). The calculations were based on a water-solid (W/S) ratio of 0.09 and a powder feed rate of 15 kg/h (APPENDIX 4). DCPA blends used for granulation with 10% (w/w) binder solution consisted of 97.11% of DCPA and 2.89% of binder (44% of the total amount of the binder was in liquid). The calculations were based on a water-solid ratio of 0.20 and a powder feed rate of 15 kg/h. MCC was granulated with binder solution as it is. Binder solution concentration was 4.39% (w/w) (Chapter 8.4). APPENDIX 5 shows the masses of the materials in granulation blends used with binder solution.

Table 7. The used blenders and the bulk densities and masses of the blends that were used to calculate the fill level of the drum.

Blend	Blender	Bulk density of the formulation (g/cm^3)*	Mass of the blend (g)	Nominal fill level (%)
Mannitol_PVP _prestudy	Muller	0.43	3160	37
MCC_PVP _prestudy	Muller	0.32	3160	49
MCC_PVP_dry _2 runs	Muller	0.32	3897	60
MCC_HPC_dry _2 runs	Muller	0.33	3897	59
Mannitol_PVP_dry _2 runs	Muller	0.43	3897	46
Mannitol_HPC_dry _2 runs	Muller	0.43	3897	45
Mannitol_PVP_wet _2 runs	Muller	0.43	3950	46
Mannitol_HPC_wet _2 runs	Muller	0.43	3950	46
DCPA_PVP _prestudy	Pharmatech	0.76	3160	42
DCPA_PVP _replicate	Pharmatech	0.76	2264	30
Mannitol_PVP _ replicate	Pharmatech	0.43	2264	53
MCC_PVP _ replicate	Pharmatech	0.32	2264	35
DCPA_PVP_dry _2 runs	Pharmatech	0.76	3897	51
DCPA_HPC_dry _2 runs	Pharmatech	0.77	3897	51
DCPA_PVP_wet _2 runs	Pharmatech	0.76	3915	52
DCPA_HPC_wet _2 runs	Pharmatech	0.77	3915	51
DCPA_PVP_wet _4 ke_new	Pharmatech	0.76	2265	30

***** Bulk densities: MCC 0.32 g/cm^3, mannitol 0.43 g/cm^3, DCPA 0.78 g/cm^3 (A-TAB), PVP 0.39 g/cm^3, HPC 0.50 g/cm^3 (Rowe et al. 2012). Mass fraction of the main excipient was 94.95% and binder 5.05%.

Pharmatech blender (Pharmatech blender, LD1533, Pharmatech Ltd., England) with a 10 L drum and Müller blender (Müller blender, FTMF 200 MG10, Fördertechnik AG, Switzerland) with a 20 L drum were used to achieve a fill level of 30-60% in mixing. The Pharmatech (drum) and Müller blenders (IBC) are tumbling mixers that rotate about an axis and impart shear mixing as a layer of granules flows over another layer and diffusive mixing as tumbling allows the granule bed to dilate and particles fall due to gravitational force. Table 7 shows the used blender for each batch. The blending time in mixing was 10 minutes and speed 13 rpm.

Blending tool (developed at AstraZeneca) in Excel spreadsheet (Microsoft, USA, 2007) was used to choose the right drum volume for blends based on the fill level (30-60%). Blending tool calculates fill level (%) based on the mass of the batch (kg), bulk density (g/cm^3) of the formulation and the available volume (L) of the blending bowl (Table 7).

8.4 Binder solution preparation and pump calibration

Concentration of the binder solutions to be used with mannitol and DCPA were 10% (w/w). Binder solutions were prepared by adding the binder in purified water in small sections and continuously mixing with an overhead stirrer (Heidolph overhead stirrer, RZR2101 Electronic, Germany). Mixing was continued overnight until the binder was dissolved in the liquid. Table 8 shows the masses of water and the binder in the granulation liquid.

Table 8. Binder solution concentration and the masses of the materials in the solutions.

Batch of the binder solution	Mass of water (g)	Mass of binder (g)	Binder solution concentration (% w/w)
PVP (for MCC)	5000.3	229.5	4.39
HPC (for MCC)	4801.5	220.4	4.39
PVP (for mannitol)	1400.0	155.6	10.0
HPC (for mannitol)	1400.0	155.6	10.0
PVP (for DCPA)	1400.0	155.6	10.0
HPC (for DCPA)	1400.0	155.6	10.0

* Approximately 1000 g of the binder solution was used for pump calibration

The binder solution concentration 4.39% (w/w) and the corresponding amount of the binder (g) in the binder solution to be used with MCC were calculated as follows:

$$m_{water} = L/S * m_{powder} \quad (14)$$

$$m_{binder} = 0.0505 * m_{powder} \quad (15)$$

$$Binder\ solution\ concentration\ (w/w)\ \% = \frac{m_{binder}}{(m_{binder} + m_{water})} \quad (16)$$

The used peristaltic pump (Peristaltic pump 1, Flexicon, Denmark and Peristaltic pump 2, Watson Marlow, England) was "calibrated" in order to find the right speed (rpm) of the pump to achieve the wanted liquid feed rate (g/min). This was conducted by running the pump for one minute with different speeds and measuring the mass of the granulation liquid. The necessary speed of the pump for different granulation liquids was solved by making a plot of the liquid feed rate against speed and using the equation of the line to solve the corresponding speed.

8.5 Twin screw granulation

Wet granulation was carried out using the ConsiGma™ 1 twin screw extruder (GEA ConsiGma™ 1, GEA Pharma Systems, Belgium) having a length to diameter ratio of 21:1 and 24 mm outer diameter (D) screws. The ConsiGma™ 1 twin screw granulator is shown in Figure 18. Only the powder feeder and the twin screw granulator were used in the current study. Drying was conducted separately after the granulation. The powder feed rate, screw speed and barrel temperature were held constant at 15 kg/h, 500 rpm and 25°C, respectively during the granulation.

Configuration 1 represents the screw configuration with four kneading elements arranged in two blocks (Figure 19). Configuration 2 shows the screw configuration with eight kneading elements in two blocks (Figure 20).

Figure 18. ConsiGma™ 1 granulator.

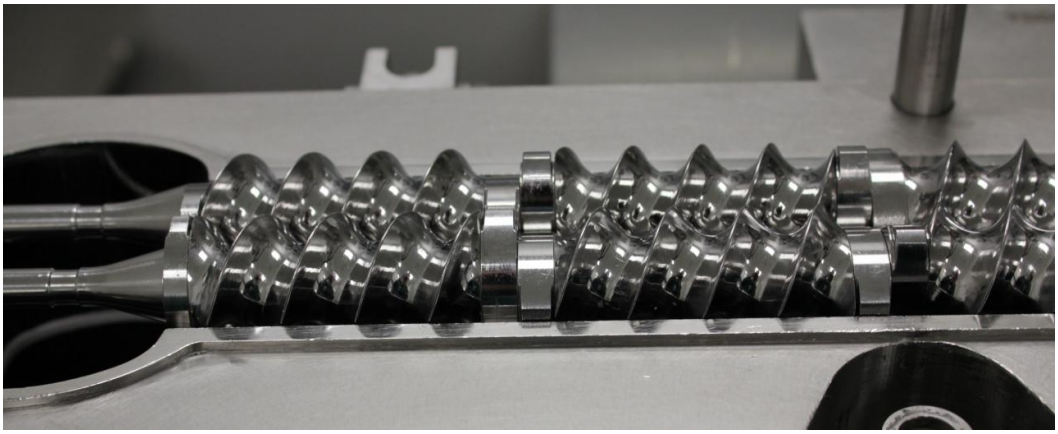

Figure 19. Screw configuration 1.

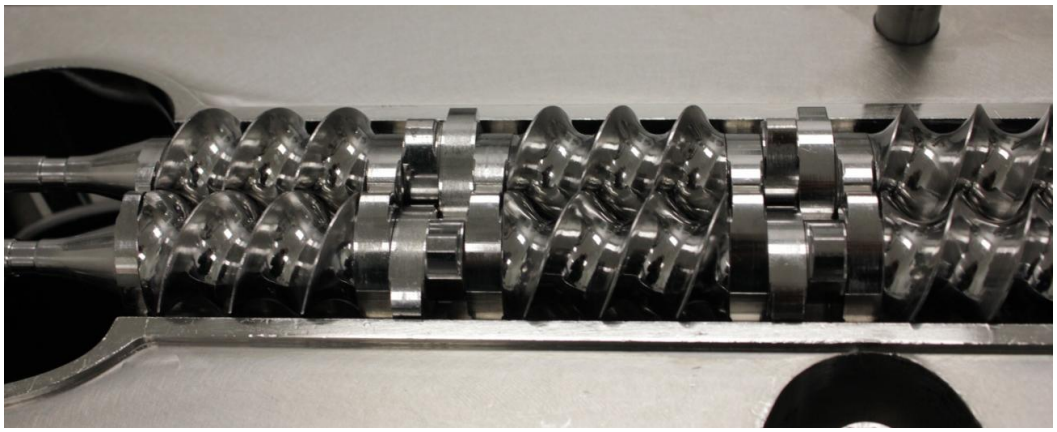

Figure 20. Screw configuration 2.

Screw configurations (from the barrel outlet):

(Config. 1) $$\frac{K}{6} - 2C - 2\frac{K}{4}60°\text{f} - 2C - 2\frac{K}{4}60°\text{f} - 14C - 2\frac{K}{6}$$

(Config. 2) $$\frac{K}{6} - 1.5C - 4\frac{K}{4}60°\text{f} - 1.5C - 4\frac{K}{4}60°\text{f} - 14C - 2\frac{K}{6}$$

In the configurations C is a conveying element with length equal to one D. Correspondingly, 2C and 1.5C have lengths equal to 2 D and 1.5 D. K/4 and K/6 are kneading elements with height of a quarter and one-sixth of D, respectively. The alignment of the kneading disks was 60° forward.

When purified water was used as a granulation liquid the liquid feed rate for MCC, mannitol and DCPA were 275.0, 22.5 and 50.0 g/min, respectively [L/S ratio*powder feed rate]. The binder solution feed rates used with each material and the equations of the calculations are shown in APPENDIX 4. The liquid feed rate was checked by running the pump for one minute and measuring the mass of the liquid before each granulation to make sure the feed rate was appropriate. Table 9 shows the speed of the pump and the actual liquid feed rate for each batch. Digital thermometer (Electronic thermometer, 3821, H-B Instrument, USA) was used to measure the temperature of the granulation liquid prior granulation.

An external peristaltic pump (Peristaltic pump 1, Flexicon, Denmark and Peristaltic pump 2, Watson Marlow, England) was used to pump the granulation liquid through two tubes and 1.8 mm (inner diameter) nozzles in to the granulator barrel. A peristaltic pump is a positive displacement pump that has elastic tubes and a rotor with number of rollers inside a (semi)cylindrical chamber (Allen 1881; Clay and Doering 1972). The fluid is pushed forward by the rotating rollers that squeeze the tubes. At the same time the tubes recover behind the rollers creating a vacuum thus drawing the fluid into the tubes, which is again pushed forward by the rollers.

Table 9. Speed of the pump and the liquid feed rate.

Batch (run order)	Speed of the pump (rpm)	Liquid feed rate (g/min)
MCC_PVP_dry_8 [1]	190	275.0
MCC_PVP_dry_4 [1]	190	275.0
MCC_HPC_dry_4 [1]	193	275.0
MCC_HPC_dry_8 [1]	190	275.0
MCC_PVP_wet_4 [1]	204	287.8
MCC_PVP_wet_8 [1]	203	286.6
MCC_HPC_wet_4 [1]	237	287.2
MCC_HPC_wet_8 [1]	238	287.1
MCC_PVP_dry_4_rep [1]	185	275.6
Mannitol_HPC_dry_4 [1]	52	22.7
Mannitol_HPC_dry_8 [1]	52	22.5
Mannitol_PVP_dry_4 [1]	53	22.4
Mannitol_PVP_dry_8 [1]	53	22.6
Mannitol_PVP_dry_4_rep [1]	53	22.5
Mannitol_PVP_wet_4 [2]	12	25.0
Mannitol_PVP_wet_8 [2]	13	25.3
Mannitol_HPC_wet_4 [2]	17	25.4
Mannitol_HPC_wet_8 [2]	17	25.7
DCPA_PVP_wet_8 [2]	26	56.6
DCPA_HPC_dry_4 [1]	102	50.1
DCPA_HPC_dry_8 [1]	105	50.0
DCPA_HPC_wet_4 [1]	80	56.8
DCPA_HPC_wet_8 [1]	80	56.9
DCPA_PVP_dry_4_rep [1]	109	50.2
DCPA_PVP_dry_4 [1]	110	50.1
DCPA_PVP_dry_8 [1]	111	49.8
DCPA_PVP_wet_4 [2]	30	56.8

[1] Peristaltic pump 1, Flexicon, Denmark
[2] Peristaltic pump 2, Watson Marlow, England

Two different peristaltic pumps were used in order to achieve the right liquid feed rate in the granulation process. Table 9 shows the pumps used for each granulation run. Tubes with inner diameter (i.d.) of 1.6 mm were used for the granulation of mannitol and DCPA when purified water was used as the granulation liquid. For the other granulation runs wider tubes were used with i.d. of 3.2 mm due to higher liquid feed

rate or higher viscosity of the liquid. The granules produced during the first two minutes were discarded. After two minutes, approximately one kilogram of granules was collected.

8.6 Drying and milling

MCC and mannitol granules were dried in a separate fluid bed dryer (Strea Fluid Bed Dryer, Niro-Aeromatic, Germany) at 90°C. In a fluidized bed dryer the velocity of air through the granule bed is increased so that the bed is fluidized and the particles can move freely in the air. Thus, the hot air has a good contact with the particles causing an efficient heat and moisture transfer and consequently dries the granules with high drying rates.

DCPA granules were dried in a tray dryer (Tray Dryer, SS, Leec Ltd., England) in order to prevent the formation of agglomerates. In fluid bed drying the wet granules stuck together and formed big lumps that were not separated by the fluid bed dryer. The same agglomerate formation was seen with wet sieving in preliminary L/S ratio studies (Chapter 7.1 and Figure 16). Tray drying did not form those large agglomerates. The tray dryer consists of three perforated shelves and a heating element situated at the bottom of the dryer. The granules are spread on shallow trays and the warm air coming through the holes in the shelves dries the granules. The granules were dried overnight with a drying temperature of approximately 70°C.

The moisture content to aim for was determined by using a DVS (Dynamic Vapour Sorption) tool in Excel. The tool has a list of moisture contents for different materials in several relative humidities and it takes into account the proportional amounts of the materials in the formulation to form a graph where the moisture content at a certain relative humidity can be seen. Table 10 lists the moisture contents at 40% relative humidity for the formulations used. Based on the moisture contents, less than 5% and 1% were selected as the end points of drying for MCC, and mannitol and DCPA, respectively.

Table 10. Moisture content at 40% relative humidity.

Batch	Moisture content (%)
MCC_PVP	5.22
MCC_HPC	4.89
Mannitol_PVP	0.71
Mannitol_HPC	0.38
DCPA_PVP	0.78
DCPA_HPC	0.45

In order to detect the end point of drying, the moisture contents of the batches were analysed (LOD) (HB43 Halogen, Mettler-Toledo, Switzerland) during drying. The drying was stopped and approximately 1-2 g of sample was taken to measure the moisture content. Temperature was 90ºC and measuring time 15 minutes. The drying was stopped when the appropriate moisture content was reached. Table 11 shows the total drying times.

Table 11. Drying time.

Batch	Drying time		
	MCC (min)	Mannitol (min)	DCPA (h)
PVP_dry_4	55	10	21
PVP_dry_8	60	9	19
HPC_dry_4	45	10	21
HPC_dry_8	38	5	21
PVP_wet_4	60	6	17
PVP_wet_8	55	5	18
HPC_wet_4	55	6	22
HPC_wet_8	45	7	19
PVP_dry_4_rep	45	8	23

The granules were dry milled with Glatt GS100 Cone Mill (GS100 Cone Mill, Glatt, Germany). The Cone Mill is a conical-screening mill that has a rotating impeller inside a conical screen placed in a chamber (Rekhi GS and Sidwell R 2010). The impeller sizes the material by imparting compression and shear forces to the granules, which are

transferred to the screen surface by centrifugal acceleration together with vortex flow caused by the impeller. For the milling of the granules the mill was fitted with a 1.4 mm screen (round) and 2 mm and 6 mm spacers. The impeller speed was 650 rpm.

8.7 Sampling of the granules

The granules were divided into samples by using an automatic (Rotary Sample Divider, Laborette 27, Fritsch, Germany) and a hand held manual (Manual Sample Divider, Endecotts, England) sampler dividers. The automatic sampler divider has a feeding funnel that directs the material into a rotating cone. The rotation movement causes the material to be divided through identical channels into ten glass bottles. The hand held sample divider has a divider that subdivides the material into two samples.

The unmilled granule samples for particle size measurement were collected by using the automatic sample divider twice to get two samples of 10 g which were divided once with the manual sample divider to get three samples of approximately 5 g. The samples of milled granules were collected by first dividing the granulation batch into ten samples of approximately 100 g. The samples of milled granules for particle size measurement were collected with manual sample divider by dividing the sample of 100 g three times to get two samples of 12 g and subdividing those samples to get three samples of 6 g. Two to five samples of 100 g were sieved with 1.00-1.18 mm sieve (Endecotts Ltd., England) to get a granule sample of one size class for the bulk density analysis. Additionally, two samples of 100 g were used to prepare the batches for tableting.

8.8 Mixing of the lubricant

Magnesium stearate was sieved (850 μm) (Endecotts Ltd., England) and added in the middle of the granule batch before mixing. Turbula blender was used for mixing at 33 rpm for 2 minutes. The amount of the lubricant was calculated by using the Equations 17, 18 and 19. APPENDIX 6 shows the masses of the granules and the lubricant.

$$Mass\ fraction\ (main\ excipient + binder) = 94\% + 5\% = 99\% \quad (17)$$

$$Mass\ fraction\ (lubricant) = 1\% \quad (18)$$

$$Amount\ of\ lubricant\ (g) \quad (19)$$
$$= \frac{Mass\ fraction\ (lubricant)}{Mass\ fraction\ (main\ excipient + binder)} * m\ (granules; excipient + binder)$$
$$= 0.010101 * m(granules)$$

8.9 Compaction of the granules

The granules were conditioned in a stability cabinet (7392, Vindon Scientific Limited, England) in 25°C and 40% relative humidity overnight and the moisture content was analysed (HB43 Halogen, Mettler-Toledo, Switzerland) before tableting.

Styl`One tablet press (Styl`One Evolution Single Station Tablet Press, Romaco Kilian, Germany) was used to produce compacts of the granules with variety of compaction forces. The Styl'One Evolution is a single-punch tablet press where the displacement of the lower punch was determined based on the target weight of the tablet. During the compaction the hopper shoe moves over the die by rotational motion and the powder or granules flow into the die. After the hopper shoe has moved aside the punches move towards each other and compress the granules into a tablet. The compact is subsequently ejected by the lower punch and pushed from the die table by the hopper shoe.

For the compaction of the granules the punches used were 10 mm in diameter, round and flat faced. The speed used was 25% of full speed (~35 mm/s) and the target mass was set up to be 400 mg. 8-12 forces were used between 3 kN to 45 kN and 8-10 tablets were produced with each force.

8.10 Characterisation of the granules and tablets

The understanding of the powder and granule properties is important for the understanding of the tablet formation and the strength of the tablets. The following chapters will explain the analysis of the properties represented in Table 12.

Table 12. Characterisation of the main excipients, granules and tablets.

		Property	Test method
Direct-compacted blend		Particle size, PSD and shape	Qicpic
		Moisture content	Moisture analyser
Granules	Unmilled	Particle size, PSD and shape	Qicpic
	Milled	Moisture content	Moisture analyser
		Particle size, PSD and shape	Qicpic
		Bulk density	Geopyc
		Morphology	SEM
Tablets		Crushing force → tensile strength	Hardness tester
		Porosity	Dimensions

8.10.1 Particle size distribution analysis

Particle size of the granules was analysed with Qicpic (SympaTec Inc., Germany), a dynamic image analyser that has a dispersion system (Witt et al. 2004). Qicpic uses VIBRI/L as the vibratory feeder and Windox 5.0 software as the instrument control program. Figure 21 demonstrates the set-up of the equipment. A light source generates visible light pulses which are expanded by a beam expansion unit (Witt et al. 2004) .The formed beam of light illuminates the particles which are dispersed by the dispersion unit. Subsequently, the images of the particles are captured by a high-speed camera that works synchronously with the light source.

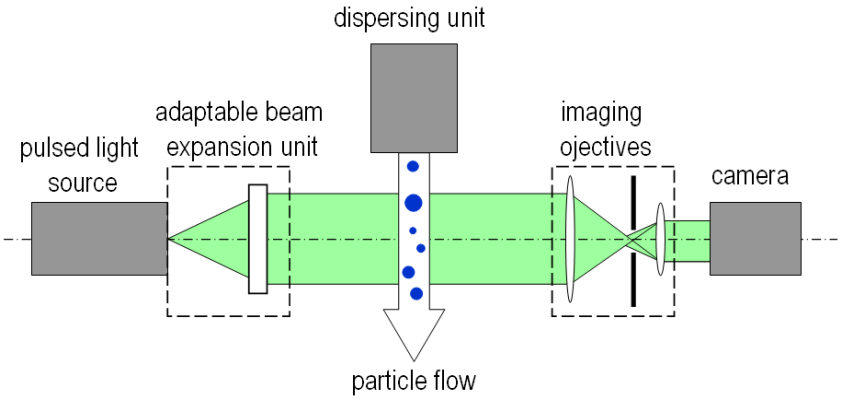

Figure 21. Principle set-up of Qicpic (Witt et al. 2004).

In the current study, the flash rate of the light source was 450 Hz and the synchronized camera took 450 images per second, accordingly. RODOS disperser (dispersion pressure of 0.2 bar, lens M7 10–3410 µm) was used for the dispersion of milled granules. Three samples of approximately 5 g were analysed for each granulation batch. For the analysis of unmilled granules three samples of 5 g were subdivided from the batch as explained in chapter 8.7. Two samples were analysed using GRADIS disperser (lens M8 20–6820 µm). The third sample was sieved with 1.7 mm sieve (Endecotts Ltd., England) (the smallest part of the funnel in RODOS was 2 mm) and subdivided into two samples of approximately 1.5–2.0 g for the analysis with RODOS disperser. This was done in order to get representative results for both small and large granules of the unmilled granule sample which had wide particle size distribution. In consequence, if only GRADIS was used there would have been loss of information about fine particles. Moreover, RODOS can only measure particles up to 3500 µm. Record was made of the mass fractions of the samples for further data analysis. Additionally, the particle size of the three main excipients (MCC, mannitol, DCPA) was analysed by measuring two samples (~1 g) of each material with RODOS disperser.

For the diameter analysis the equivalent projected circle (EQPC Diameter of a Circle of Equal Projection Area) was used as the size descriptor in Qicpic. The EQPC is the diameter (x) of a circle that has the same area as the real particle. Qicpic gives the particle size distribution as a logarithmic density distribution, q3(x) log, as a function of

particle size (x_i). Equations 20-24 were used to calculate the size class limits (x_0) and the fractional volume distribution, p3(x), from the density distribution.

$$r = \frac{x_{0,i+1}}{x_{0,i}} = \frac{x_{i+1}}{x_i} \tag{20}$$

$$x_i = \sqrt{x_{0,i+1} * x_{0,i}} = \sqrt{r * x_{0,i} * x_{0,i}} = x_{0,i} * \sqrt{r} \tag{21}$$

$$x_{0,i} = \frac{x_i}{\sqrt{r}} \tag{22}$$

$$x_{0,i} = \sqrt{x_{i+1} * x_i} = \sqrt{r * x_i * x_i} = x_i * \sqrt{r} \tag{23}$$

$$p3_i = q3_{log}\,(\log x_{0,i+1} - \log x_{0,i}) \tag{24}$$

In the equations r is the geometric ratio, x_i the particle size and x_0 the corresponding size class limits. Equation 22 was used to calculate the lower limit for the first size class. Equation 23 was used to calculate the upper size class limit and the following size classes. Subsequently, Equation 24 was used to calculate the volume distribution. For each batch an average volume distribution and a standard deviation (Eq. 25) of the distribution were calculated. In the Equation 25, x_i represents each value in the sample, $\bar{x}$ is the mean value of the sample and n is the number of the values in the sample.

$$STDV = \sqrt{\frac{\sum_{i=1}^{n}(x_i - \bar{x})^2}{n-1}} \tag{25}$$

For unmilled MCC granules only the results from GRADIS were used because there was no large difference between the particle size distributions measured with RODOS and GRADIS. For mannitol and DCPA granules, the particle size results from RODOS

and GRADIS were combined. In this method it was assumed that particle density was constant across all the sizes i.e. interchangeability of mass and volume fractions.

The Rodos distribution data were used for small particles (e.g. below a cut-off size, x_c, of 364.64 μm). The average p_3 values of the granules measured with RODOS ($p_{3,R}$) that were smaller than the cut-off size were rescaled to take account that only granules smaller than 1.7 mm were measured and not the entire sample volume. This was done by multiplying the p_3 values with the mass fraction (X_R) of the RODOS sample (Eq. 26).

$$p_{3,i,final} = p_{3,i,R} \cdot x_R \qquad x_i < x_c \tag{26}$$

For size fractions larger than x_c, the GRADIS data were used. The GRADIS volume fractions ($p_{3,G}$) were rescaled so that the total volume of the size fractions above x_c was equal to:

$$\sum_{x_c}^{\infty} \hat{p}_{3,i,G} = 1 - \sum_{0}^{x_c} p_{3,i,R} \cdot x_R \tag{27}$$

To achieve this, the GRADIS volume fractions were normalised by their total volume above x_c and multiplied by the factor above, to give Equation 28.

$$p_{3,i,final} = \begin{cases} p_{3,i,R} \cdot x_R & x_i < x_c \\ \dfrac{p_{3,i,G}}{\sum_{x_c}^{\infty} p_{3,i,G}} \left(1 - \sum_{0}^{x_c} p_{3,i,R} \cdot x_R \right) & x_i \geq x_c \end{cases} \tag{28}$$

This ensured that the sum of the p_3 values in the combined PSD was equal to 1 (Eq. 29). Finally, the new p_3 values formed the new particle size distribution.

$$\sum p_{3,i,final} = 1 \tag{29}$$

Additionally, a volume mean diameter (VMD) and a volume specific surface area (SSA) were determined. For milled granules VMD and SSA were calculated as an average from the results attained from Qicpic. For unmilled mannitol and DCPA granules Equations 30 and 31 were used to calculate the average values from the combined RODOS and GRADIS distributions.

$$VMD = D[4,3] = \sum x_i * p_{3,i} \tag{30}$$

$$SSA = \frac{Surface\ of\ all\ particles}{Volume\ of\ all\ particles} = 6 \sum x_i^{(-1)} * p_{3,i} \tag{31}$$

In the Equations 30 and 31, x_i is the particle size and $p_{3,i}$ is the volume fraction of that size class. For unmilled MCC granules VMD was calculated as an average of the results attained from Qicpic and SSA was calculated by using the Equation 31.

Moreover, 10% percentile (q10), 50% percentile (median size or q50) and 90% percentile (q90) of the PSD were determined. For MCC granules and milled mannitol and DCPA granules the values were calculated as an average from the Qicpic results. For unmilled mannitol and DCPA granules Matlab software (The MathWorks, USA) was used to calculate the fractiles. In the current study, particles smaller than 150 µm, were considered as fines and granules over 1400 µm as oversized agglomerates.

8.10.2 Bulk density measurement

Bulk density (ρ) is known as the mass of the material (m) divided by its volume (V) including interparticulate voids (Webb 2001). The Geopyc envelope density analyser (1360, Micromeritics, USA) (Figure 22) was used to measure the bulk density of the milled granules because true porosity could not be measured due to the segregation of the granules and the Dry Flow (Micromeritics, USA), i.e. small spheres with good flowability. Consequently, the granules moved to the surface of the cylinder and caused gaps between the Dry Flow and the granules in the analysis thus resulting in

unreasonable high porosity values. Bulk density was used as an indication of the porosity of the granules as bulk density is directly proportional to true density.

Figure 22. Geopyc density analyser.

The bulk density was measured with the T.A.P (Transverse Axial Pressure) Density option of Geopyc. Geopyc measures the packing volume and calculates the bulk density based on the entered sample weight. In the analysis, the displacement of the piston in an empty chamber is measured first. Next, the piston is inserted into the chamber containing weighed sample of granules. Once the chamber and the piston have been placed in Geopyc the measurement starts. The chamber rotates and agitates and the piston applies a predetermined consolidation force to the sample (Figure 23). The piston displacement is determined several times based on the number of consolidation cycles chosen beforehand. After the analysis Geopyc calculates the difference between the distances ($h = h_0 - h_s$) the piston travels in the empty chamber (h_0) and in the chamber containing the sample (h_s) (Webb 2001). This distance (h) is used to calculate the bulk volume of the sample with Equation 32 for the volume of a cylinder

$$V = \pi r^2 \mathrm{h}, \tag{32}$$

where r is the radius of the chamber. Finally, Geopyc calculates the average bulk density (g/cm^3) of the sample based on the sample volume, the prefilled sample weight and the number of consolidation cycles.

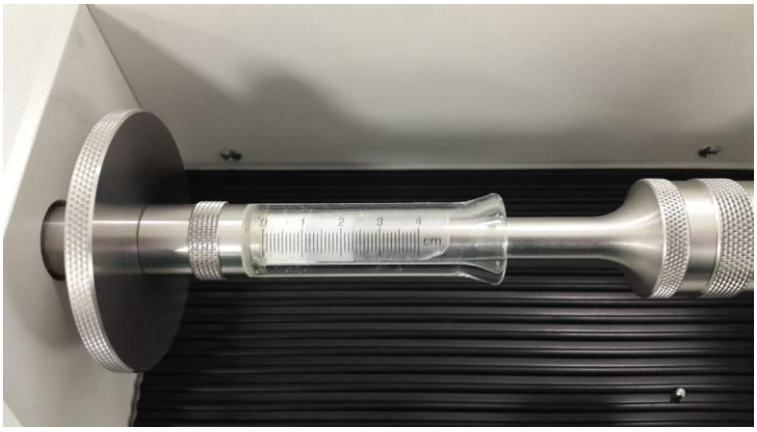

Figure 23. Consolidation of the sample in the density tester.

Size class of 1.00-1.18 mm was chosen for the measurement of bulk density. Chamber diameter was 12.7 mm and consolidation force 4 N. Two to three samples were analysed for each granulation batch and the Geopyc measured three consolidation cycles for each sample. Sample amount was approximately 1.0-1.5 cm of granules measured in the chamber. Record was made of the sample weight and entered in the Geopyc. Average bulk density was calculated for each granulation batch.

8.10.3 SEM imaging

SEM Tabletop Microscope (TM-1000, Hitachi High-Technologies Corporation, Japan) was used to take images of the milled granule batches (MCC_PVP_wet_4 and 8, MCC_HPC_dry_4 and 8, MCC_PVP_dry_4_rep, mannitol_PVP_wet_4 and 8). Scanning electron micrographs were taken in order to get information about the morphology of the granules including alignment of the particles and porosity of the granules.

The SEM (Scanning Electron Microscope) has a column that consists of electron source, number of condenser lenses and openings, scan coils and an objective lens (Gignac and Wells 2012). The sample is placed in a chamber and the chamber and the column are evacuated with vacuum pumps. A pre-centered cartridge filament is used as the electron source and the condenser lenses focus the beam of electrons. The beam is

controlled with two scanning coils that enable the scanning of the sample surface through the objective lens. As the beam interacts with the sample, backscattered electrons (BSE) are formed and collected by a BSE semiconductor detector to form an image.

Quorum (Q150R S, Quorum Technologies Ltd., England), a rotary-pumped sputter coater, was used to coat the samples twice with a gold film of 10 nm before imaging. The gold-coating prevents image distortion and thus optimizes the image quality. Magnifications of 100x, 300x and 500x were used and two to five images were taken with each magnification.

8.10.4 Tablet dimensions and strength

The diametric compression test (Figure 24) was used to measure the breaking force of a tablet and the tensile strength was calculated using the Equation 1 (Chapter 3.2).

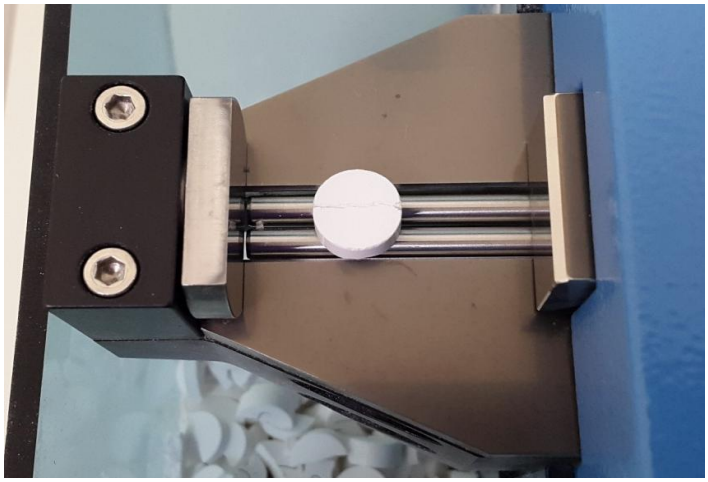

Figure 24. Mannitol_PVP tablet after compression test.

The tablets were allowed to stand for at least 48 hours after compaction before any analysis. Three to four tablets for each force were weighed and their dimensions (diameter and thickness) measured (Absolut Digimatic Caliper, Mitutoyo Ltd., England) before measuring the strength of the tablets (Sotax Hardness Tester HT1, Sotax, Switzerland). The mass and dimensions were used to calculate the tablet porosity as explained in Chapter 8.11.

8.11 Data analysis

The tabletability, compactability and compressibility curves were produced from the collected data. For the graphs, the punch pressure (MPa) was calculated by using the Equation 33

$$p = \frac{F}{A}, \tag{33}$$

where F is the average compression force (N) calculated from upper and lower punch pressures and A is the punch area (mm^2) of a 10 mm round punch. The tablet porosity (%) was calculated with Equation 34.

$$Porosity = 1 - \frac{\rho_{envelope}}{\rho_{true}} * 100 \tag{34}$$

The envelope density ($\rho_{envelope}$) was calculated from the mass (g) of the tablet and the tablet volume (mm^3) with Equation 35

$$\rho_{envelope} = \frac{m}{V} = \frac{m}{\pi r^2 * t}, \tag{35}$$

where r and t are the radius and the thickness of the tablet. The true density (ρ_{true}) was determined by using the mass fractions and the true densities of the materials in the tablet shown in Table 13 (Rowe et al. 2012).

Table 13. True density of the materials.

Material	True density (g/cm^3)
MCC (94%)	1.55
Mannitol (94%)	1.49
DCPA (94%)	2.89
PVP (5%)	1.18
HPC (5%)	1.22
MgSt (1%)	1.09

The difference between the tensile strengths of the DC and granulated tablets at zero porosity, T0g-T0dc, represents the improvement (+) or loss (-) in the compactability after granulation compared with the direct compacted tablets. For the calculation of T0g-T0dc, the tensile strength of both DC (T0dc) and granulated (T0g) tablets at zero porosity was determined. This was done by solving the intercept of the y-axis of the compactability graph (ln TS vs. porosity) with the intercept function in Excel.

Additionally, tablet tensile strength at 12% (MCC and mannitol) and 25% (DCPA) porosity and at 200 MPa pressure were determined. For MCC this was done by using the Equations 36 and 37

$$T = T_{max} * (1 - e^{-bP}) \tag{36}$$

$$T = T_0 e^{-k_b \varepsilon}, \tag{37}$$

where ε is the porosity of the tablet, P is the punch pressure (200 MPa) and k_b is an exponent parameter that is solved as the slope of the tabletability (TS vs. punch pressure) curve. T_{max}, the maximum tensile strength of a tablet, and b, a material-specific exponent parameter, were solved as explained in Chapter 5.1.

The Equation 37 was used to calculate the tensile strength at specific porosity for DCPA and mannitol as well. The tablet strength at 200 MPa punch pressure was determined by using the compressibility (ln punch pressure vs. porosity) and compactability models because the fit of the tabletability curve to the experimental data was not precise. The Equation 38 was used to get tablet porosity from specific punch pressure (200 MPa). Subsequently, the Equation 37 was used to obtain tablet tensile strength from the calculated porosity.

$$\varepsilon = \frac{ln\, P - ln\, P_0}{(-K)} \tag{38}$$

In the Equation 38 P_0 is the pressure at zero porosity determined from the compressibility graph the same way as T_0. K is an exponent parameter determined as the slope of the same compressibility curve.

Substantial part of the data analysis consisted of fitting the loss in compressibility models to the produced data. Additionally, P_{WG} and T_{WG} of MCC and DCPA batches were determined as demonstrated in Chapter 5.2. For the calculation of εWG data for MCC and DCPA the Equation 13 (Chapter 5.4) was modified for wet granulation to be applicable in the current study to yield Equation 39 where ε_{WG} is the porosity of the granules produced by wet granulation.

$$T = T_0 e^{-k_b \varepsilon_T} - T_0 e^{-k_b \varepsilon_{WG}} \quad (39)$$

The Equation 12 was used to fit to DC data. T_0 was determined with the intercept function in Excel as explained earlier. The bonding capacity (k_b) was solved as the slope of the compactability curve. Equation 39 was fitted to wet granulation data by using the "goal-seek" function and LSES by varying ε_{WG}. T_0 and k_b were attained from the fitting of the DC data and were kept constant for each formulation. Furthermore, the average torque for each batch was calculated from the real time data collected by ConsiGma1 during granulation.

The effects of process parameters on the responses mentioned above together with bulk density, VMD and SSA were analysed with regression analysis using Design Expert 9 software (Stat-ease, Inc., USA). The objective was to find statistically significant ($p<0.05$) variables that have an impact on the responses and to understand how these variables affect.

9. RESULTS AND DISCUSSION

The main results of the granule and tablet characterisations are gathered in APPENDIX 7. The corresponding values for powders are represented in APPENDIX 8. Additionally, the results from the regression analysis conducted with Design Expert are represented in APPENDIX 9. The values in the APPENDIX 9 represent the p-values of the factors. The symbols AC, AB and BC indicate the interactions of the individual process parameters. Table 14 shows the abbreviations and levels of the process parameters used in the regression analysis.

Table 14. Abbreviations of the process parameters and their levels in regression analysis.

Abbreviation	Factor	Minimum	Maximum
A - Binder	Binder type	PVP	HPC
B - BinAM	Binder addition method	Dry	Wet
C- KE	Number of kneading elements	4	8

9.1 Results of the experimental conditions

APPENDIX 10 shows the temperature of the granulation liquid before granulation. The difference in the temperature of PVP binder solution between the batches was 0.3ºC at the highest for each material so the temperature did not probably have any influence on the viscosity of the PVP binder solutions as the viscosity of 10% PVP solution is hardly affected by temperature (Bühler 2008). Additionally, the difference in the temperature of HPC binder solutions varied between 0.1-0.6ºC for each material. The viscosity of a HPC solution is known to decrease as temperature is increased, typically by about 50% for every 15.0ºC rise (Ashland Inc 29.7.2016). Thus, the maximum variation of 0.6ºC could have made only a 2% change in the viscosity that probably did not influence the results significantly. APPENDIX 11 represents the results of the moisture analysis of the granules after drying and of the powder and granules after conditioning before tablets were compressed.

9.2 Results from the analysis of MCC

9.2.1 Torque of MCC granulation

The results of average torque of the granulation of MCC are shown in Figure 25 and APPENDIX 7. Based on the regression analysis all the variables had a significant effect on torque. The torque was higher with HPC, eight kneading elements and the wet addition of binder. There was also an interaction between the binder type and the number of kneading elements so that the difference in torque between four and eight kneading elements was clearer with HPC (dry/HPC: 2.77 Nm, wet/HPC: 3.11 Nm) compared with PVP (dry/PVP: 2.16 Nm, wet/PVP: 1.62 Nm) and the difference in torque between the binder types was clearer with eight kneading elements (dry/8ke: 1.35 Nm, wet/8ke: 1.95 Nm) compared with four kneading elements (dry/4ke: 0.74 Nm, wet/4ke: 0.45 Nm). Higher torque with eight kneading elements was expected as a longer kneading section is known to resist the powder flow more than a shorter one causing higher friction thus resulting in higher power needed to rotate the screws that is converted into torque (Dhenge et al. 2011; 2012b; Vercruysse et al. 2012).

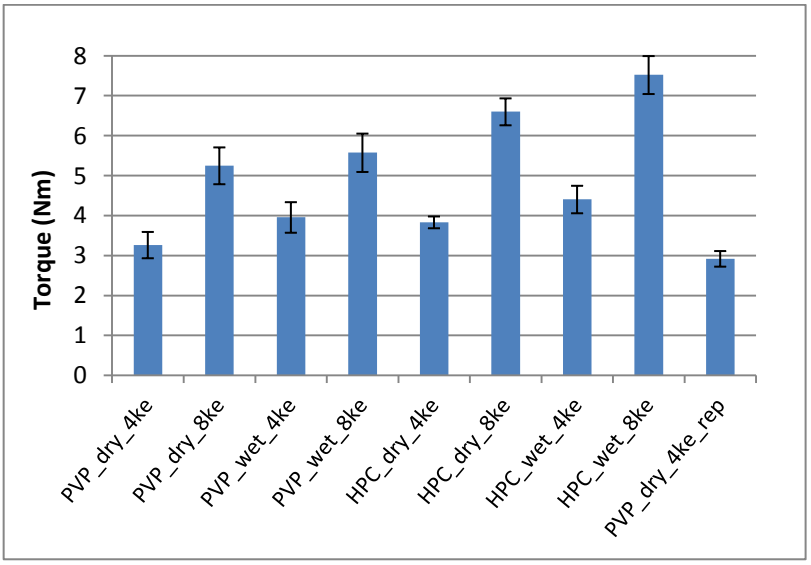

Figure 25. Torque of MCC granulation with standard deviations.

Higher torque with wet addition was believed to result from the higher viscosity of the binder solution (10% HPC Klucel EXF 300-600 mPas at 25ºC, 10% PVP Kollidone K28/32 5.5-8.5 mPas at 20ºC, (Rowe et al. 2012)) compared to water (0.9 mPas at 25ºC (Rowe et al. 2012)) which caused stronger liquid bridges and higher wet mass rheology of the material inside the barrel thus restricting the flow of the powder resulting in higher torque as the motor had to put more work into the process to rotate the screws (Dhenge et al. 2012b). The model of the regression analysis had a good fit to the data based on the R^2 value ($R^2 = 0.99$), which is the coefficient of determination. From Q^2, i.e. quality factor, it could be seen that the model was reliable as it predicted the data well ($Q^2 = 0.95$). The number of kneading elements had the strongest effect on torque followed by the binder type and binder addition method, respectively. This could be seen from the p-values of the variables presented in APPENDIX 9.

9.2.2 Bulk density of MCC granules

The significant variable having an effect on the bulk density of MCC was the number of kneading elements. Eight kneading elements resulted in higher bulk density and thus less porous granules than four kneading elements (Figure 26). This was expected as higher number of kneading elements is thought to produce more shear forces and compaction than a shorter kneading section resulting in denser granules. The results found here were in line with earlier studies (Djuric and Kleinebudde 2008; Vercruysse et al. 2012). Moreover, the torque results presented in the previous chapter support the bulk density results as eight kneading elements resulted in higher torque, which is an indication of the extent of the shear and compaction forces the material experiences during granulation (Dhenge et al. 2011; 2012b). The regression model had a good fit and predictability based on the R^2 and Q^2 values ($R^2 = 0.95$, $Q^2 = 0.92$).

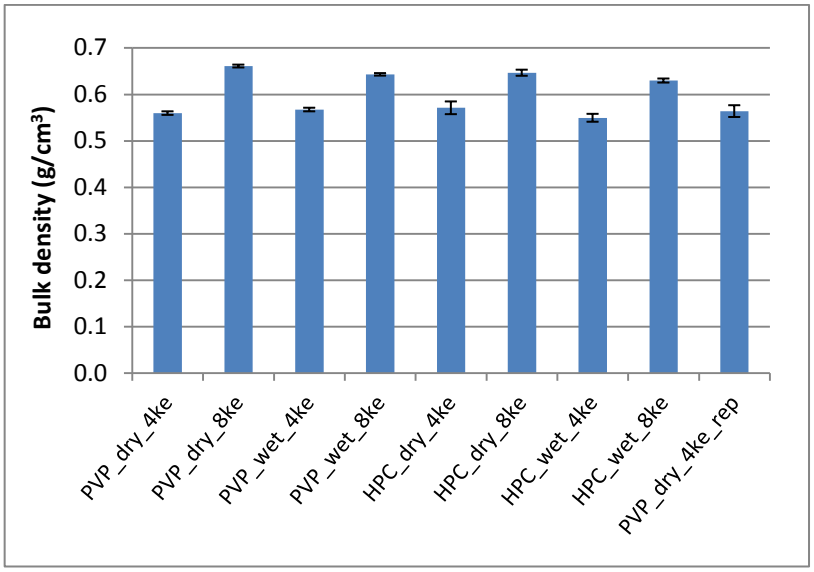

Figure 26. Bulk density of milled MCC granules with standard deviations.

9.2.3 Particle size distribution of MCC

Figures 27 and 28 represent the particle size distributions of powder and unmilled and milled MCC granules. From the mono-modal distributions of unmilled granules it could be seen that almost all of the powder had been granulated as there were not much primary particles left and large granules had been created. This was probably due to the high water level (L/S of 1.1) as high L/S ratios are known to increase the amount and size of the granules compared with smaller L/S ratios and in some cases result in mono-modal distribution (Keleb et al. 2004b; Dhenge et al. 2010; 2012a; 2012b; El Hagrasy et al. 2013; Yu et al. 2014; Vercruysse et al. 2015). The distributions of milled granules show that the large granules broke down creating fine particles when milled resulting in granule sizes that were more suitable for tableting (<1000 µm) compared with the unmilled granules. Relative standard deviation was 25% at the highest for milled MCC granules below 500 µm and 173% at worst for the largest particle size (1727 µm) above 500 µm. Large standard deviation was expected for the coarse MCC granules.

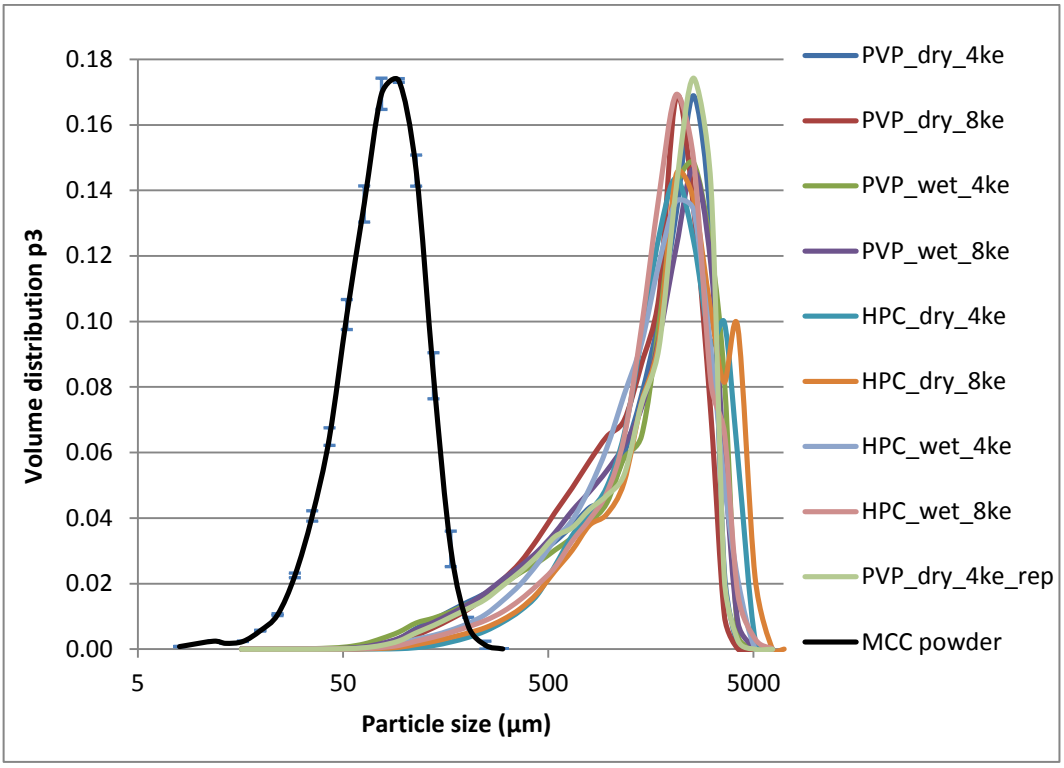

Figure 27. Average particle size distribution of unmilled MCC granules (n = 2) and powder (n = 2).

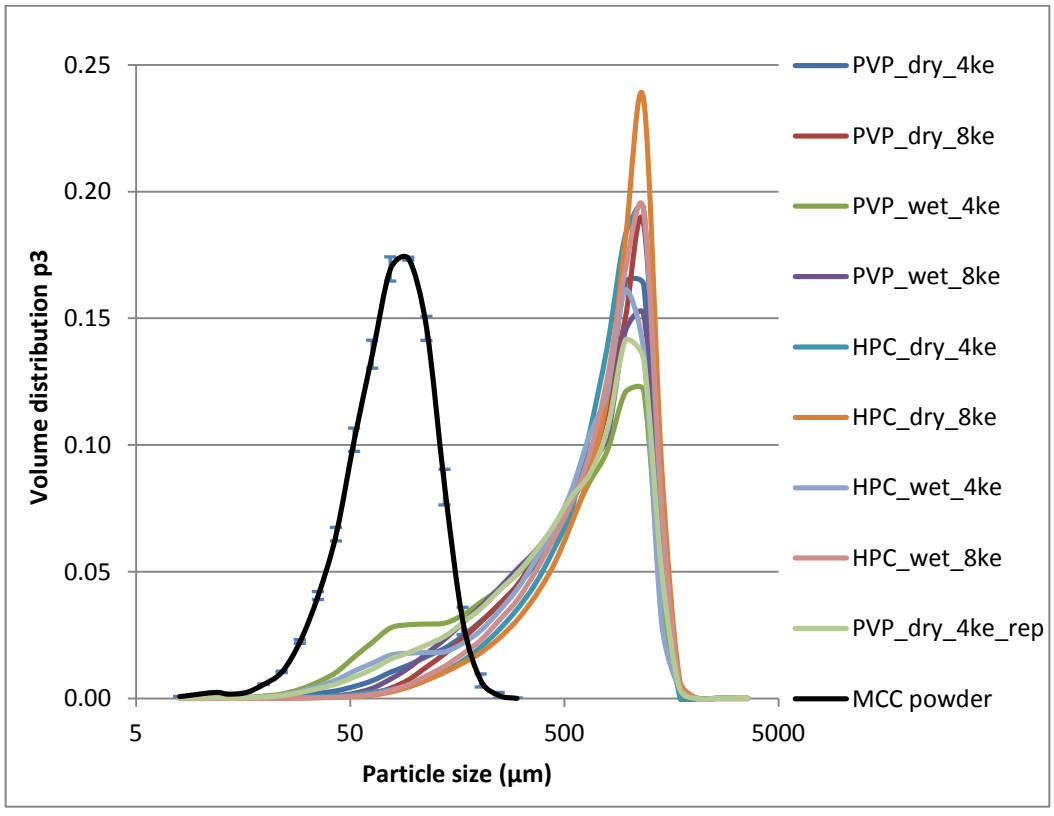

Figure 28. Average particle size distribution of milled MCC granules (n = 3) and powder (n = 2).

The particle size distributions and VMD results of the milled granules and MCC powder proved that the granules remained much larger than the powder particles even after milling (APPENDIX 7 and 8). The SSA results were expected based on the VMD and particle size distribution results. The SSAs of milled granules were much larger than those of the unmilled granules but smaller than the SSA of the MCC powder. Additionally, the 10%, 50% and 90% percentiles supported the observations discussed above. Relative standard deviation of q10, q50 and q90 of the milled MCC granules was 13% at the highest probably because the granules were coarse. Relative standard deviation of q10, q50 and q90 of MCC powder was only 3.5% at the highest.

Based on the regression analysis the binder type had an impact on VMD of the unmilled granules. HPC resulted in larger granules probably due to higher toughness and better binding properties compared with PVP hence resulting in increased growth and stronger granules i.e. higher dynamic yield stress (Krycer et al. 1983; Reading and Spring 1984; Iveson and Litster 1998; Joneja et al. 1999; Iveson et al. 2001; Stoyanov et al. 2014a). Moreover, the strong particle bonds resisted the breakage of the granules in the granulator leading to decreased breakage rates. Additionally, the results were supported by the torque results as the higher torque with HPC could be considered as an indication of higher extent of compaction during granulation leading to increased liquid pore saturation and thus enhanced growth through coalescence or layering (Ennis and Litster 1997; Iveson et al. 2001; Ennis 2010; Dhenge et al. 2011; 2012b).

Furthermore, the binder type had significant interactions with both the binder addition method and the number of kneading elements. Thereby, HPC resulted in larger VMD when dry addition was used. With wet addition, the difference in VMD between the binder types was not significant as the confidence intervals overlapped. The confidence interval range symbols indicate the result of least significant difference (LSD) calculations performed at the 95 percent confidence level. Additionally, when HPC was used dry addition produced larger granules with higher VMD. Again, the difference in VMD between dry and wet addition was not significant with PVP.

The observation that HPC resulted in smaller granules with wet binder addition was not expected as in earlier studies the stickiness of the more viscous granulation liquid had led into larger granules due to stronger liquid bonds and a longer residence time caused by the higher wet mass rheology (Dhenge et al. 2012b; Yu et al. 2014; Saleh et al. 2015). Probably, here the wet addition of HPC produced smaller granules because the higher viscosity of HPC binder solution led to decreased liquid penetration and distribution thus resulting in limited growth of the granules compared with water (Ennis and Litster 1997; Hapgood et al. 2002; Ennis 2010). This was in line with the observations by Dhenge et al. (2013) who noticed that granule size decreased when the binder viscosity increased. However, the limited liquid distribution was attributed to the low shear forces of the granulation due to screw design containing conveying screws only. On the other hand, the effect of 60º forward kneading elements is noticed to be similar to conveying elements (Djuric and Kleinebudde 2008). Moreover, it is possible that MCC is more able to absorb water and swell when using water as the granulation liquid. Additionally, surface tension of water was higher than that of HPC binder solution (10% HPC 45.8 mN/m at 20ºC, water 72.0 mN/m at 25ºC (Rowe et al. 2012)) thus it had higher adhesion tension and better wettability of the powder resulting in enhanced granule growth compared with binder solution (Ennis and Litster 1997; Hapgood et al. 2002; Ennis 2010).

The lack of impact of the binder addition method when PVP was used may have resulted because the difference in viscosity between water and the PVP binder solution was not as large as between HPC and water. This result was in agreement with the finding by Keleb et al. (2002), who did not detect significant differences in granule size between the wet and dry addition of PVP binder. Based on R^2 and Q^2 values the regression model had a good fit and predictability (R^2 = 0.97, Q^2 = 0.71, pure error of 1252.1).

Based on the regression analysis the SSA of unmilled MCC granules was affected by the binder type and addition method. PVP led to higher SSA compared with HPC as well as wet addition compared to dry addition. This was supported by the VMD results presented previously as HPC and dry addition resulted in larger VMD and here in

smaller SSA. The reasons behind these results are the same as discussed in the previous chapter. The binder type had a stronger effect on SSA compared with the binder addition method based on the p-values shown in APPENDIX 9. As with VMD the regression model of SSA was reliable and fitted the data well ($R^2 = 0.94$, $Q^2 = 0.87$).

As with unmilled granules the VMD ($R^2 = 0.93$, $Q^2 = 0.79$, pure error of 1492.0) and SSA ($R^2 = 0.93$, $Q^2 = 0.74$) results of milled MCC granules were analysed. It was found that all the variables had significant effect on both of the responses. HPC, dry addition and eight kneading elements produced larger granules and higher VMD compared with PVP, wet addition and four kneading elements, respectively. HPC produced larger granules than PVP probably due to greater toughness as discussed with VMD results of unmilled granules (Krycer et al. 1983; Reading and Spring 1984; Joneja et al. 1999; Stoyanov et al. 2014a). The production of larger granules with the dry addition of the binder contradicts the study by El Hagrasy et al. (2013), who noticed that wet addition increased the mean particle size of the granules due to better solubilization of the binder. In the current study, the water used in dry addition had lower viscosity and higher surface tension compared with the binder solutions (10% HPC 45.8 mN/m at 20ºC, 10% PVP ~53.6 mN/m, water 72.0 mN/m at 25ºC). This was believed to enable better liquid penetration and distribution resulting in enhanced coalescence and layering of the granules with fine powder producing larger granules (Ennis and Litster 1997; Hapgood et al. 2002; Ennis 2010; Rowe et al. 2012).

Furthermore, the distribution of granulation liquid increased with a longer kneading section leading to larger granules. This was in line with earlier studies (Vercruysse et al. 2012; El Hagrasy and Litster 2013). Additionally, eight kneading elements produced higher forces than four kneading elements based on the torque results thereby causing higher extent of compaction and consolidation resulting in higher pore saturation and increased growth of the granules as with unmilled granules (Ennis and Litster 1997; Iveson et al. 2001; Ennis 2010; Dhenge et al. 2011; 2012b). Overall, the number of kneading elements had the strongest effect on VMD of the milled granules (APPENDIX 9).

PVP resulted in higher SSA of the milled MCC granules than HPC but the difference was not significant as the confidence intervals overlapped. Wet addition produced larger SSA than dry addition but the difference was not significant when eight kneading elements were used. The higher shear forces produced with eight kneading elements probably minimized the effect of the binder addition method which was seen with four kneading elements.

Four kneading elements resulted in higher SSA compared with eight kneading elements but the difference was not significant when dry addition was used (confidence intervals overlapped). A potential reason why the number of kneading elements did not have significant effect on SSA when dry addition was used could have been the good liquid penetration and distribution of water even with four kneading elements due to low viscosity of water. This enabled the coalescence of the granules and layering with fines thus resulting in smaller SSA which evened out the difference between four and eight kneading elements. On the other hand, with wet addition of the binder the difference was more pronounced as the four kneading elements did not produce enough shear forces to distribute the viscous liquid sufficiently thus restricting the coalescence and layering hence resulting in more fines and higher SSA than with eight kneading elements. Based on R^2 and Q^2 values the regression models for VMD and SSA of milled MCC granules had good fits and predictability.

9.3 Results from the analysis of mannitol

9.3.1 Torque of mannitol granulation

The regression analysis showed only one significant variable that had an influence on the torque of mannitol granulation that is the number of kneading elements (Figure 29). The torque was higher with eight kneading elements due to the restricted flow of material as with MCC granulation (Vercruysse et al. 2012). However, the standard deviation was large as seen in Figure 29. Furthermore, the regression model had only an adequate fit and poor predictability ($R^2 = 0.61$, $Q^2 = 0.35$). Thereby, it was uncertain if the number of kneading elements had an actual effect on torque of the granulation.

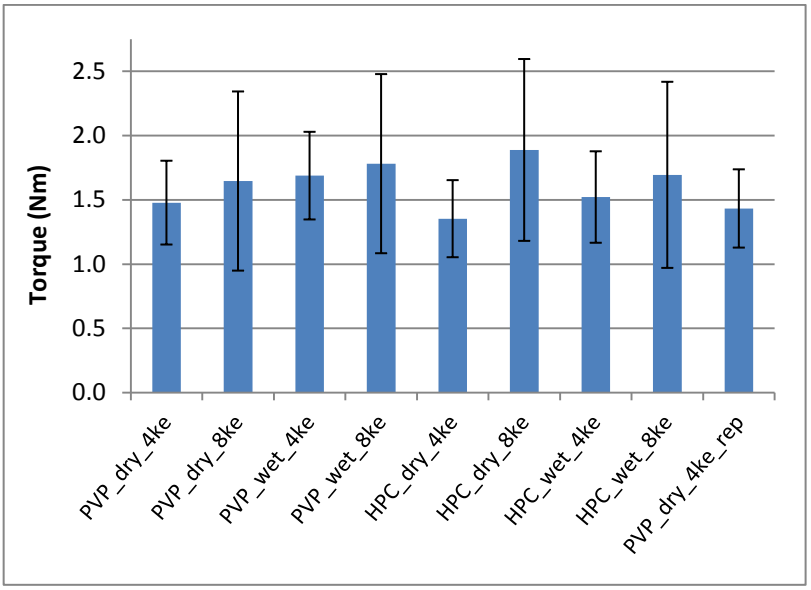

Figure 29. Torque of mannitol granulation with standard deviations.

9.3.2 Bulk density of mannitol granules

The significant factors having an effect on the bulk density of mannitol (Figure 30) were the binder addition method and the interactions of the binder type and the addition method as well as the binder type and the number of kneading elements. The wet addition method gave higher bulk density than dry addition but due to the interaction with the binder type, HPC showed clearer difference between the two binder addition methods compared with PVP (difference; HPC/4ke 0.038 g/cm^3, PVP/4ke 0.019 g/cm^3, HPC/8ke 0.037 g/cm^3, PVP/8ke 0.015 g/cm^3). The formation of denser granules with more viscous binder was in line with published studies (Dhenge et al. 2012a; 2012b). The increased stickiness of the material probably enabled improved binding of the particles producing higher number and strength of the liquid bonds leading to densified granules as the binder viscosity increased. Additionally, higher wet mass rheology resulted in a longer residence time improving liquid distribution and increasing compaction and consolidation leading to densified granules.

Due to the other interaction, eight kneading elements showed higher bulk density when PVP was used and four kneading elements resulted in higher bulk density when HPC was used. This was unexpected as more kneading elements were expected to densify the

granules more. One reason for the phenomenon could have been a different shape distribution of the granules. Hence, even though the size was normalized by measuring density of a particular size class, the granules could have had a different packing effect due to a different shape distribution for example the granules produced with eight kneading elements could have been more elongated and thus resulted in looser packing and in lower bulk density compared with granules produced with four kneading elements. All in all, the regression model was reliable and fitted the data well (R^2 = 0.99, Q^2 = 0.95).

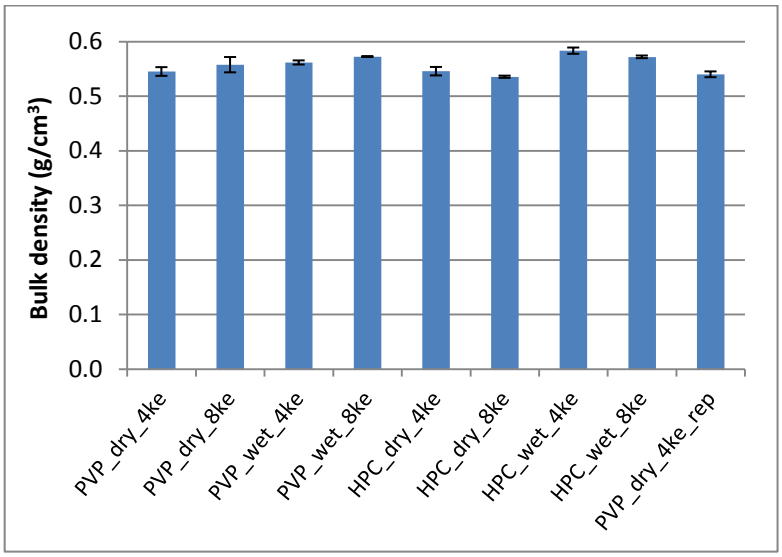

Figure 30. Bulk density of milled mannitol granules with standard deviations.

9.3.3 Particle size distribution of mannitol

Figures 31 and 32 represent the particle size distributions of unmilled and milled mannitol granules and powder. From the bimodal distributions of unmilled granules it could be seen that the powder had been granulated forming some large and some small granules and that there was still some primary particles left. A bimodal particle size distribution is typical for twin screw granulation (Dhenge et al. 2010; 2012b; Lee et al. 2013; Fonteyne et al. 2014; Vercruysse et al. 2015). The distributions of milled granules show that milling broke down some of the large granules creating fine particles. The distributions were still bimodal after milling but the bimodality was not that clear

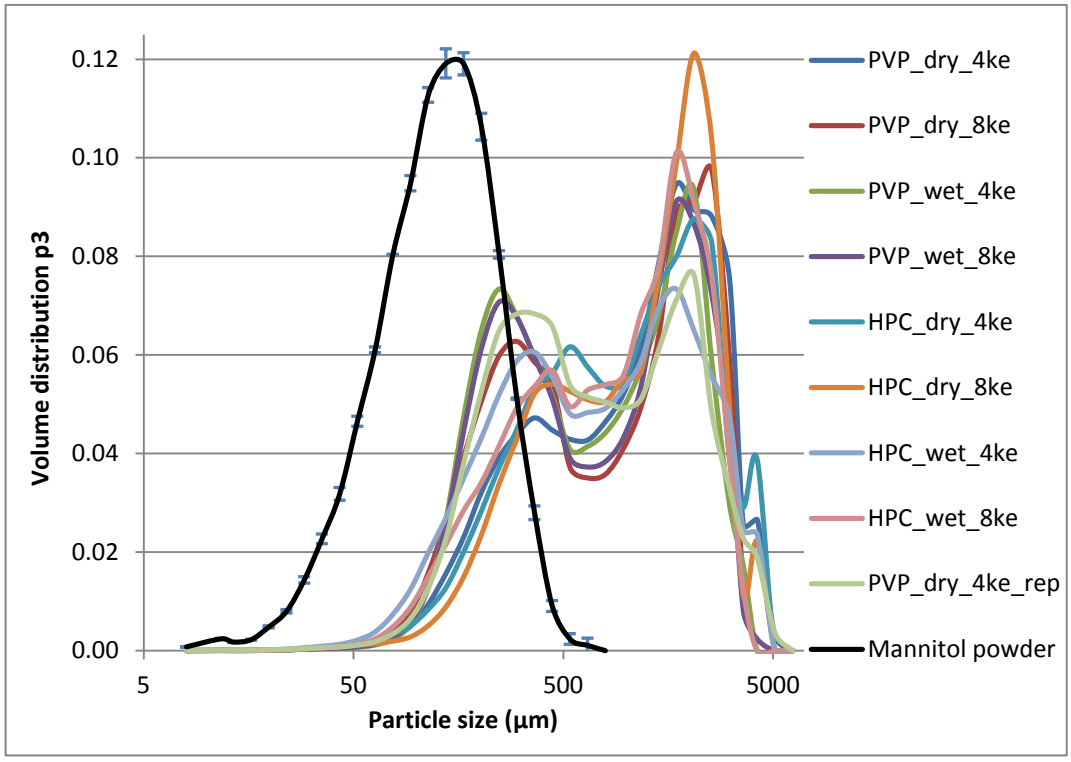

Figure 31. Average particle size distribution of unmilled mannitol granules (n = 2) and powder (n = 2).

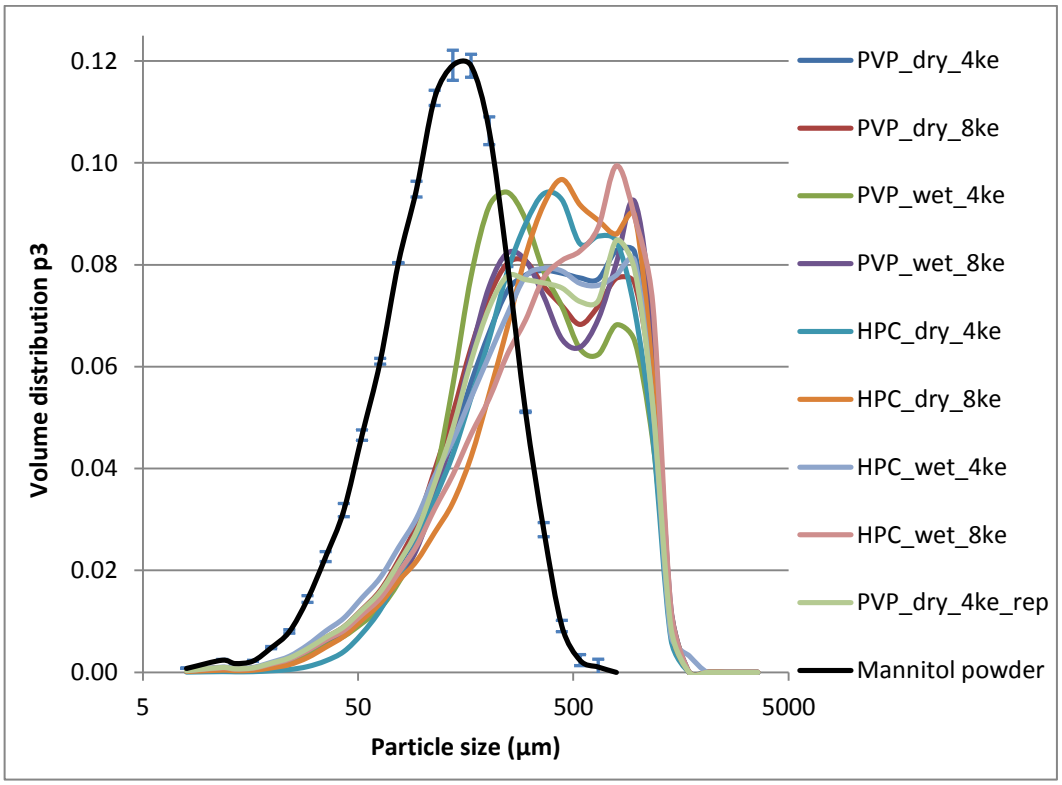

Figure 32. Average particle size distribution of milled mannitol granules (n = 3) and powder (n = 2).

anymore and the two peaks had moved closer to each other. Narrower and more mono-modal particle size distribution is favorable because it reduces the risk of particle segregation during for example tableting and capsule filling and thus enables uniform drug distribution in tablets and capsules (Vercruysse et al. 2015). Relative standard deviation was 11% at the highest for milled mannitol granules below 500 μm and 173% at worst for the largest particle size (1422 μm) above 500 μm. Large standard deviation was expected for the largest particle sizes.

The VMD results of the mannitol powder and unmilled and milled granules showed that the mean particle size of the milled granules was much smaller than that of the unmilled granules but that it remained larger than the mean size of the mannitol powder (APPENDIX 7 and 8). The 10%, 50% and 90% percentiles supported these observations. Relative standard deviation of q10, q50 and q90 of the milled mannitol granules was 7% at the highest. The low relative standard deviation resulted probably from the use of manual and automatic sample divider. Relative standard deviation of q10, q50 and q90 of mannitol powder was only 1.8% at the highest. The SSAs of milled granules were larger than those of the unmilled granules but smaller than the SSA of the mannitol powder. The results were expected based on the VMD and particle size distribution results.

With mannitol the regression models for VMD and SSA of the unmilled and milled granules were not significant (p-values > 0.05) and could not predict the data satisfactorily (small Q^2-value). This was probably due to the large variance in VMD and SSA values of the replicates. Even though the models were not significant the factors having an effect on the size and surface area of the granules are shown below to discuss the results in more detail.

Based on the regression analysis there was one significant factor to affect the VMD of unmilled mannitol granules which was the binder addition method (R^2 = 0.60, Q^2 = 0.24, p = 0.063). The dry addition method showed larger VMD values compared with wet addition contradicting the results by El Hagrasy et al. (2013), as discussed with the milled MCC granules. The observations seen in the current study resulted probably

from the better liquid distribution of water due to lower viscosity and higher surface tension compared with binder solutions (Ennis and Litster 1997; Hapgood et al. 2002; Ennis 2010; Rowe et al. 2012). However, the difference was not significant as the confidence intervals overlapped. Additionally, the pure error was large (53581.4) due to the large variance in VMD values of the replicates. In the case of SSA of the unmilled mannitol granules there were no significant model terms (R^2 = 0.54, Q^2 = 0.02, p = 0.099).

VMD of the milled mannitol granules was influenced by the binder type and the number of kneading elements (R^2 = 0.85, Q^2 = 0.27, pure error of 67.5, p = 0.058). HPC produced larger granules than PVP but the difference was not significant as the confidence intervals overlapped. Eight kneading elements resulted in higher VMD values than four kneading elements probably due to better liquid distribution (Vercruysse et al. 2012; El Hagrasy and Litster 2013). However, the difference was not significant when dry addition was used because the confidence intervals overlapped. The same effect was observed with the SSA values of milled MCC granules and the reason was attributed to the good liquid penetration and distribution of water even with four kneading elements which enabled the enhanced growth of the granules and thus evened out the difference in granule size between four and eight kneading elements. On the other hand, wet addition resulted in more pronounced difference in VMD as the lower shear forces of four kneading elements could not distribute the viscous binder solution properly thus restricting more the granule growth compared with eight kneading elements.

The binder type had a significant impact on SSA of the milled mannitol granules (R^2 = 0.92, Q^2 = 0.05, p = 0.075). Additionally, it had an interaction with the binder addition method (Figure 33). Hence, HPC resulted in smaller SSA than PVP when dry addition was used presumably due to the better binding properties of HPC leading to increased incorporation of fines into granules and production of larger granules during granulation as well as reduced generation of fines during milling due to stronger agglomerates (Krycer et al. 1983; Reading and Spring 1984; Joneja et al. 1999; Stoyanov et al.

2014a). The difference between binder types was not significant when wet addition was used (confidence intervals overlapped).

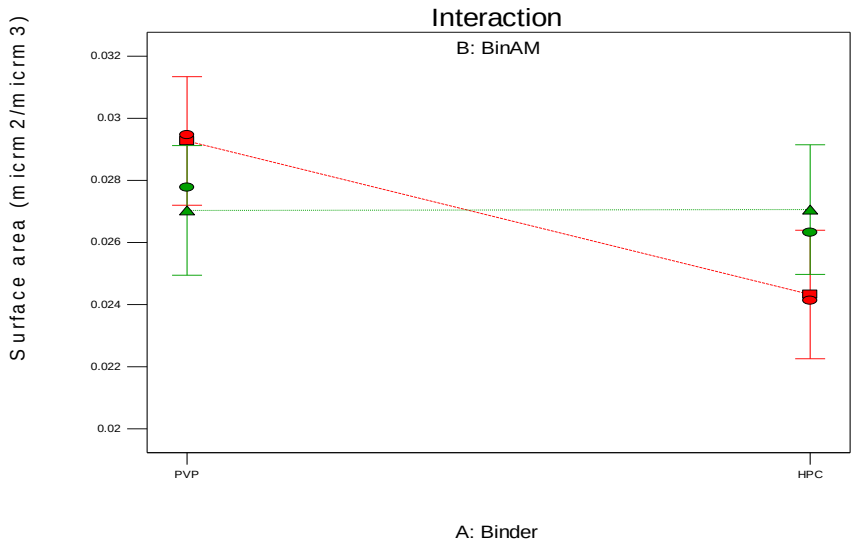

Figure 33. The interaction between the binder type and binder addition method in the regression analysis of the SSA of milled mannitol granules (BinAM=binder addition method, □ = dry binder, Δ = wet binder, 8 kneading elements).

For HPC, the SSA was larger when wet addition was used compared with dry addition. This was probably due to the high viscosity and low surface tension of the binder solution and thus inadequate liquid distribution resulting in restricted growth and more fines compared with the granulation when using water (Ennis and Litster 1997; Hapgood et al. 2002; Ennis 2010; Rowe et al. 2012). The opposite was observed with PVP which showed larger SSA with dry addition compared to wet addition. This was thought to result from the better solubilization of PVP when added to granulation liquid prior to granulation thus increasing the binding efficiency and resulting in increased incorporation of fines into granules compared with the dry addition. This was in line with a study by El Hagrasy et al (2013). Moreover, the viscosity of PVP binder solution was not too high to restrict the liquid distribution substantially.

9.4 Results from the analysis of DCPA

In the regression analysis of DCPA data the run 9 (PVP_wet_4ke) was noticed to act as an outlier in some models. One reason for the observation could be that the blend used for that granulation run was prepared from a different DCPA batch than the other DCPA granulation blends (APPENDIX 2). For this reason, the run 9 was excluded from the regression analysis of ε_{WG}, VMD and SSA of unmilled and milled DCPA granules and the tablet tensile strength results attained at specific porosity and pressure.

9.4.1 Torque of DCPA granulation

Based on the regression analysis the binder type had a significant effect on the torque (Figure 34) of DCPA granulation. PVP gave higher torque than HPC, in contrast to that seen with MCC. However, as with mannitol, the regression model fitted the results only moderately and could not predict as seen from the R^2 and Q^2 values (R^2 = 0.57, Q^2 = 0.33, pure error 0.05). This was probably due to the large variation in the torque values of the replicates. Moreover, the standard deviation was large as seen in Figure 34. Therefore, it was not certain that the binder type had an actual effect on the torque of the DCPA granulation.

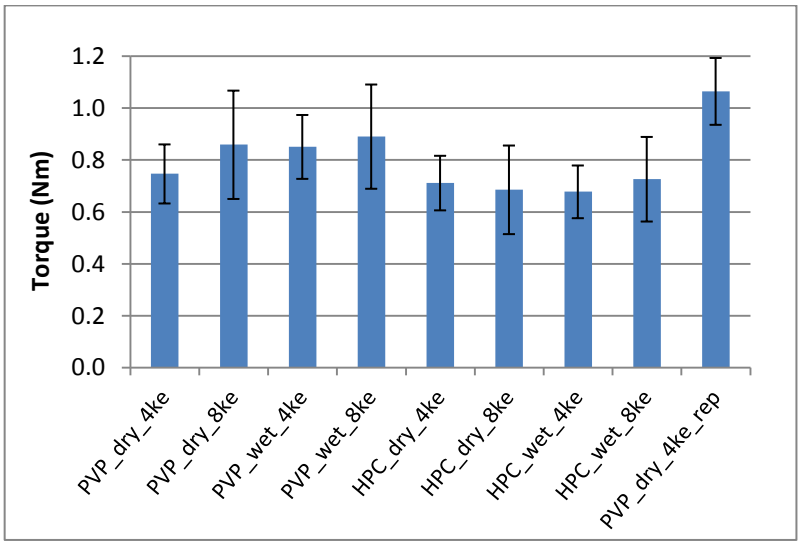

Figure 34. Torque of DCPA granulation with standard deviations.

9.4.2 Bulk density of DCPA granules

The binder type and the number of kneading elements had a significant impact on the bulk density (Figure 35) of DCPA granules based on the regression analysis. The regression model had a good fit and predictability (R^2 = 0.94, Q^2 = 0.87). PVP as well as four kneading elements resulted in higher bulk density compared to HPC and eight kneading elements, respectively. The binder type had a stronger effect on the bulk density than the number of kneading elements based on the p-values of the regression analysis. The higher torque values with PVP discussed in the previous chapter support the results seen here with the bulk density as based on the torque the material experienced more shear and compaction forces with PVP and thus resulted in denser granules (Dhenge et al. 2011; 2012b). The higher bulk density with four kneading elements was not expected as usually a shorter kneading section provides less compaction and thus more porous granules than a longer one which was not the case here (Djuric and Kleinebudde 2008; Vercruysse et al. 2012; Yu et al. 2014).

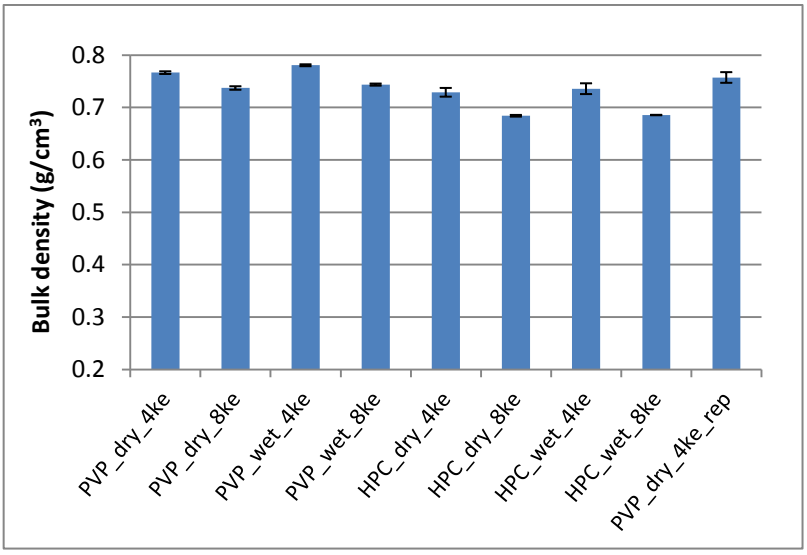

Figure 35. Bulk density of milled DCPA granules with standard deviations.

9.4.3 Particle size distribution of DCPA

Figures 36 and 37 represent the particle size distributions of the DCPA powder and unmilled and milled granules. The distributions of the granules were bimodal both

before and after milling. The distribution of unmilled granules showed that the DCPA powder had been granulated forming both large and small granules. However, some of the primary particles had probably stayed ungranulated. The distributions of milled granules had shifted to the left indicating that granules had broken down during milling and fine particles had formed. Due to the formation of fines the bimodalities of the distributions were more pronounced after milling. Bimodal particle size distribution is typical for twin screw granulation as mentioned earlier (Dhenge et al. 2010; 2012b; Lee et al. 2013; Fonteyne et al. 2014; Vercruysse et al. 2015). Relative standard deviation was 12% at the highest for milled DCPA granules below 500 µm and 173% at worst for the largest particle size (1422 µm) above 500 µm. Large standard deviation was expected for the largest particle sizes. The abrupt end to the particle size distribution of DCPA powder did not indicate an absence of particles below that size but probably was an indication of a detection limit of Qicpic.

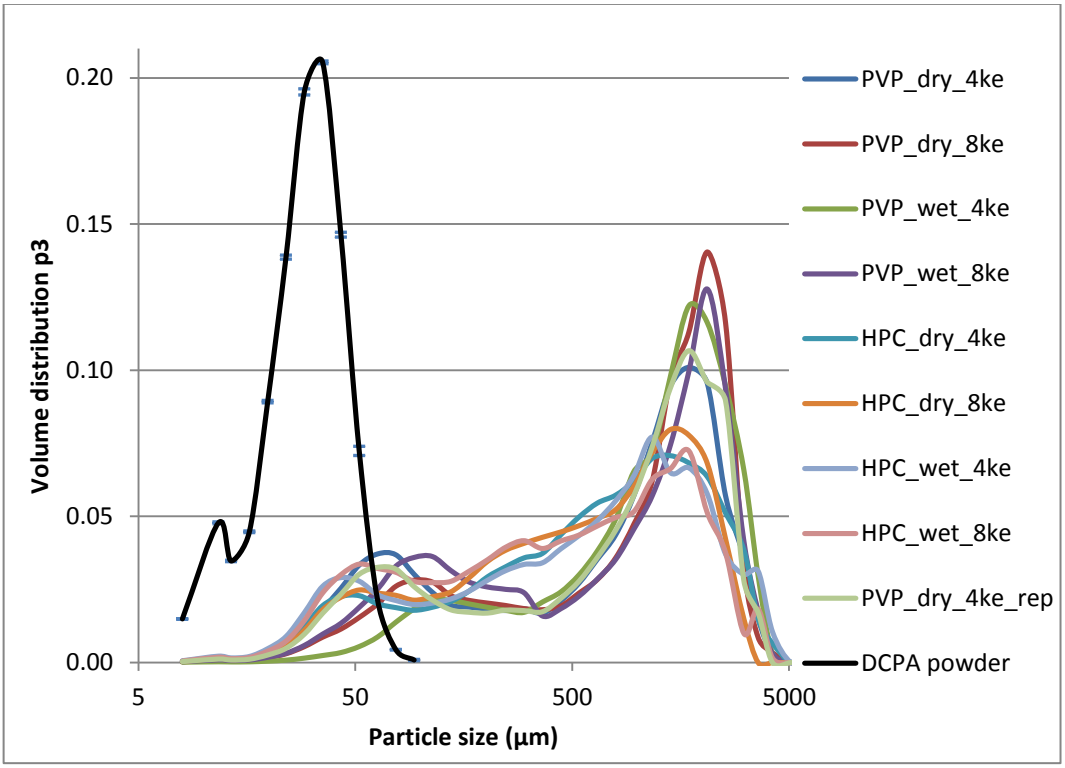

Figure 36. Average particle size distribution of unmilled DCPA granules (n = 2) and powder (n = 2).

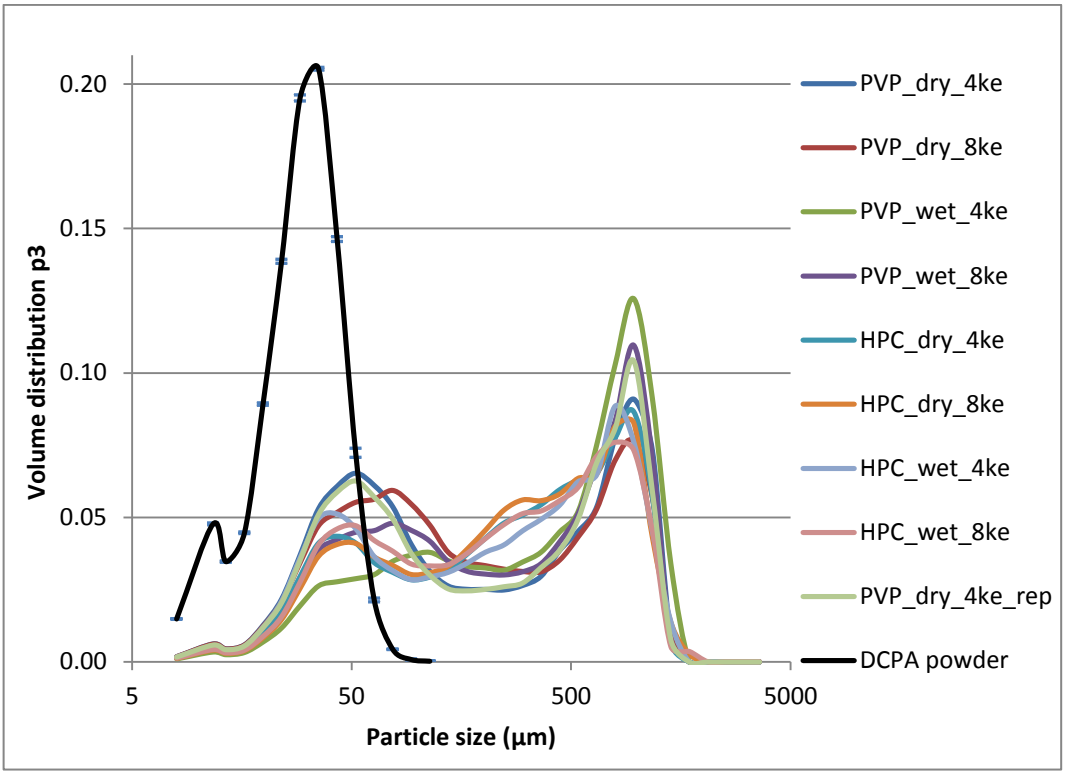

Figure 37. Average particle size distribution of milled DCPA granules (n = 3) and powder (n = 2).

Based on the VMD results of the DCPA powder and unmilled and milled granules the mean particle size of the milled granules was much smaller than that of the unmilled granules (APPENDIX 7 and 8). However, the mean size of the granules remained larger than the mean size of DCPA powder even after milling. The SSA results correlated with the VMD results. The SSAs of milled granules were larger than those of the unmilled granules but smaller than the SSA of the DCPA powder. Additionally, the 10%, 50% and 90% percentiles supported the observations. Relative standard deviation of q10, q50 and q90 of the milled DCPA granules was 14% at the highest, probably due to the elongated and irregular granules. Relative standard deviation of q10, q50 and q90 of DCPA powder was only 0.4% at the highest.

Results from the regression analysis showed that the binder type had an effect on the VMD values of the unmilled DCPA granules. PVP resulted in larger granules but the number of kneading elements had a significant interaction with the binder type thus eight kneading elements showed a bigger difference between the binder types compared

with four kneading elements (Figure 38). The formation of larger granules with PVP was supported by the torque results as PVP resulted in higher torque suggesting that the material had experienced higher shear and compaction forces leading to consolidation and increased liquid pore saturation resulting in enhanced growth (Ennis and Litster 1997; Iveson et al. 2001; Ennis 2010; Dhenge et al. 2011; 2012b).

Furthermore, due to the interaction HPC showed larger VMD with four kneading elements compared with eight kneading elements. This was not expected as usually a longer kneading section provides more compaction and higher pore saturation leading to enhanced growth (Vercruysse et al. 2012; El Hagrasy and Litster 2013). PVP, on the other hand, showed opposite results as eight kneading elements resulted in larger VMD. The regression model fitted the data well and showed good predictability, however the pure error was large probably due to the large variation in the VMD results of the replicates (R^2 = 0.97, Q^2 = 0.87, pure error of 1818.8, aliased terms).

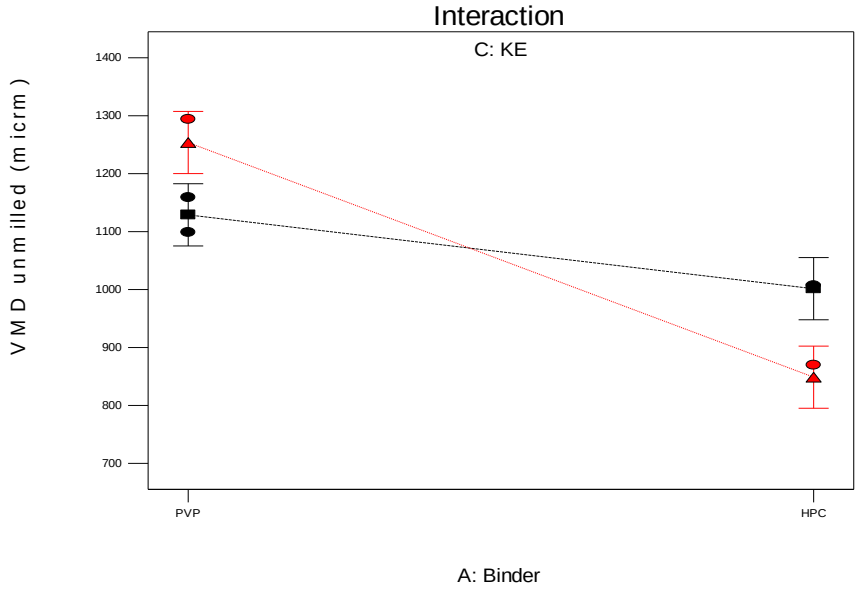

Figure 38. The interaction between the binder type and the number of kneading elements in the regression analysis of the VMD of unmilled DCPA granules (KE=kneading elements, □ = 4 ke, Δ = 8 ke, dry binder).

All the factors had a significant influence on the SSA values of unmilled DCPA granules. The wet addition method resulted in larger SSA probably due to high viscosity

and low surface tension and thus decreased distribution of the liquid as mentioned before (Ennis and Litster 1997; Hapgood et al. 2002; Ennis 2010; Rowe et al. 2012). However, this effect was not seen with PVP/four kneading elements as the difference between the binder addition methods was not significant as the confidence intervals overlapped because the run 9 (PVP_wet_4 ke) was excluded, thus resulting in wider error bars. HPC resulted in higher SSA values than PVP when eight kneading elements were used but there was no significant difference in SSA between the binder types when four kneading elements were used.

On the other hand, four kneading elements showed larger SSA compared with eight kneading elements when PVP was used but again there was no significant difference when HPC was used. These observations were due to an interaction between the binder type and the number of kneading elements. Furthermore, these results were supported by the VMD results discussed earlier as four kneading elements with PVP resulted in smaller VMD and larger SSA than eight kneading elements, and HPC with eight kneading elements resulted in smaller VMD and larger SSA than four kneading elements. However, it was unexpected that HPC resulted in larger SSA because it has better binding properties than PVP (Krycer et al. 1983; Reading and Spring 1984; Joneja et al. 1999; Stoyanov et al. 2014a). Based on the R^2 and Q^2 values the regression model had a good fit and predictability ($R^2 = 0.97$, $Q^2 = 0.79$).

Based on the regression analysis, the binder addition method and the number of kneading elements had an effect on the VMD of the milled DCPA granules. The regression model fitted the data well but it could not be considered significant as the p-value of the model was above 0.05 ($R^2 = 0.98$, Q^2 = N/A, model not significant $p = 0.051$). Moreover, there was no value for Q^2 thus the predictability of the model could not be assessed. Additionally, an interaction between the binder type and addition method was significant (Figure 39). Hence, PVP resulted in higher VMD when wet addition was used presumably resulting from the lower viscosity of the PVP binder solution compared with HPC (Ennis and Litster 1997; Hapgood et al. 2002; Ennis 2010; Rowe et al. 2012). HPC, on the other hand, produced larger granules if dry addition was used probably due to better binding properties of HPC leading to increased growth and

decreased breakage rates compared with PVP (Krycer et al. 1983; Reading and Spring 1984; Joneja et al. 1999; Stoyanov et al. 2014a). However, the difference between PVP and HPC was not significant when four kneading elements were used as the confidence intervals overlapped.

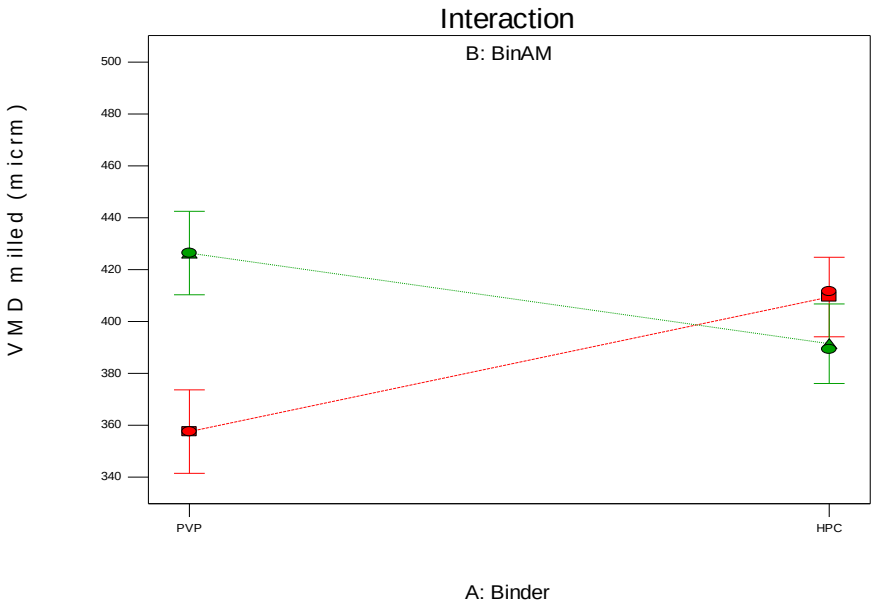

Figure 39. The interaction between the binder type and binder addition method in the regression analysis of the VMD of milled DCPA granules (BinAM=binder addition method, □ = dry binder, Δ = wet binder, 8 kneading elements).

From the Figure 39, it could also be seen that the difference between dry and wet addition was not significant when HPC was used. On the contrary, the binder addition method had a significant effect on VMD when PVP was used. Thus, wet addition produced larger granules compared with dry addition when PVP was used presumably due to better solubilization of PVP as mentioned before (El Hagrasy et al. 2013). It was not expected that the binder addition method would have an effect with PVP and not with HPC even though the difference in viscosity between water and the binder solution was greater with HPC compared with PVP (Rowe et al. 2012). Furthermore, the solubilization of HPC could be assumed to be slower compared with PVP due to the lower hydrophilicity of HPC hence the difference in granule size between the binder addition methods would have been expected to be larger with HPC than with PVP which was not the case here (Stoyanov et al. 2014b). The number of kneading elements

had a significant effect on VMD only when PVP was added as dry powder in the powder blend at that case four kneading elements resulted in larger granules than eight kneading elements.

The binder type and its interaction with the binder addition method had a significant impact on the SSA of milled DCPA granules. Thus, PVP produced larger SSA than HPC when dry addition was used. This was probably due to better binding properties of HPC thus resulting in larger granules and reduced generation of fines during milling leading to smaller SSA compared with PVP (Krycer et al. 1983; Reading and Spring 1984; Joneja et al. 1999; Stoyanov et al. 2014a). There was no significant difference between the binder types with wet addition as confidence intervals overlapped. The dry addition method resulted in higher SSA compared with wet addition when PVP was used. The same effect was seen with milled mannitol granules and was attributed to the reduction in binding efficiency due to the reduced solubilization of PVP compared with wet addition and hence reduced incorporation of fines into granules (El Hagrasy et al. 2013). Additionally, the viscosity of the PVP binder solution did not restrict the liquid distribution significantly and the granule growth and layering was improved despite the slightly higher viscosity compared with water. Wet addition showed larger SSA when HPC was used however the confidence intervals overlapped thus the difference was not significant. Overall, the regression model had a good fit based on R^2 value but the predictability of the model could not be assessed as there was no value for Q^2 (R^2 = 0.91, Q^2 = N/A, aliased terms).

9.5 Compactability and tabletability of the materials and the feasibility of the “loss in compressibility” models

9.5.1 Compactability and tabletability of the materials

Twin screw granulation had an effect on the tabletability and compactability as can be seen from the graphs in Figure 40 and 41. The points in the graphs represent individual tablets. Next the impact of twin screw granulation on the compactability and tabletability of each material will be discussed in more detail.

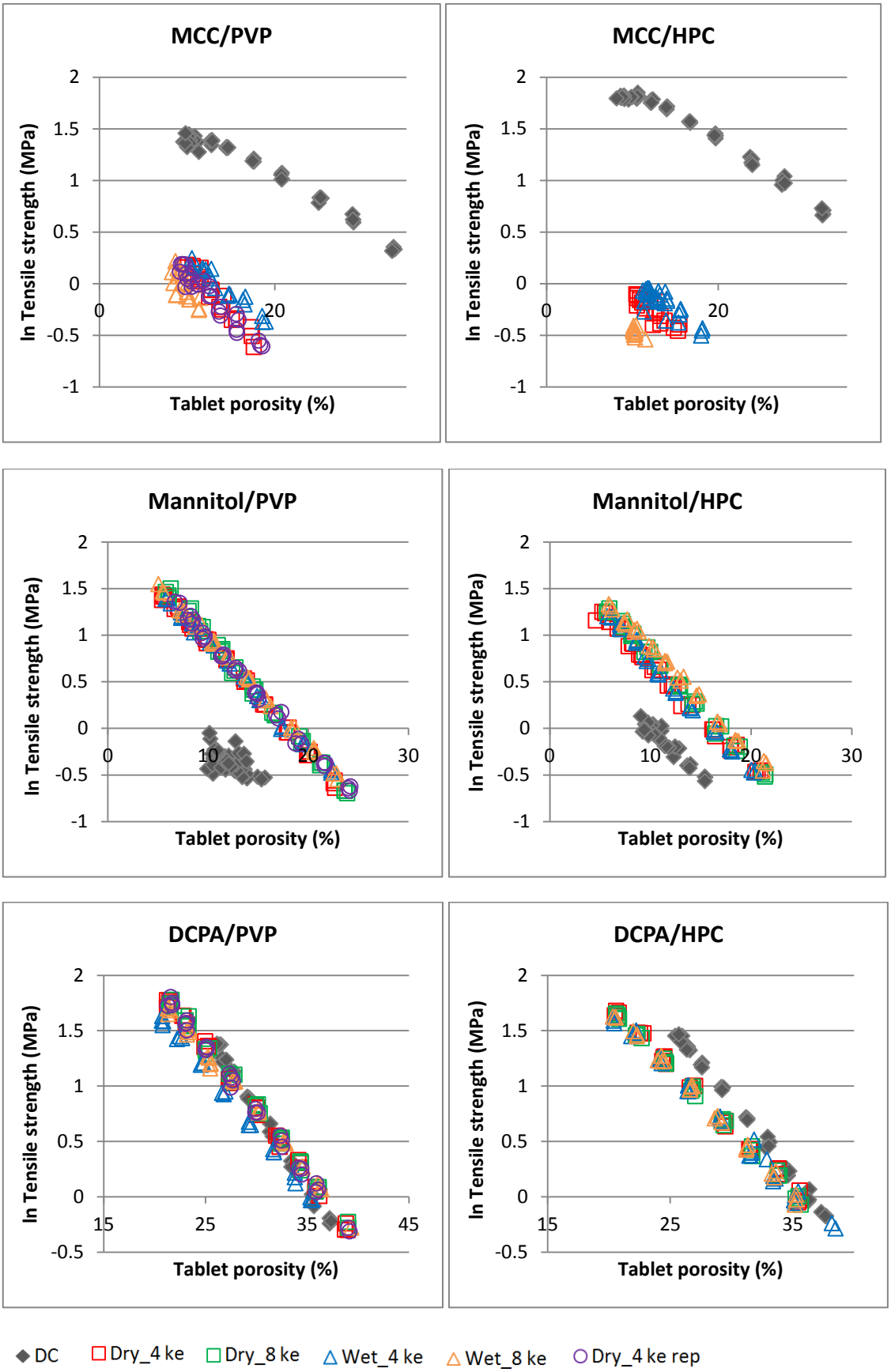

Figure 40. Compactability of the direct compaction blends and granules.

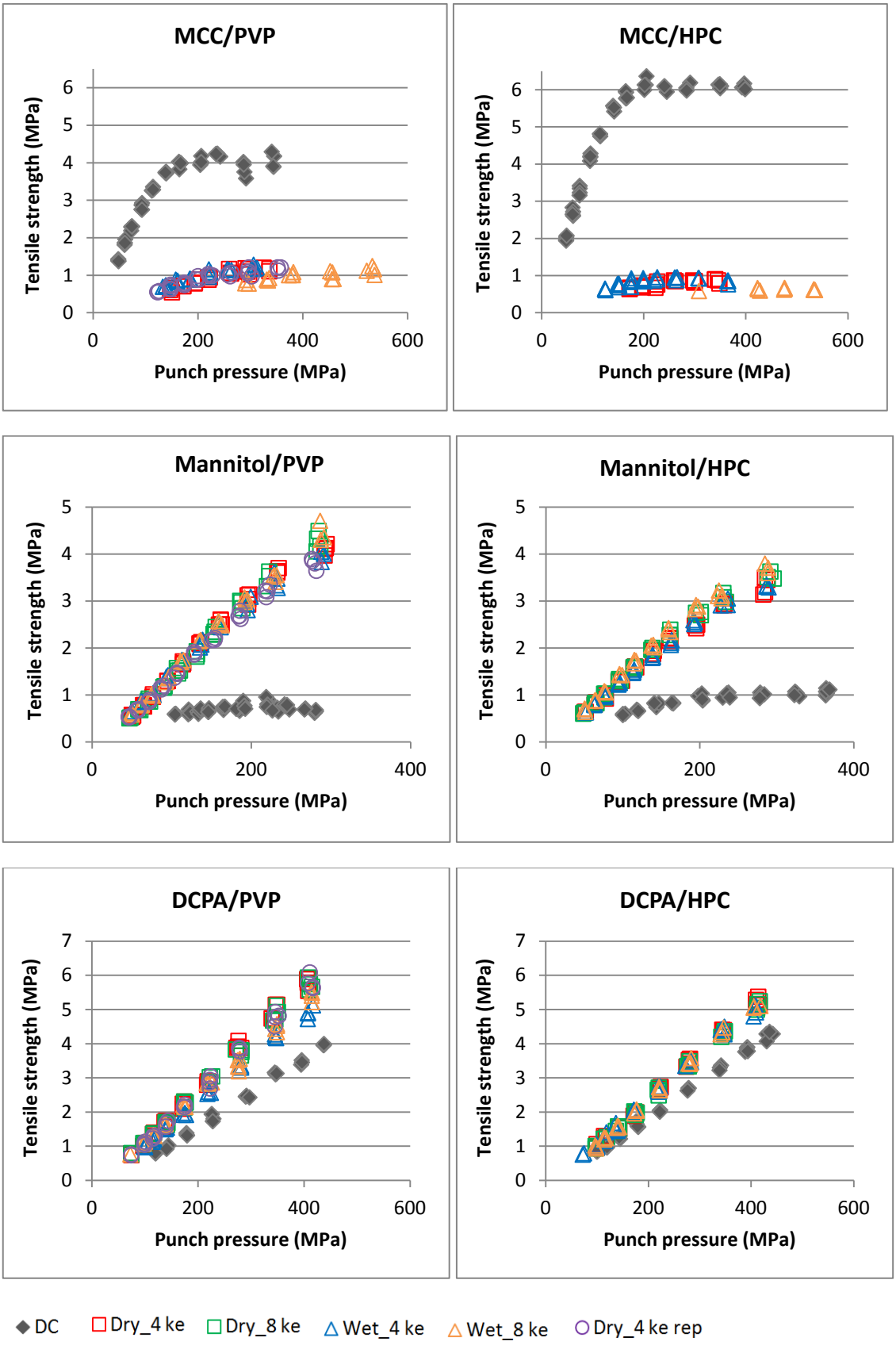

Figure 41. Tabletability of the direct compaction blends and granules.

Figures 40 and 41 demonstrate the clear loss in the compactability and tabletability of MCC after continuous wet granulation. The loss was clear despite dry milling, which can sometimes improve the compatcability of MCC when particle surface area is increased due to a reduction in particle size (Badawy et al. 2006). The change in tensile strength between DC tablets and the tablets made from granules at 12% porosity was approximately 2.90-3.25 MPa for PVP and 5.20-5.43 MPa for HPC. The tensile strength at 200 MPa pressure dropped approximately 3.16-3.48 MPa for PVP and 5.07-5.38 MPa for HPC. The exact tensile strength values are shown in APPENDIX 7. The loss in tabletability and compactability of MCC after wet granulation was in line with other studies (Jayme 1944; Staniforth J. 1988; Millili et al. 1990; Kleinebudde 1997; Westermarck et al. 1999; Shi et al. 2010; 2011a; 2011b; Nguyen et al. 2013).

Based on the tensile strength results of the tablets it seemed that the granules were overgranulated which supported the loss in tabletability and compactability results. Granules are considered overgranulated if the formed tablets do not generate tensile strengths of 2 MPa or higher when compressed with typical compaction pressures (50-400 MPa) (Shi et al. 2010). Shi et al. (2010) proved that the loss in tabletability of MCC was not due to size enlargement as a reduction in tabletability was seen after batch wet granulation before any significant granule growth occurred. The loss in tabletability was attributed to particle rounding and decreased binding surface area. Similar results were observed by Shi et al. (2011b) and Nguyen et al. (2013).

Even though the decrease in binding surface area and mechanical inter-locking due to particle rounding and surface smoothing might have an impact on the loss in compactability and tabletability of MCC, probably more important factor is the “hornification” phenomenon or other network formation, which can be considered as a fundamental property of MCC. It is believed that in the current study MCC experienced the “hornification” effect and thus the amount of hydrogen bonds increased during wet granulation. Subsequently, the formed network shrunk upon drying resulting in densified granules which had reduced deformability compared with ungranulated powder (Jayme 1944; Chatrath 1992; Kleinebudde 1994; Minor 1994). Figure 42 represents a SEM image of MCC granules supporting the theory of a dense granule

structure. The decreased deformability of the granules probably resulted in long separation distance and reduced contact area thus restricting the number and strength of the contact bonds. Thereby, the formed tablets were weaker compared with the direct compacted tablets. The densities of the granules and MCC powder support this theory as the bulk densities of the granules varied around 0.55-0.66 g/cm^3 and the bulk and tapped densities of the powder were 0.32 g/cm^3 and 0.45 g/cm^3, respectively (Rowe et al. 2012).

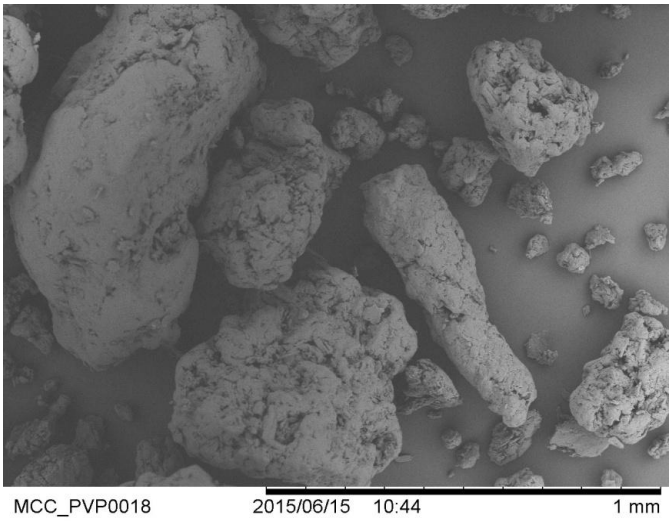

Figure 42. SEM image of milled MCC granules (batch MCC_PVP_wet_8ke, magnification 100X)

Figures 40 and 41 show that the compactability and tabletability of mannitol had improved, after twin screw granulation, compared with ungranulated powder. Especially tabletability improved markedly. The differences in the compactability between powder and the granules at 12% porosity were 1.28-1.41 MPa for PVP and 0.78-1.09 MPa for HPC. The differences were somewhat smaller at higher porosities. The differences in tabletability at 200 MPa were 2.22-2.47 MPa for PVP and 1.69-1.97 MPa for HPC. The difference between DC tablets and the tablets made from granules was even larger at higher compaction pressures.

From the particle size distributions of powder and milled mannitol granules (Figure 32) it could be seen that there were still lot of large mannitol granules left after milling. It was believed that the improvement in the compactability and tabletability of mannitol

was due to the formation of porous granules that had better deformability compared with the hard primary particles thus resulting in stronger tablets due to greater extent and strength of particle bonding. The same phenomenon had been observed before in published studies (Krycer et al. 1982; Juppo et al. 1995; Westermarck et al. 1998). Figure 43 and 44 represent the SEM images of milled mannitol granules. The images demonstrate that the primary particle size and shape had been retained in granulation and that the primary particles had formed granules with internal porosity which supports the theory mentioned previously.

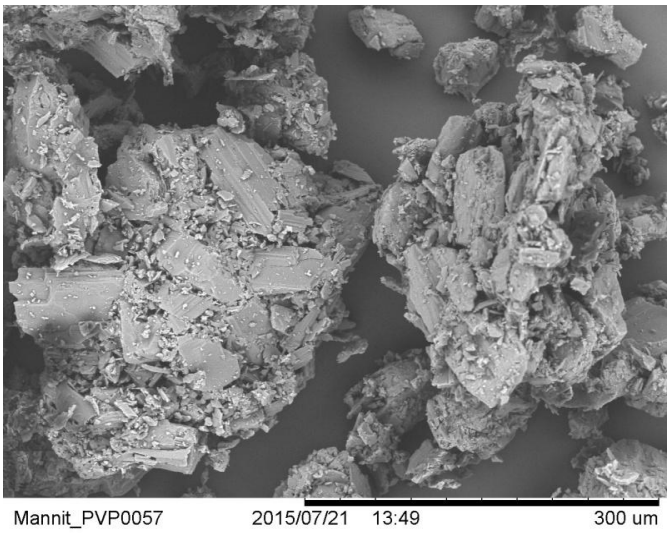

Figure 43. SEM image of milled mannitol granules (batch mannitol_PVP_wet_8 ke, magnification 300X)

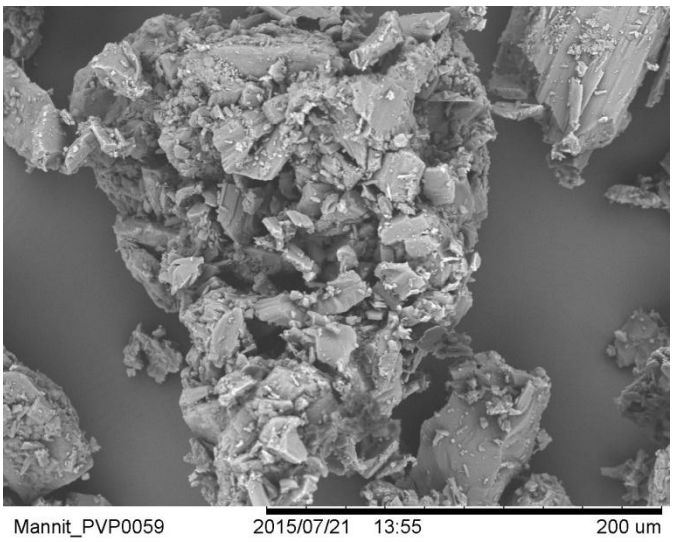

Figure 44. SEM image of milled mannitol granules (batch mannitol_PVP_wet_8 ke, magnification 500X)

The bulk densities of the granules were approximately 0.54-0.58 g/cm^3 (APPENDIX 7). The bulk and tapped densities of the powder were 0.43 g/cm^3 and 0.73 g/cm^3, respectively (Rowe et al. 2012). Due to the characterisation method of the bulk density of the granules with repetitive consolidation cycles with the force of 4 N, the corresponding density of the powder is probably more close to the tapped density than the bulk density. Thus, without having the bulk density of the powder measured with the same method as the granules it could be still concluded that the granules were more porous than the primary particles of the powder which would support the improvement in compactability and tabletability and the theory explained above. Additionally, the compressibility of mannitol granules and powder (Figure 45) supported the theory as the granules had better compressibility (porosity below 15%) and produced denser tablets compared with the powder, when the same compaction pressures were used.

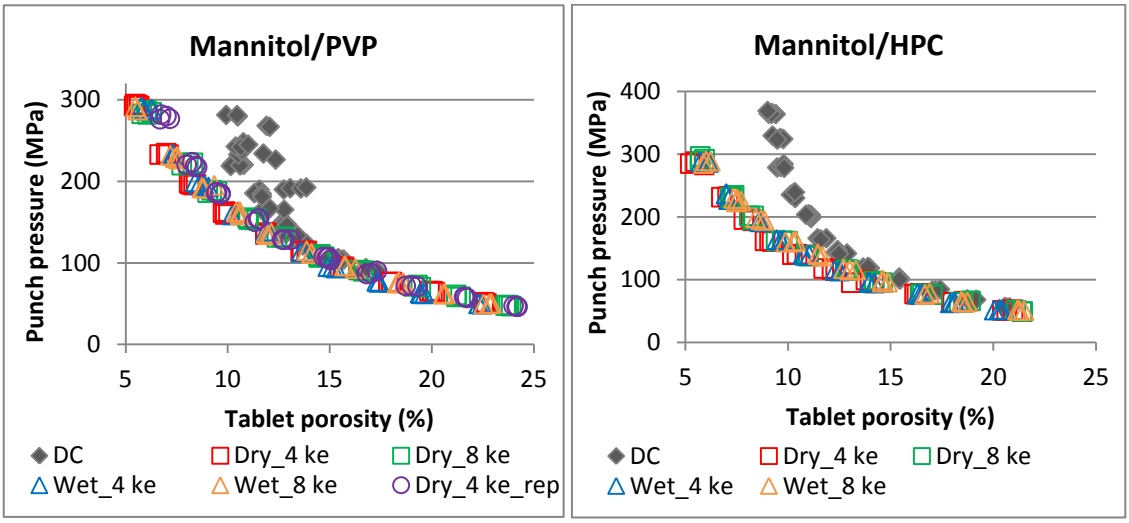

Figure 45. Compressibility of mannitol powder and granules.

Figures 40 and 41 show that the compactability of DCPA decreased and the tabletability increased slightly. For example, the difference in tensile strength between the DC tablets and the granulated tablets at the porosity of 27% varied from 0.34 MPa to 0.94 MPa for granulation with PVP and was approximately 1.00 MPa for HPC. Moreover, the differences were smaller at higher porosities. The differences in tabletability between the DC blends and the granules at 200 MPa were around 1.00 MPa and 0.50 MPa for PVP and HPC, respectively. The differences were larger at higher pressures.

Bulk densities of the granules were slightly smaller than that of the DCPA powder (bulk density 0.78 g/cm^3, tapped density 0.82 g/cm^3) (Rowe et al. 2012). Thus, it was speculated that the tabletability was somewhat improved after wet granulation because the more porous granules fractured more during compression and thus formed shorter separation distance and larger contact area compared with powder. Thereby, the granules resulted in greater number of strong particle bonds and stronger tablets. This could also be seen from the compressibility graphs (Figure 46) as the granules could be compressed into denser tablets at the same compaction pressure compared with the powder and thus the granules had better compressibility.

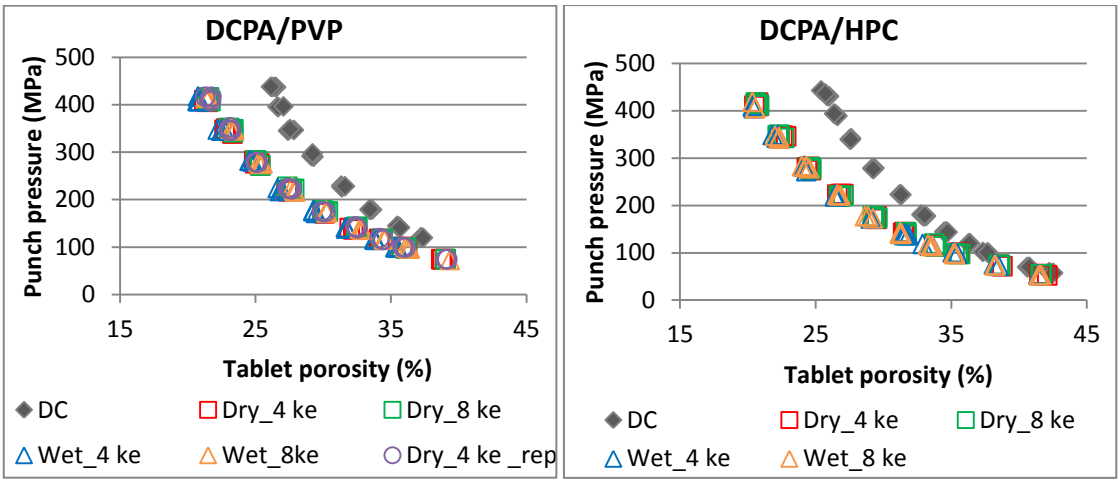

Figure 46. Compressibility of DCPA powder and granules.

Because DCPA fractures during compression and should form new surfaces for particle bonding, the reason for the slightly different tensile strength of DC and granulated tablets at the same tablet density (compactability) might have resulted from a different pore shape or pore size distribution of the tablets or from the different strength of the bonds (Shi et al. 2011a; Nguyen et al. 2013).

However, despite of the markedly different size distributions and somewhat different bulk densities of the DCPA powder and milled granules, the compactability and tabletability changed only little after continuous wet granulation. This can probably be attributed to DCPA's very brittle nature and extensive fracturing of the granules

resulting in large bonding area and strong tablets during compaction. Thereby, the effects of different porosities and sizes of the granules and powder on the tablet tensile strength were minimized. Similar results has been found earlier (Wu and Sun 2007; Djuric et al. 2009; Djuric and Kleinebudde 2010; Souihi et al. 2013). Additionally, DCPA is insoluble and does not recrystallise or go through hornification during granulation so it does not change chemically in wet granulation in contrast to MCC and mannitol. This is another reason why wet granulation does not affect the compaction behavior of DCPA. Furthermore, due to its brittle fracturing and only a small change in the compactability and tabletability after twin screw granulation, DCPA could probably be used to improve the tabletability and compactability of otherwise plastic formulations (Wu and Sun 2007; Osei-Yeboah et al. 2014).

The impact of process parameters on T0g-T0dc results and tensile strengths of the tablets at specific porosity and punch pressure was analysed with the regression analysis in order to find out if the binder had an effect on the compactability and tabletability of the excipients used and to understand the granulation process. The results are discussed below.

The effect of process variables on the tensile strengths of MCC and mannitol tablets at 12% porosity and DCPA tablets at 25% porosity (Figure 47) was studied. For all the excipients PVP produced stronger tablets compared with HPC. In the case of mannitol and MCC this was probably due to the hydrophilicity of PVP and the fillers (Shiromani and Bavitz 1988; Savolainen et al. 2003; Takács et al. 2010; Hoekman and Ho 2011; Thoorens et al. 2014; Stoyanov et al. 2014b). It had been noticed before that stronger tablets were formed when a hydrophilic binder was used with hydrophilic materials and vice versa (Stoyanov et al. 2014b). This had been attributed to the theory that hydrophilic materials compete for water either for dissolution or swelling during granulation and thus a hydrophilic binder (PVP) is better option as it swells and/or dissolves faster (creates more liquid bridges) than a more hydrophobic binder (HPC). With DCPA, PVP resulted in stronger tablets probably because of the faster dissolution of the binder compared with the less hydrophilic HPC (Stoyanov et al. 2014b).

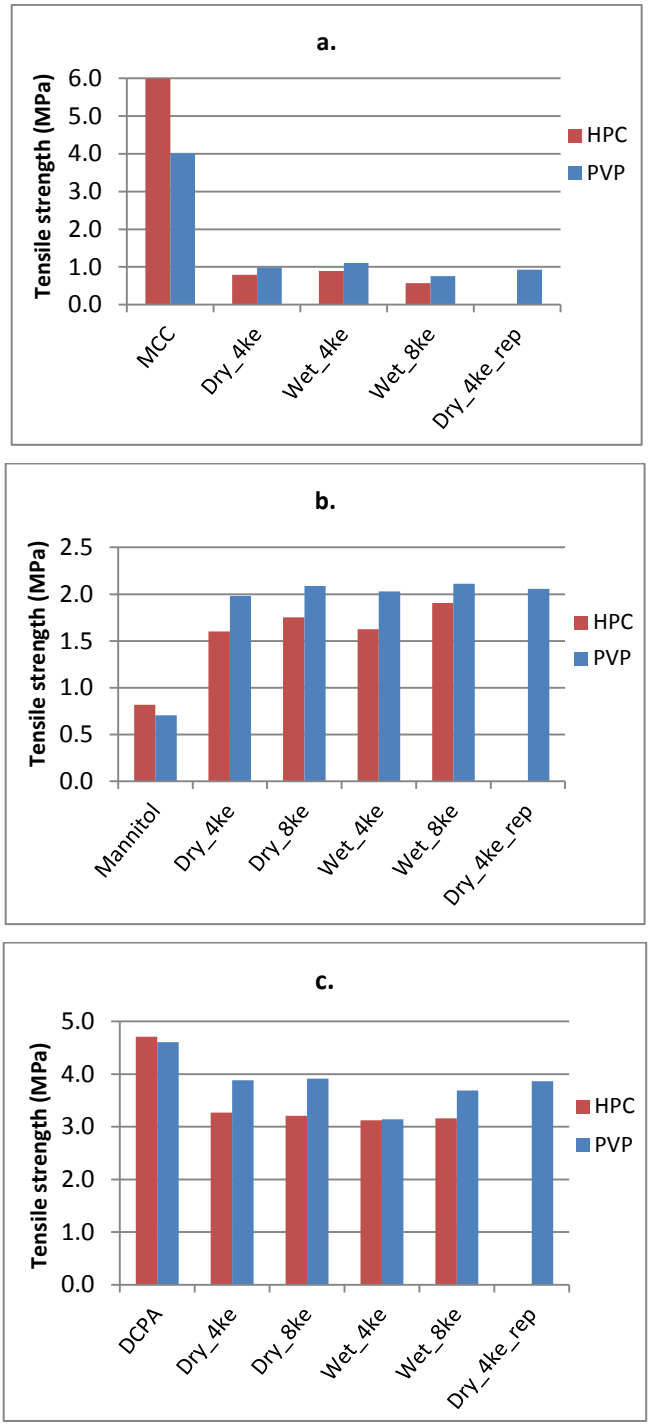

Figure 47. Tensile strength of tablets at 12% porosity (a.MCC, b.mannitol) and 25% porosity (c.DCPA), n = 1.

Additionally, HPC probably produced stronger bonds and denser granules due to better binding properties thus with MCC this probably restricted the deformability of the granules and resulted in weaker tablets (Krycer et al. 1983; Reading and Spring 1984;

Joneja et al. 1999; Stoyanov et al. 2014a). The loss in compactability of MCC due to strong and dense granules was in line with earlier studies (Johansson et al. 1995; Shi et al. 2011a; 2011b; Nguyen et al. 2013).

The tensile strength of MCC (R^2 = 0.98, Q^2 = 0.94) tablets (12% porosity) was also higher with four kneading elements and the wet addition of the binder (except with eight kneading elements). The shorter kneading section resulted in stronger tablets probably because the granules were less densified as seen from the regression analysis of the bulk density (9.2.2) and had better deformability compared with the kneading section of eight disks. This theory was supported by earlier studies where a longer kneading section resulted in denser granules (Djuric and Kleinebudde 2008; Vercruysse et al. 2012). Additionally, the results were in agreement with a twin screw granulation study by Lian et al. (2014) where the wet addition of the binder resulted in stronger tablets. However, the reasons behind the phenomenon were not discussed.

The tensile strength of mannitol (R^2 = 0.92, Q^2 = 0.81) tablets (12% porosity) was also affected by the number of kneading elements, eight kneading disks producing stronger tablets. This could be attributed to the increased number of granules that were more porous than the primary particles and had better deformability. The theory was supported by earlier studies where longer kneading sections had increased the size and number of the granules (Vercruysse et al. 2012; El Hagrasy and Litster 2013). The strength of the DCPA (R^2 = 0.99, Q^2 = 0.97) tablets (25% porosity) were influenced by the binder addition method in addition to the binder type mentioned before. Dry addition generated stronger tablets compared with wet addition. This was probably due to less viscous granulation liquid and thus better liquid penetration and distribution as discussed earlier (Krycer et al. 1983; Reading and Spring 1984; Joneja et al. 1999; Stoyanov et al. 2014a). The number of kneading elements had the strongest effect on MCC tablets and the binder type on mannitol and DCPA tablets as could be seen from the p-values of the regression analysis (APPENDIX 9). Based on the R^2 and Q^2 values all the regression models had good fits and predictability.

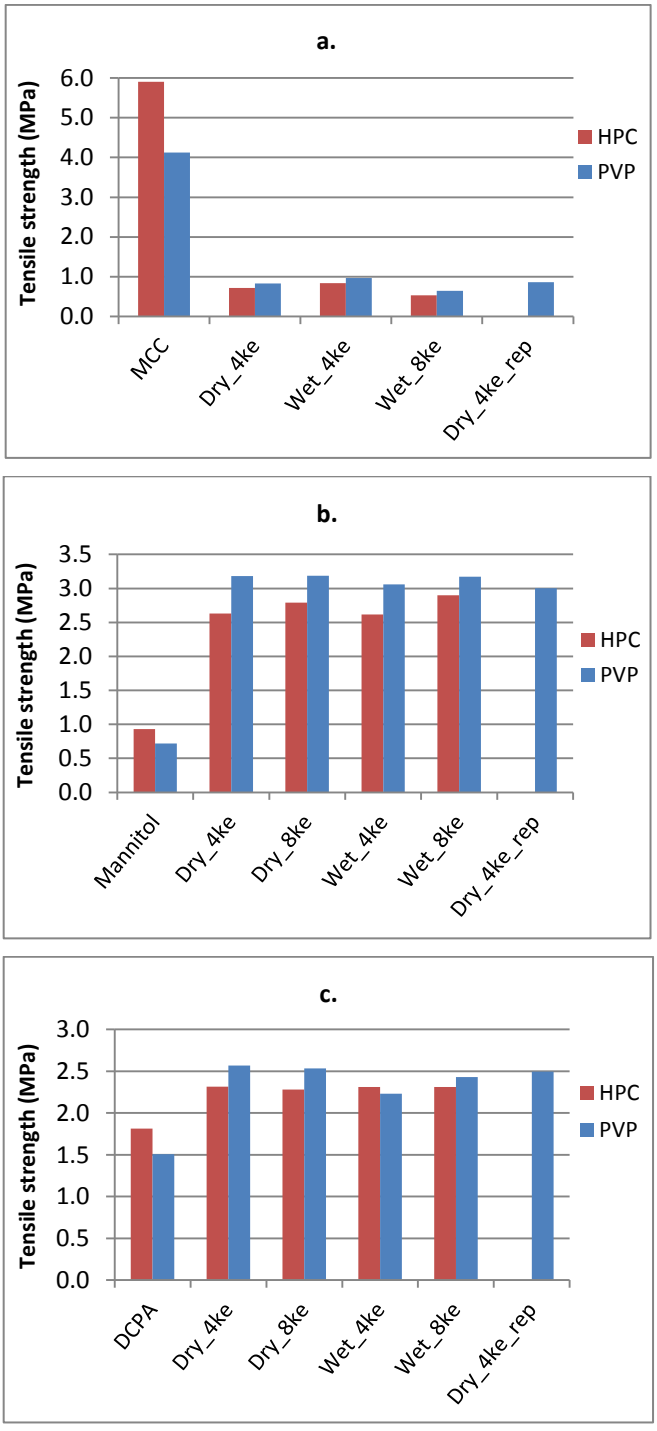

Figure 48. Tensile strength of tablets at a punch pressure of 200 MPa (a.MCC, b.mannitol, c.DCPA), n = 1.

Based on the regression analysis all the variables had a significant effect on the tensile strength of MCC tablets (R^2 = 0.99, Q^2 = 0.98, aliased terms) produced at 200 MPa punch pressure (Figure 48). PVP, four kneading elements and the wet addition of the

binder produced stronger tablets compared with HPC, eight kneading elements and dry addition as seen with the tensile strength results at 12% porosity. The reasons behind the observations were the same as discussed previously. The number of kneading elements had the strongest effect followed by the binder type and binder addition method (APPENDIX 9).

Stronger mannitol tablets (R^2 = 0.92, Q^2 = 0.84) were produced with PVP and eight kneading elements. The reasons for the results were the same as with the tensile strengths at 12% porosity discussed earlier. The binder type had a stronger influence on tablet strength than the number of kneading elements based on the p-values of the regression analysis (APPENDIX 9). Only the binder type had an effect on DCPA tablets (R^2 = 0.88, Q^2 = 0.79, aliased terms) PVP yielding higher tensile strengths. This was probably due to the higher hydrophilicity of PVP compared with HPC as mentioned earlier (Stoyanov et al. 2014a). As could be seen from the R^2 and Q^2 values all the regression models had good fits and predictability.

The direction of the effect of granulation on the compactability and tabletability could be seen from the values of T0g-T0dc (APPENDIX 7), which described the difference in tensile strength between granulated and DC tablets at zero porosity. Positive number (+) indicated improvement and negative number (-) loss in compactability after granulation. MCC and DCPA had negative values and mannitol positive values as demonstrated in Figures 49, 50 and 51.

Only the binder type had an effect on the T0g-T0dc values of MCC based on the regression analysis. PVP showed smaller negative difference suggesting that the tablet tensile strength was higher and that the reduction in compactability smaller with PVP than with HPC. The observations were supported by the tensile strength results at specific porosity and pressure and the reasons behind the phenomenon have been explained in the corresponding chapters. The R^2 and Q^2 values (R^2 = 0.99, Q^2 = 0.98, aliased terms) showed that the regression model fitted and predicted the data well.

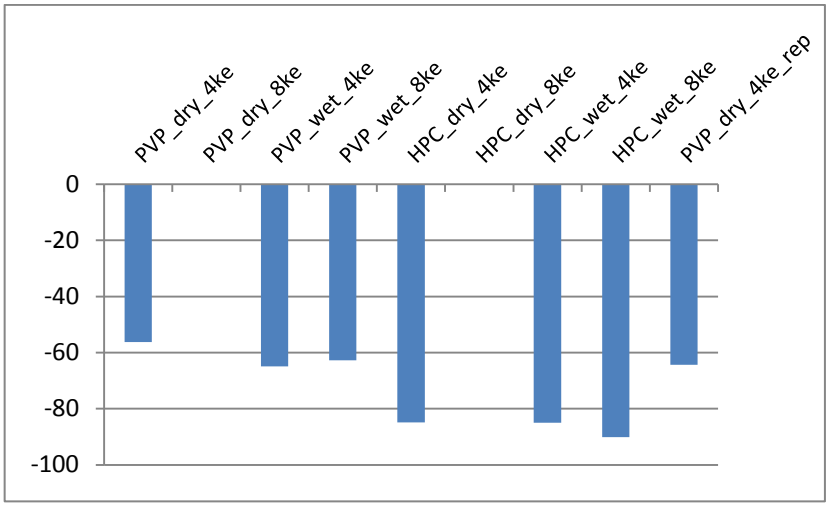

Figure 49. The T0g-T0dc/T0dc (%) results of MCC.

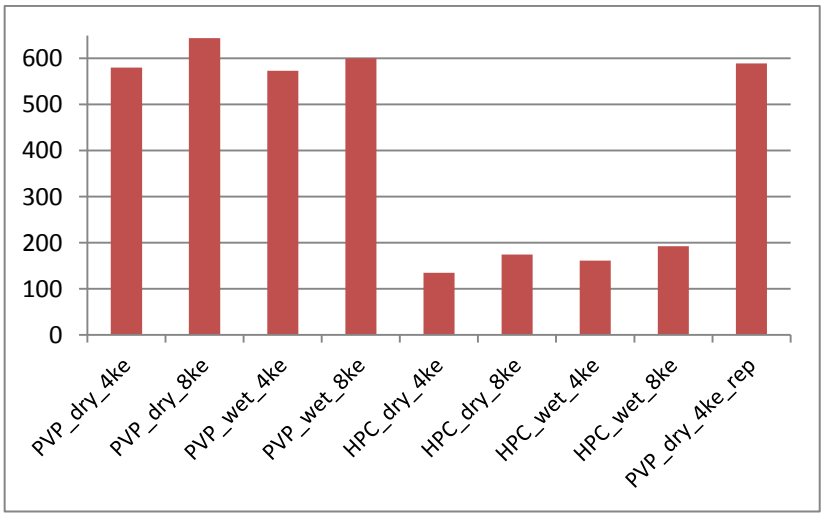

Figure 50. The T0g-T0dc/T0dc (%) results of mannitol.

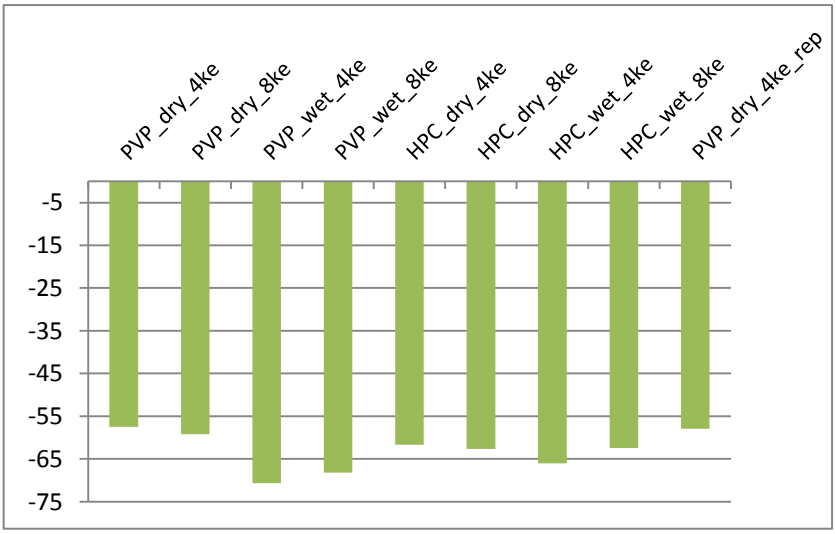

Figure 51. The T0g-T0dc/T0dc (%) results of DCPA.

The binder type and the number of kneading elements had an impact on the T0g-T0dc values of mannitol. PVP led to larger positive difference than HPC indicating that the compactability was more improved and the tablets were stronger with PVP than with HPC. As with MCC, this was in line with the tensile strength results and the underlying reasons were discussed in the corresponding chapters. There was also an interaction between the binder type and binder addition method so that the difference between the binder types was more pronounced with the dry addition of the binder (difference between binder types: dry/4ke 3.56, wet/4ke 2.73, dry/8ke 3.24, wet/8ke 2.26). Moreover, eight kneading elements had a similar effect as PVP, showing more improved compactability compared to four kneading elements as with the tablet strength results. This was probably due to the higher amount of granules that were more porous than primary particles as mentioned before. The binder type had more significant effect than the number of kneading elements which could be seen from the p-values of the regression analysis. Overall, the regression model had a good fit and predicted the data well ($R^2 = 0.99$, $Q^2 = 0.96$).

All the variables had an influence on the T0g-T0dc values of DCPA. HPC showed smaller negative difference compared with PVP indicating that the tablet tensile strengths were higher with HPC. This could have resulted from the higher plasticity and toughness of HPC thus resulting in better binding properties (Krycer et al. 1983; Reading and Spring 1984; Joneja et al. 1999; Stoyanov et al. 2014a). Due to the fracturing of DCPA during compression this resulted in different outcome compared with MCC. Additionally, the effect of the binder type was clearer when the binder was added in the granulation liquid (difference between binder types: dry/4ke 11.77, wet/4ke 27.62, dry/8ke 12.87, wet/8ke 28.42).

The dry addition method gave smaller negative difference (except with eight kneading elements, HPC) with clearer effect with PVP (difference between addition methods: PVP/4ke 21.91, HPC/4ke 6.06, PVP/8ke 15.23, (HPC/8ke 0.32)). This could be attributed to the lower viscosity and higher surface tension of the granulation liquid and thus better liquid penetration and distribution (Krycer et al. 1983; Reading and Spring 1984; Joneja et al. 1999; Stoyanov et al. 2014a). There was also an interaction between

the binder addition method and the number of kneading elements so that eight kneading elements gave smaller negative value when wet addition was used and four kneading elements gave smaller negative value with dry addition. However, the differences in T0g-T0dc values between four and eight kneading elements were much smaller (difference between number of ke: PVP/dry 2.53, PVP/wet 4.16, HPC/dry 1.42, HPC/wet 4.96) compared with the binder type and binder addition method (above). The regression model had a good fit and predictability based on the R^2 and Q^2 values (R^2 = 0.99, Q^2 = 0.99).

Based on the results discussed above and the results seen in APPENDIX 9 it could be concluded that the binder type had a significant effect on the compactability, tabletability and tablet strength of the materials. In most of the cases PVP resulted in stronger tablets. The binder addition method showed only little change in the responses when being part of the model and did not have any impact on the compactability and tabletability behavior of mannitol which suggested that the binder activation and distribution is not that important for the tablet strength. This was a favorable result as dissolving of the binder in the granulation liquid forms another process step that usually takes a long time and forms a bottleneck in the tablet production line.

The number of kneading elements had a significant impact on the responses when MCC and mannitol were used. This was probably due to the observation that the tablet strengths of MCC and mannitol were dependent on the granule properties, for example porosity and size, on which the number of kneading elements had significant impact. With DCPA, the number of kneading elements had mainly effect on granule properties that is density, size and surface area of the granules. The same effect could not be seen with the tablet strength, compactability or tabletability probably due to the very brittle nature of DCPA and the fracturing of the granules during compression. Thereby, the effects of the differences in porosity, particle size and surface area between granules and primary particles on the tablet strength were minimized. Hence, for example the flowability of DCPA could be improved with wet granulation without markedly affecting the compactability or tabletability of the material and the tensile strength of the tablets.

9.5.2 “Loss in compressibility” models

The UCC model and the porosity model were fitted to the DC and granulation data. P_{WG}, T_{WG} and ε_{WG} values were attained as explained earlier in the thesis. Additionally, the feasibility of the “loss in compressibility” models was evaluated. The observations are discussed below.

The effect of process parameters on P_{WG} (APPENDIX 7) of MCC granulation attained from the UCC model was analysed. The binder type and the number of kneading elements had a significant effect on P_{WG}. P_{WG} was larger with HPC compared with PVP indicating that the tabletability and tablet strength were lower with HPC. This was probably due to the hydrophilic nature of MCC as it competed for water and hence hydrophobic HPC did not perform as well as hydrophilic PVP which dissolved faster (Stoyanov et al. 2014b). Additionally, due to the higher toughness of HPC the formed bonds were stronger thus resulting in stronger and denser granules hence restricting further the compactability of MCC during tableting (Krycer et al. 1983; Reading and Spring 1984; Joneja et al. 1999; Stoyanov et al. 2014a).

Eight kneading elements resulted in larger P_{WG} compared with four kneading elements which was expected because a longer kneading section produces higher friction as discussed earlier (Vercruysse et al. 2012). Additionally, the torque and bulk density results supported the P_{WG} results as torque was higher and the granules were denser with the longer kneading section and thus had lower deformability resulting in weaker tablets. This led to larger difference in tabletability between the powder and the granules and thus higher P_{WG} according to the calculations of the UCC model. However, the difference between four and eight kneading elements could not be considered significant as the confidence intervals overlapped slightly. All in all, the regression model had fairly good predictability (R^2 = 0.94, Q^2 = 0.70, aliased terms). However, the lack of fit was significant (p = 0.0006) which indicated that the P_{WG} values of the replicates were close to each other but probably offset from the regression model and thus resulted in lack of fit.

Based on the regression analysis, the same variables had a significant effect on T_{WG} of the MCC granules calculated with the UCC model as on the P_{WG}. HPC produced stronger granules which could be attributed to the toughness of HPC as discussed previously (Krycer et al. 1983; Reading and Spring 1984; Joneja et al. 1999; Stoyanov et al. 2014a). Eight kneading elements resulted in stronger granules due to improved liquid distribution and the densification of the granules which was in line with earlier studies (Djuric and Kleinebudde 2008; Vercruysse et al. 2012). However, as with P_{WG} the confidence intervals overlapped thus the difference between four and eight kneading elements was not significant. As with the regression model of P_{WG}, the regression model for T_{WG} had good predictability (R^2 = 0.99, Q^2 = 0.99, aliased terms) and significant lack of fit based on the p-value (p = 0.0007).

The porosity values (ε_{WG}) of MCC granules attained from the porosity model varied between 12-20%. The low porosity results were supported by the SEM images of MCC granules and correlated with the seen loss in tabletability and compactability as well as with the hornification theory. The porosity values were analysed with the regression analysis. The regression model had a good fit and fairly good predictability (R^2 = 0.89, Q^2 = 0.75, aliased terms). The binder type and the number of kneading elements had a significant impact on ε_{WG}. PVP resulted in higher ε_{WG} compared with HPC probably due to better binding properties of HPC as mentioned earlier (Krycer et al. 1983; Reading and Spring 1984; Joneja et al. 1999; Stoyanov et al. 2014a). However, with eight kneading elements the difference was not significant as the confidence intervals were larger than with four kneading elements and thus they overlapped. This may have resulted from the lack of data for the dry addition with eight kneading elements as those tablets were too weak to give breaking forces larger than zero. Granulation with four kneading elements produced more porous granules than eight kneading elements. This was supported by the bulk density results as four kneading elements resulted in lower density. Additionally, the observations were in line with published studies (Djuric and Kleinebudde 2008; Vercruysse et al. 2012). The effect of the binder type and the number of kneading elements had equally strong effect on ε_{WG}. Moreover, the ε_{WG} values attained from the porosity model were smaller for HPC than PVP supporting the results seen for P_{WG} and the UCC model.

The ε_{WG} values of DCPA granules varied between 32-41% which seemed high. However, the porosity of DCPA/PVP granules produced with twin screw granulation have varied between 22-48% for different screw configurations including kneading block with 90º offset angle to long pitch conveying elements only, respectively (Djuric and Kleinebudde 2010).

Similarly as with MCC granules, PVP produced more porous (ε_{WG}) DCPA granules compared with HPC and the reasons behind the phenomenon have been discussed in previous chapters. Moreover, the binder addition method was a significant variable as wet addition produced denser granules compared with dry addition. This could be attributed to the higher number and strength of viscous bridges as well as to the increased compaction and consolidation due to the longer residence time resulting from the higher wet mass rheology of the binder solution (Dhenge et al. 2012b; Yu et al. 2014; Saleh et al. 2015). Between the two variables, the binder type had a stronger effect on ε_{WG} compared with the binder addition method. The regression model was reliable and had a very good fit to the data (R^2 = 0.99, Q^2 = 0.99, aliased terms, power transformation).

Figures 52 and 53 represent the fittings of the UCC model to MCC granulation data. The black line shows the fit of Equation 3 to direct compaction data. The points on the line represent the calculated tensile strength values i.e. the unified compaction curve data. The Figures 52 and 53 demonstrate that the fit of the UCC model to the twin screw granulation data of MCC was good. The results were in agreement with earlier studies (Farber et al. 2008; Mosig and Kleinebudde 2013; Nguyen et al. 2013).

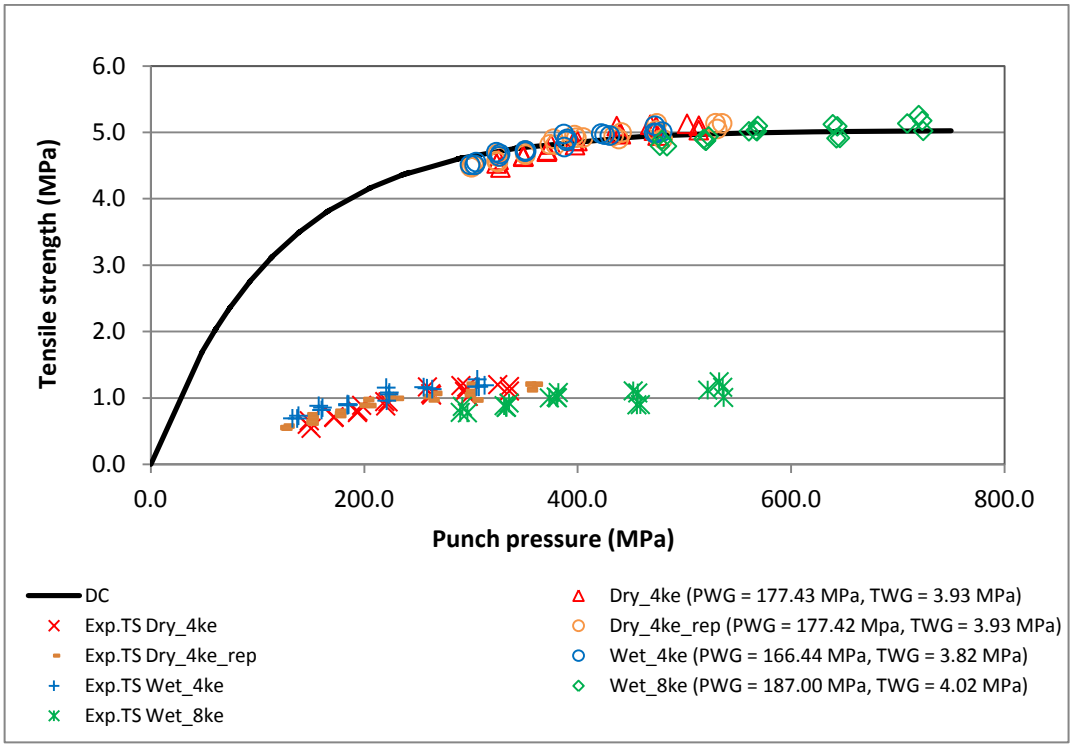

Figure 52. Unified compaction curve and the transported data points of MCC/PVP tablets (Exp.TS = experimental tensile strength data, Tmax = 5.0 MPa, b = 0.009).

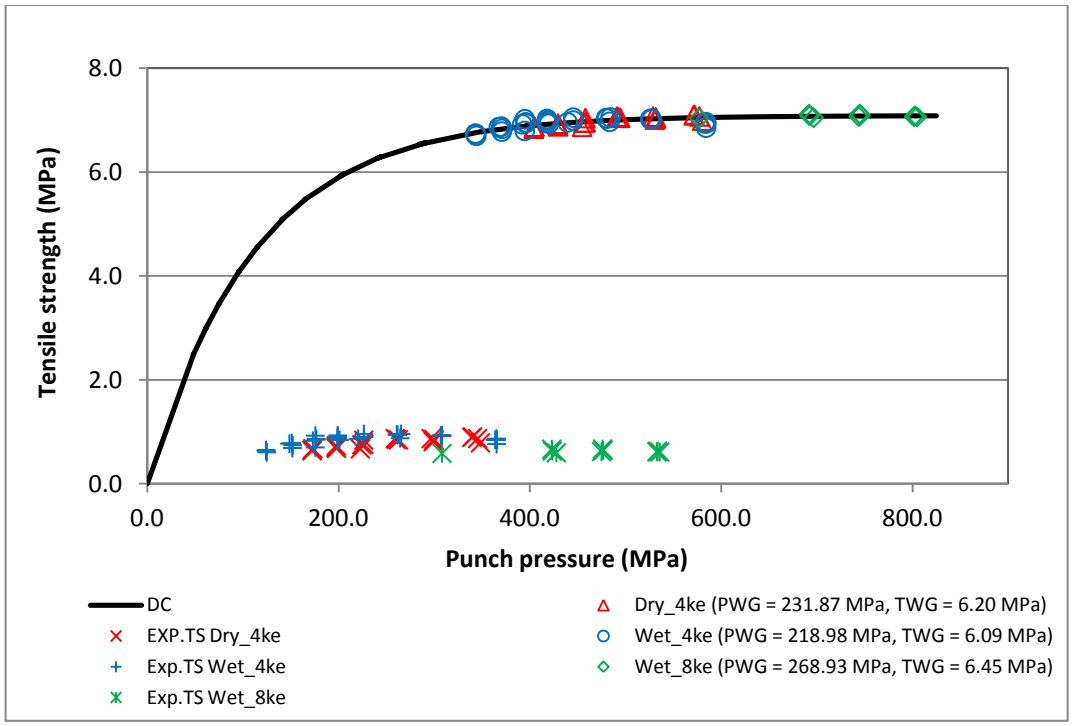

Figure 53. Unified compaction curve and the transported data points of MCC/HPC tablets (Exp.TS = experimental tensile strength data, Tmax = 7.1 MPa, b = 0.009).

However, the pressure values of the granulation (P_{WG}) varied from 166-269 MPa and it is arguable if the pressure experienced by the material during granulation could have been that high. For example in studies by Chan et al. (2012; 2013), the impeller stress in high shear granulation varied between 1000-4000 Pa that is orders of magnitude smaller compared with the stresses attained from the UCC model. Additionally, in earlier studies considering the UCC model, the P_{WG} values have varied from 20-135 MPa for high shear granulation and from 75-107 MPa for roller compaction (Farber et al. 2008; Nguyen et al. 2013). Tensile strength values of the ribbons produced by roller compaction were 1.60-2.84 MPa which were much smaller than in the current study (Farber et al. 2008). The high P_{WG} and T_{WG} values seen here might have resulted from extensive hornification and shrinkage of the cellulose fibers due to drying of the granules to low moisture contents (APPENDIX 11) and/or higher compaction and shear forces experienced by the material during twin screw granulation compared with high shear granulation and roller compaction where roller pressure can be controlled (Keleb et al. 2002; Miller 2010; Dhenge et al. 2012b).

The UCC model was not applicable to mannitol and DCPA because the tabletability of the materials improved after continuous wet granulation. Furthermore, if they had had experienced loss in compactability they probably would not still had fitted the UCC model due to their linear tensile strength-pressure relationship (Figure 41) seen in earlier studies as well (Farber et al. 2008; Mosig and Kleinebudde 2013). This supported the assumption that the UCC model is applicable only for formulations that contain sufficient amount of plastically deforming material.

Figures 54 and 55 demonstrate the fits of the porosity model to MCC granulation data. The fit of the model to tablets produced after granulation was moderate below tablet porosities of 15%. However, there was uncertainty in the fitting due to the linearity of the data and the lack of data points. The lack of data points resulted from the inability of the hardness tester to give crushing strength values for the weak tablets. In order to be able to draw conclusions of the feasibility of the porosity model to the twin screw granulation of MCC a more comprehensive tensile strength-porosity relationship would have been needed.

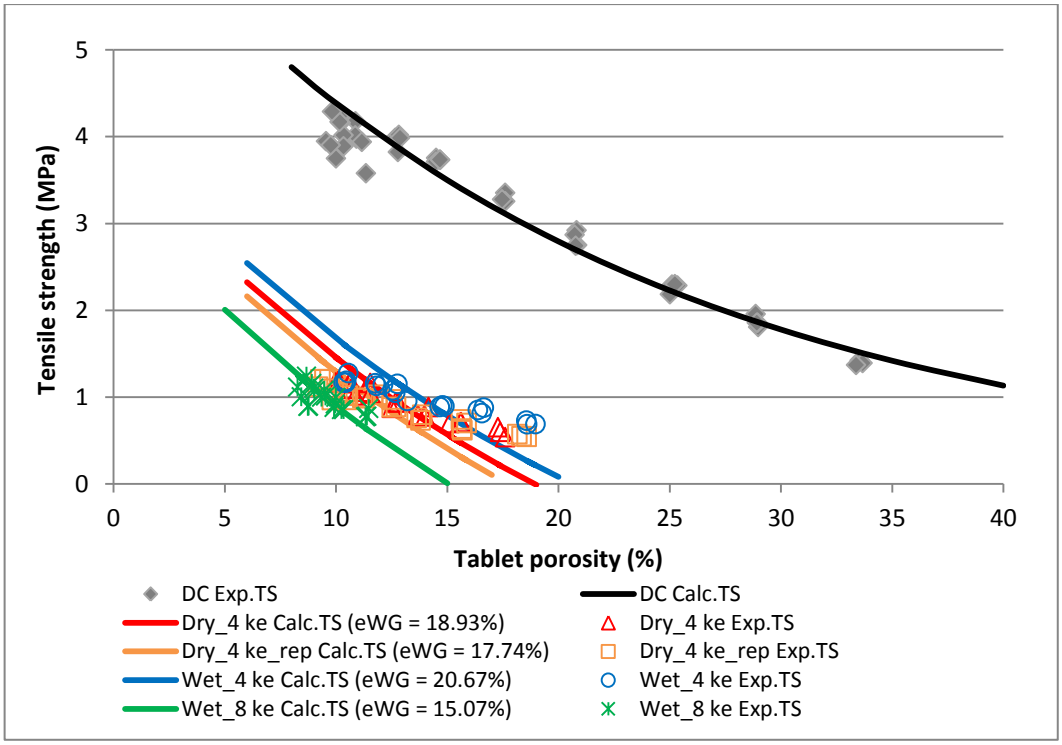

Figure 54. Fits of the porosity model to DC (Eq. 12) and granulation (Eq. 39) data of MCC/PVP tablets (DC: T0 = 6.9 MPa, kb = 0.045).

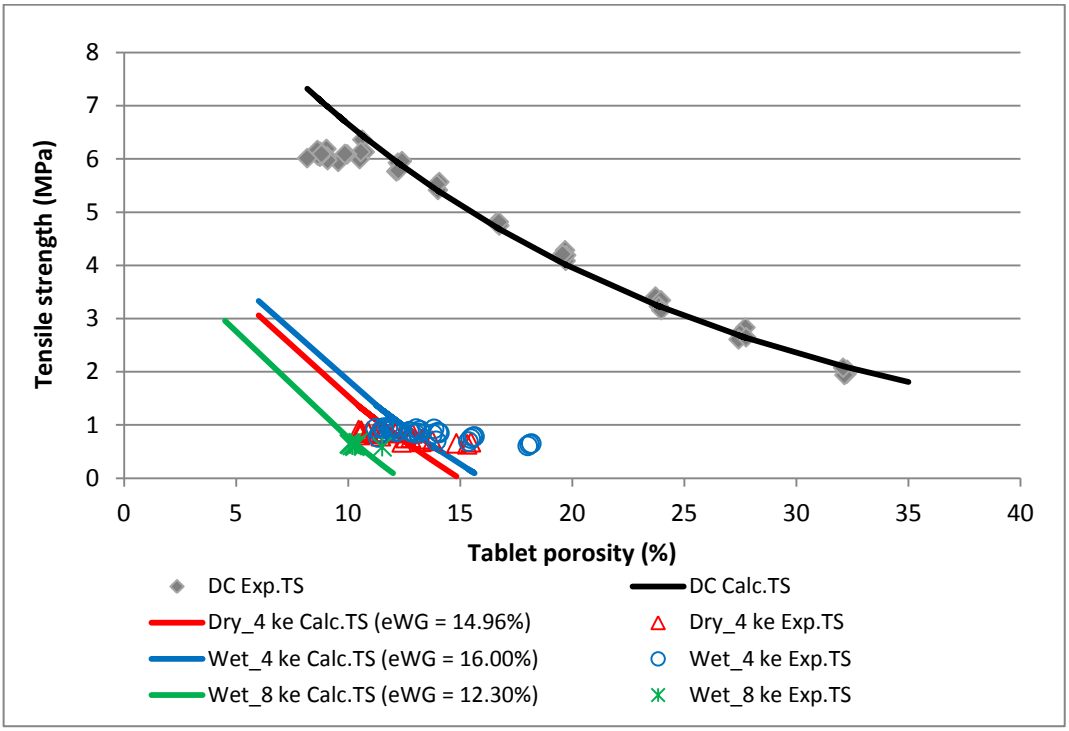

Figure 55. Fits of the porosity model to DC (Eq. 12) and granulation (Eq. 39) data of MCC/HPC tablets (DC: T0 = 11.2 MPa, kb = 0.052).

Figures 56 and 57 represent the fits of porosity model to the DCPA granulation data. The model fitted the data well with tablet porosities of 22-27%. Based on the compressibility of DCPA (Figure 46) those porosities were attained when compaction pressures used in the industry (200-300 MPa) were applied. As a consequence the porosity model was feasible to describe the loss in compactability of DCPA after continuous twin screw granulation. These results were in line with a study by Gavi and Reynolds (2014) who concluded that the porosity model was feasible to predict the tensile strength of tablets when intermediate compaction pressures were used. At low compaction pressure (5 kN) the tablets were crushed locally and did not exhibit tensile failure and thus deviated from the model. Over-compression took place at high compaction pressure (20 kN) which resulted in flaws in the tablets and lower tensile strength than was predicted by the model. This could have happened in the current study as well because with tablet porosities above 27% the model overestimated the reduction in tensile strength from the granule porosity and below 22% the model underestimated it. Reynolds et al. (2015) developed the model further by including a granule porosity dependent coefficient to take into account different extents of loss in compactability. This way the prediction of the loss in compactability of different materials was improved.

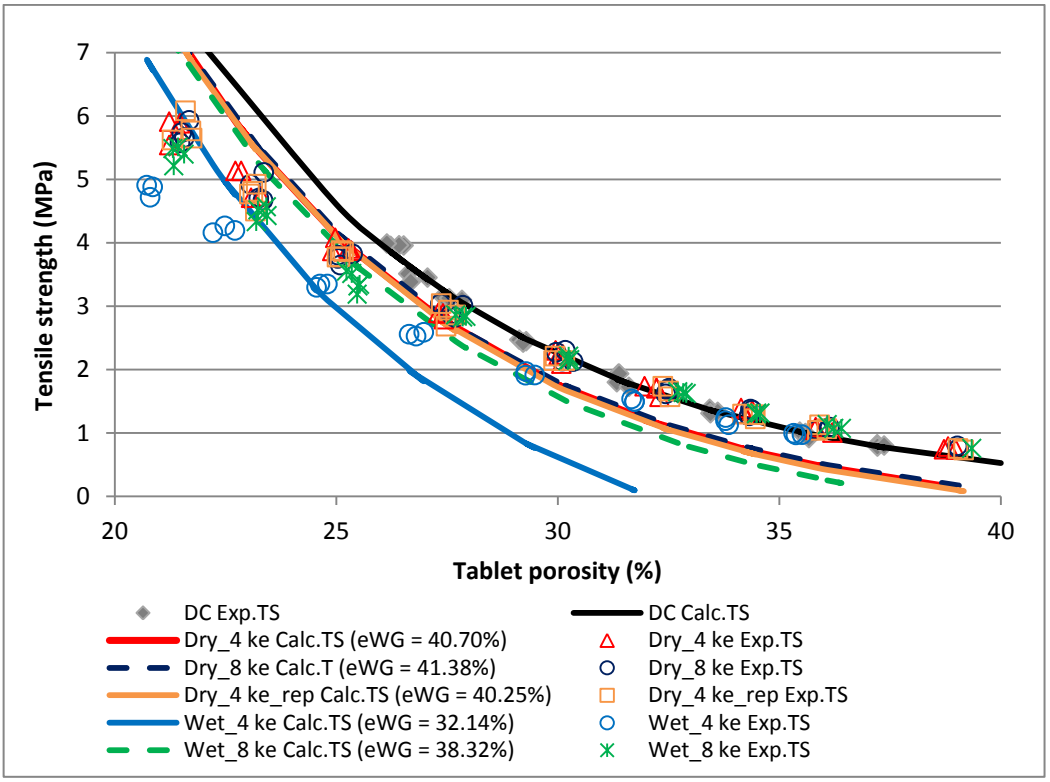

Figure 56. Fits of the porosity model to DC (Eq. 12) and granulation (Eq. 39) data of DCPA/PVP tablets (DC: T0 = 169.5 MPa, kb = 0.144).

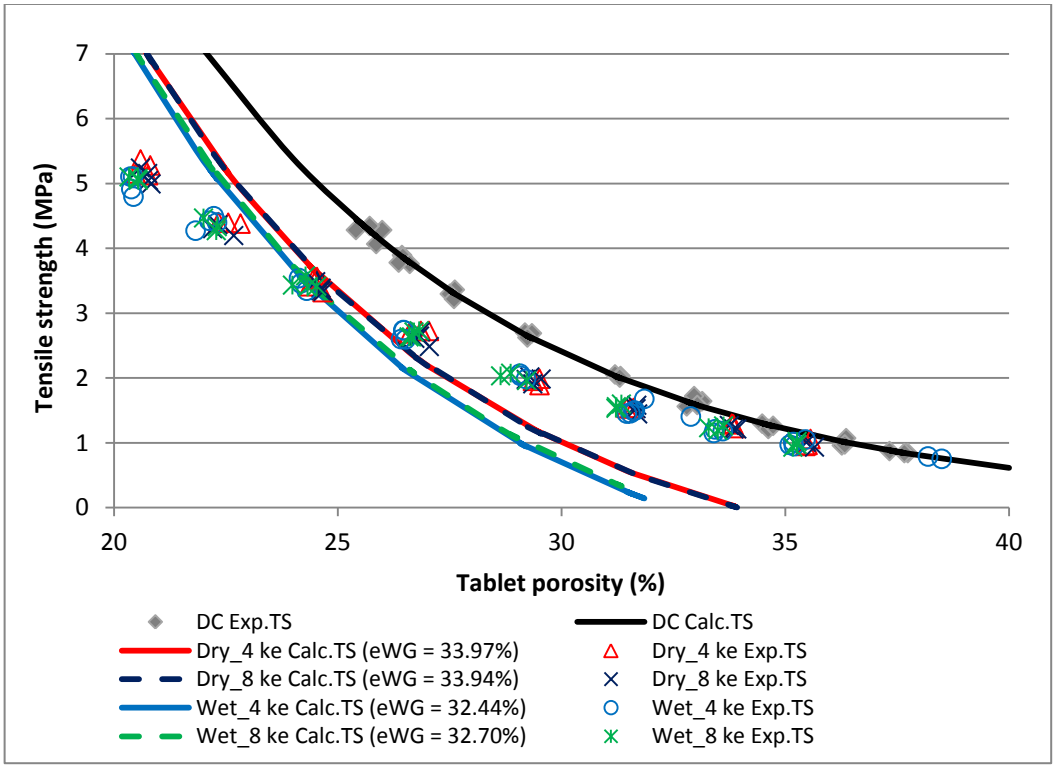

Figure 57. Fits of the porosity model to DC (Eq. 12) and granulation (Eq. 39) data of DCPA/HPC tablets (DC: T0 = 139.6 MPa, kb = 0.136).

10. CONCLUSIONS

The main objective of the study was to gain understanding on how twin screw granulation affects the compactability and tabletability of MCC, mannitol and DCPA. Additionally, the impact of binder on the compaction behavior and tablet strength was studied. Loss in compactability and tabletability of MCC was detected as expected due to the hornification of MCC. On the other hand, the compactability and tabletability of mannitol was improved resulting from the formation of porous granules. Additionally, there was only a small change in the compactability and tabletability of DCPA due to its brittle and insoluble nature.

The binder type had an impact on the tabletability and compactability of the materials, PVP yielding stronger tablets compared with the less hydrophilic HPC. This indicated that the compaction behavior of a formulation and tablet strength can be affected by the properties of the binder. The binder addition method, however, showed only a small effect or did not have any impact on the compaction behavior of the materials. This indicated that it is irrelevant for the final tablet strength whether the binder is dissolved in the granulation liquid or added as dry powder in the formulation blend. This observation supports the elimination of the time consuming process step of binder dissolving which saves resources in the tablet production chain and enables continuous tablet manufacturing with twin screw granulation.

Additionally, this study was the first to evaluate the feasibility of two "loss in compressibility" models to twin screw granulation. Because the loss in compactability and tabletability behaviors were not applicable across all the materials the models were not feasible to all of the excipients. However, there was a general mechanism in the results that stronger or tougher granules led to weaker tablets. This did fit, in principle, with the "loss in compressibility" models, even though the data did not fit the models exactly for each of the materials.

The UCC model was applicable to MCC and its loss in tabletability behavior. Thereby, the prediction of tablet tensile strength for different granulation conditions or the design of the granulation process to achieve a specific tensile strength based on small scale

preliminary studies is possible with the UCC model. Consequently, the UCC model can be used to help optimize the twin screw granulation process and therefore reduce the resources needed to conduct case-studies.

However, the model was not feasible to mannitol and DCPA because they experienced improvement in tabletability after twin screw granulation. The porosity model was applicable to MCC and DCPA but not to mannitol as it exhibited improvement in compactability. The porosity model described the loss in compactability of MCC only moderately due to lack of tensile strength data points and the linearity of the tensile strength-porosity relationship. However, the model described well the loss in compactability of DCPA at tablet porosities achieved with compaction pressures used in industry.

As a conclusion, the current study demonstrated that the twin screw granulation process can influence the final tablet tensile strength and that the compaction behavior of the formulation can change either way depending on the materials used. Thus, there is no universal model or theory that would describe or explain the change in compaction behavior after granulation for all the materials. That is why it should be studied further how materials behave in granulation and subsequent compaction to understand the characteristics of the phenomenon. Therefore, it would be relevant to study in the future how the materials behave in mixtures and what are the percentages needed to achieve the compactability and tabletability behaviors seen with the certain excipients in the current study. Also, the feasibility of the “loss in compressibility” models to tablet formulations used in production would be important to assess. The results from those studies would improve the understanding of the twin screw granulation process and further aid the designing of formulations for continuous wet granulation processing routes.

REFERENCES

Allen EE: Instrument For The Transfusion Of Blood. United States patent US 249285: 1881

Ashland Inc: Excipient information: Klucel™ hydroxypropylcellulose (HPC) physical and chemical properties. Ashland Inc., USA, Purchased from internet 29.7.2016: http://www.ashland.com/Ashland/Static/Documents/ASI/PC_11229_Klucel_HPC.pdf

Badawy SI, Gray DB, Hussain MA: A study on the effect of wet granulation on microcrystalline cellulose particle structure and performance. Pharm Res 23: 634-640, 2006

Bassam F, York P, Rowe RC, Roberts RJ: Young's modulus of powders used as pharmaceutical excipients. Int J Pharm 64: 55-60, 1990

Beer P, Wilson D, Huang Z, De Matas M: Transfer from High-Shear Batch to Continuous Twin Screw Wet Granulation: A Case Study in Understanding the Relationship Between Process Parameters and Product Quality Attributes. J Pharm Sci 2014

Brook DB, Marshall K: "Crushing-strength" of compressed tablets I. Comparison of testers. J Pharm Sci 57: 481-484, 1968

Buckton G, Yonemochi E, Yoon W, Moffat A: Water sorption and near IR spectroscopy to study the differences between microcrystalline cellulose and silicified microcrystalline cellulose before and after wet granulation. Int J Pharm 181: 41-47, 1999

Bühler V: Kollidon - Polyvinylpyrrolidone excipients for the pharmaceutical industry. 9th ed. BASF SE, 2008

Bultmann JM: Multiple compaction of microcrystalline cellulose in a roller compactor. Eur J Pharm Biopharm 54: 59-64, 2002

Bush L: FDA lowers barriers to process improvement. Pharm Technol 29: 54-64, 2005

Capes CE: Particle size enlargement. Elsevier Scientific Publishing Company, The Netherlands 1980

Chan EL, Reynolds GK, Gururajan B, Salman AD, Hounslow MJ: Blade-granule bed stress in a cylindrical high-shear granulator: Variability studies. Chem Eng Technol 35: 1435-1447, 2012

Chan EL, Reynolds GK, Gururajan B, Hounslow MJ, Salman AD: Blade–granule bed stress in a cylindrical high shear granulator: I—Online measurement and characterisation. Chem Eng Sci 86: 38-49, 2013

Chatrath M: The effect of wet granulation on the physico-mechanical characteristics of microcrystalline cellulose. Dissertation, University of Bath, UK 1992

Clay RB, Doering WA: Pump apparatus for slurry and other viscous liquids. United States patent US 3649138: 1972

Dave RH, Dudhat SM: To evaluate wet granulated tablet properties through the unified compaction curve using microcrystalline cellulose (mcc, avicel 101 and 200). American Association of Pharmaceutical Scientists Annual Meeting and Exposition, San Antonio, USA AAPS 2013

David ST, Augsburger LL: Plastic flow during compression of directly compressible fillers and its effect on tablet strength. J Pharm Sci 66: 155-159, 1977

Dhenge RM, Cartwright JJ, Hounslow MJ, Salman AD: Twin screw granulation: Steps in granule growth. Int J Pharm 438: 20-32, 2012a

Dhenge RM, Cartwright JJ, Doughty DG, Hounslow MJ, Salman AD: Twin screw wet granulation: Effect of powder feed rate. Adv Powder Technol 22: 162-166, 2011

Dhenge RM, Cartwright JJ, Hounslow MJ, Salman AD: Twin screw wet granulation: Effects of properties of granulation liquid. Powder Technol 229: 126-136, 2012b

Dhenge RM, Fyles RS, Cartwright JJ, Doughty DG, Hounslow MJ, Salman AD: Twin screw wet granulation: Granule properties. Chem Eng J 164: 322-329, 2010

Dhenge RM, Washino K, Cartwright JJ, Hounslow MJ, Salman AD: Twin screw granulation using conveying screws: Effects of viscosity of granulation liquids and flow of powders. Powder Technol 238: 77-90, 2013

Djuric D: Continuous granulation with a twin-screw extruder. Dissertation, University of Düsseldorf, Germany 2008

Djuric D, Kleinebudde P: Continuous granulation with a twin-screw extruder: Impact of material throughput. Pharm Dev Technol 15: 518-525, 2010

Djuric D, Kleinebudde P: Impact of screw elements on continuous granulation with a twin-screw extruder. J Pharm Sci 97: 4934-4942, 2008

Djuric D, Van Melkebeke B, Kleinebudde P, Remon JP, Vervaet C: Comparison of two twin-screw extruders for continuous granulation. Eur J Pharm Biopharm 71: 155-160, 2009

Duberg M, Nyström C: Studies on direct compression of tablets. VI. Evaluation of methods for the estimation of particle fragmentation during compaction. Acta Pharm Suec 19: 421-436, 1982

Ek R, Newton JM: Microcrystalline cellulose as a sponge as an alternative concept to the crystallite-gel model for extrusion and spheronization. Pharm Res 15: 509-512, 1998

El Hagrasy AS, Hennenkamp JR, Burke MD, Cartwright JJ, Litster JD: Twin screw wet granulation: Influence of formulation parameters on granule properties and growth behavior. Powder Technol 238: 108-115, 2013

El Hagrasy AS, Litster JD: Granulation rate processes in the kneading elements of a twin screw granulator. AIChE J 59: 4100-4115, 2013

Ennis BJ, Litster JD: Particle size enlargement. In book: Perry's chemical engineers' handbook, p. 20-56-20-89, 7. Edition. Eds. Perry R and Green D, McGraw-Hill, New York 1997

Ennis B: Theory of granulation: An engineering perspective. In book: Handbook of pharmaceutical granulation technology, p. 6-58, 3. Edition. Ed. Parikh DM, Informa Healthcare, USA 2010

Farber L, Hapgood KP, Michaels JN, Fu X, Meyer R, Johnson M, Li F: Unified compaction curve model for tensile strength of tablets made by roller compaction and direct compression. Int J Pharm 346: 17, 2008

Fell JT, Newton JM: Determination of tablet strength by the diametral-compression test. J Pharm Sci 59: 688-691, 1970

Fielden KE, Newton JM, O' Brien P, Rowe RC: Thermal studies on the interaction of water and microcrystalline cellulose. J Pharm Pharmacol 40: 674-678, 1988

Fonteyne M, Wickström H, Peeters E, Vercruysse J, Ehlers H, Peters B-, Remon JP, Vervaet C, Ketolainen J, Sandler N, Rantanen J, Naelapää K, Beer TD: Influence of raw material properties upon critical quality attributes of continuously produced granules and tablets. Eur J Pharm Biopharm 87: 252-263, 2014

Freitag F, Kleinebudde P: How do roll compaction/dry granulation affect the tableting behaviour of inorganic materials? Comparison of four magnesium carbonates. Eur J Pharm Sci 19: 281-289, 2003

Gamlen MJ, Eardley C: Continuous extrusion using a Baker Perkins MP50 (multipurpose) extruder. Drug Dev Ind Pharm 12: 1701-1713, 1986

Gavi E, Reynolds GK: System model of a tablet manufacturing process. Comput Chem Eng 71: 130-140, 2014

Ghebre-Sellasie I, Plains M, Mollan MJ, Pathak N, Lodaya M, Fessehaie M: Continuous production of pharmaceutical granulation. United States patent US 6499984 B1: 2002

Gignac L, Wells O: Characterization of semiconductor nanostructures by scanning electron microscopy. In book: Handbook of instrumentation and techniques for semiconductor nanostructure characterization, p. 1-42, 1. Edition. Eds. Haight R, Hannon J and Ross F, World Scientific Publishing Company, Singapore 2012

Habib YS, Abramowitz R, Jerzewski RL, Jain NB, Agharkar SN: Is silicified wet granulated microcrystalline cellulose better than original wet granulated microcrystalline cellulose? Pharm Dev Technol 4: 431-437, 1999

Häkkinen A: Optimization of particle size distribution in continuous wet granulation process (ConsiGma25). Master´s thesis, University of Helsinki, Finland 2016

Hapgood KP, Litster JD, Biggs SR, Howes T: Drop penetration into porous powder beds. J Colloid Interface Sci 253: 353-366, 2002

Hoekman JD, Ho RJ: Effects of localized hydrophilic mannitol and hydrophobic nelfinavir administration targeted to olfactory epithelium on brain distribution. AAPS PharmSciTech 12: 534-543, 2011

Iveson SM, Litster JD: Growth regime map for liquid-bound granules. AIChE J 44: 1510-1518, 1998

Iveson SM, Litster J, Hapgood K, Ennis B: Nucleation, growth and breakage phenomena in agitated wet granulation processes: a review. Powder Technol 117: 3-39, 2001

Jayme G: Mikro-Quellungsmessungen an Zellstoffen. Wochenbl Papierfabr 6: 187-194, 1944

Johansson B, Wikberg M, Ek R, Alderborn G: Compression behavior and compactability of microcrystalline cellulose pellets in relationship to their pore structure and mechanical-properties. Int J Pharm 117: 57-73, 1995

Joneja S, Harcum W, Skinner G, Barnum P, Guo J: Investigating the fundamental effects of binders on pharmaceutical tablet performance. Drug Dev Ind Pharm 25: 1129-1135, 1999

Juppo AM: Pore structure of lactose, glucose and mannitol tablets compressed from granules and dependence of breaking force of tablets on porosity parameters studied by mercury porosimetry. Dissertation, University of Helsinki, Finland 1995

Juppo AM, Kervinen L, Yliruusi J, Kristoffersson E: Compression of lactose, glucose and mannitol granules. J Pharm Pharmacol 1995

Juppo AM, Yliruusi J, Kervinen L, Ström P: Determination of size distribution of lactose, glucose and mannitol granules by sieve analysis and laser diffractometry. Int J Pharm 88: 141-149, 1992

Juppo AM, Yliruusi J: Effect of amount of granulation liquid on total pore volume and pore size distribution of lactose, glucose and mannitol granules. Eur J Pharm Biopharm 40: 299-309, 1994

Keleb EI, Vermeire A, Vervaet C, Remon JP: Extrusion granulation and high shear granulation of different grades of lactose and highly dosed drugs: A comparative study. Drug Dev Ind Pharm 30: 679-691, 2004a

Keleb EI, Vermeire A, Vervaet C, Remon JP: Twin screw granulation as a simple and efficient tool for continuous wet granulation. Int J Pharm 273: 183-194, 2004b

Keleb EI, Vermeire A, Vervaet C, Remon JP: Continuous twin screw extrusion for the wet granulation of lactose. Int J Pharm 239: 69-80, 2002

Khan F, Pilpel N: An investigation of moisture sorption in microcrystalline cellulose using sorption isotherms and dielectric response. Powder Technol 50: 237-241, 1987

Khan F, Pilpel N, Ingham S: The effect of moisture on the density, compaction and tensile strength of microcrystalline cellulose. Powder Technol 54: 161-164, 1988

Kleinebudde P, Jumaa M, El Saleh F: Influence of degree of polymerization on behavior of cellulose during homogenization and extrusion/spheronization. AAPS PharmSci 2: 1-10, 2000

Kleinebudde P: The crystallite-gel-model for microcrystalline cellulose in wet-granulation, extrusion, and spheronization. Pharm Res 14: 804-809, 1997

Kleinebudde P: Shrinking and swelling properties of pellets containing microcrystalline cellulose and low substituted hydroxypropylcellulose. Part 2. Swelling properties. Int J Pharm 109: 221-227, 1994

Kochhar SK, Rubinstein MH, Barnes D: The effects of slugging and recompression on pharmaceutical excipients. Int J Pharm 115: 35-43, 1995

Krycer I, Pope DG, Hersey JA: The role of intra-granular porosity in powder compaction. Powder Technol 33: 101-111, 1982

Krycer I, Pope DG, Hersey JA: An evaluation of tablet binding agents part I. Solution binders. Powder Technol 34: 39-51, 1983

Kumar A, Vercruysse J, Bellandi G, Gernaey KV, Vervaet C, Remon JP, De Beer T, Nopens I: Experimental investigation of granule size and shape dynamics in twin-screw granulation. Int J Pharm 475: 485-495, 2014a

Kumar A, Vercruysse J, Toiviainen M, Panouillot P-, Juuti M, Vanhoorne V, Vervaet C, Remon JP, Gernaey KV, De Beer T, Nopens I: Mixing and transport during pharmaceutical twin-screw wet granulation: Experimental analysis via chemical imaging. Eur J Pharm Biopharm 87: 279-289, 2014b

Lee KT, Ingram A, Rowson NA: Comparison of granule properties produced using twin screw extruder and high shear mixer: A step towards understanding the mechanism of twin screw wet granulation. Powder Technol 238: 91-98, 2013

Leuenberger H: The compressibility and compactibility of powder systems. Int J Pharm 12: 41-55, 1982

Leuenberger H: New trends in the production of pharmaceutical granules: batch versus continuous processing. Eur J Pharm Biopharm 52: 289-296, 2001

Li H, Thompson MR, O'Donnell KP: Progression of wet granulation in a twin screw extruder comparing two binder delivery methods. AIChE J 61: 780, 2015

Lian Z, Bell A, Zong Y, Birkmire A, Hullen J, Zombek J, Tewari D, Durig T: Evaluation of binders and process factors in continuous twin-screw granulation. AAPS, R6095 2014

Lindberg N: Some experience of continuous granulation. Acta Pharm Suec 25: 239-246, 1988

Lindberg N, Myrenas M, Tufvesson C, Olbjer L: Extrusion of an effervescent granulation with a twin screw extruder, Baker Perkins MPF 50D. Determination of mean residence time. Drug Dev Ind Pharm 14: 649-655, 1988a

Lindberg N, Tufvesson C, lbjer L: Extrusion of an effervescent granulation with a twin screw extruder, Baker Perkins MPF 50 D. Drug Dev Ind Pharm 13: 1891-1913, 1987

Lindberg N, Tufvesson C, Holm P, Olbjer L: Extrusion of an effervescent granulation with a twin screw extruder, Baker Perkins MPF 50 D. Influence on intragranular porosity and liquid saturation. Drug Dev Ind Pharm 14: 1791-1798, 1988b

Mashadi AB, Newton J: Characterization of the mechanical properties of microcrystalline cellulose: a fracture mechanics approach. J Pharm Pharmacol 39: 961-965, 1987

McKenna A, McCafferty D: Effect on particle size on the compaction mechanism and tensile strength of tablets. J Pharm Pharmacol 34: 347-351, 1982

Miller R: Roller compaction technology. In book: Handbook of pharmaceutical granulation technology, p. 163-182, 3. Edition. Ed. Parikh DM, Informa Healthcare, USA 2010

Millili G.: Differences in the mechanical strength of dried microcrystalline cellulose pellets are not due to significant changes in the degree of hydrogen bonding. Pharm Dev Technol 1: 239-249, 1996

Millili GP, Wigent R, Schwartz J: Autohesion in pharmaceutical solids. Drug Dev Ind Pharm 16: 2383-2407, 1990

Minor JL: Hornification - its origin and meaning. Prog Pap Recycl 3: 93-95, 1994

Mosig J, Kleinebudde P: Critical assessment of the unified compaction curve model. 6th International Granulation Workshop, Sheffield, UK 2013

Nguyen TH: Prediction of tablet strength: Development of the unified compaction curve model for wet granulation. Monash University, Australia 2014

Nguyen TH, Morton DAV, Hapgood KP: Application of the unified compaction curve to link wet granulation and tablet compaction behaviour. Powder Technol 240: 103-115, 2013

Osei-Yeboah F, Zhang M, Feng Y, Sun CC: A formulation strategy for solving the overgranulation problem in high shear wet granulation. J Pharm Sci 103: 2434, 2014

Owolabi GM, Bassim MN, Page JH, Scanlon MG: The influence of specific mechanical energy on the ultrasonic characteristics of extruded dough. J Food Eng 86: 202-206, 2008

Pitt KG, Heasley MG: Determination of the tensile strength of elongated tablets. Powder Technol 238: 169-175, 2013

Plumb K: Continuous processing in the pharmaceutical industry: changing the mind set. Chem Eng Res Design 83: 730-738, 2005

Reading S, Spring M: The effects of binder film characteristics on granule and tablet properties. J Pharm Pharmacol 36: 421-426, 1984

Rekhi GS, Sidwell R: Sizing of granulation. In book: Handbook of pharmaceutical granulation technology, p. 449-468, 3. Edition. Ed. Parikh DM, Informa Healthcare, USA, 2010

Reynolds G, Roberts R, Claxton S, Mirtič A, Parry J: Practical application of a unified compaction curve to roller compaction formulation design and equipment transfer. The 7th International Granulation Workshop, Sheffield, UK 2015

Roberts RJ, Rowe RC: The effect of punch velocity on the compaction of a variety of materials. J Pharm Pharmacol 37: 377-384, 1985

Roberts R, Rowe R: Brittle/ductile behavior in pharmaceutical materials used in tabletting. Int J Pharm 36: 205-209, 1987a

Roberts R, Rowe R: The compaction of pharmaceutical and other model materials - a pragmatic approach. Chem Eng Sci 42: 903-911, 1987b

Rowe RC, Sheskey PJ, Cook WG, Fenton ME: Handbook of pharmaceutical excipients. 7th ed. Pharmaceutical Press, London 2012

Rue PJ, Rees JE: Limitations of the Heckel relation for predicting powder compaction mechanisms. J Pharm Pharmacol 30: 642-643, 1978

Saleh MF, Dhenge RM, Cartwright JJ, Hounslow MJ, Salman AD: Twin screw wet granulation: Binder delivery. Int J Pharm 487: 124, 2015

Savolainen M, Herder J, Khoo C, Lövqvist K, Dahlqvist C, Glad H, Juppo A: Evaluation of polar lipid-hydrophilic polymer microparticles. Int J Pharm 262: 47-62, 2003

Sayin R, Barrasso D, Osorio J, Ramachandran R, Litster J: Population balance modeling of twin screw wet granulation through mechanistic understanding. 7th International Granulation Workshop, Sheffield, UK 2015a

Sayin R, El Hagrasy AS, Litster JD: Distributive mixing elements: Towards improved granule attributes from a twin screw granulation process. Chem Eng Sci 125: 165-175, 2015b

Schæfer T, Mathiesen C: Melt pelletization in a high shear mixer. IX. Effects of binder particle size. Int J Pharm 139: 139-148, 1996

Seem TC, Rowson NA, Ingram A, Huang Z, Yu S, de Matas M, Gabbott I, Reynolds GK: Twin screw granulation — a literature review. Powder Technol 276: 89-102, 2015

Seitz JA, Flessland GM: Evaluation of the physical properties of compressed tablets. I. Tablet hardness and friability. J Pharm Sci 54: 1353-1357, 1965

Shah U: Use of a modified twin-screw extruder to develop a high-strength tablet dosage form. Pharm Technol 29: 52-66, 2005

Shang C, Sinka IC, Jayaraman B, Pan J: Break force and tensile strength relationships for curved faced tablets subject to diametrical compression. Int J Pharm 442: 57-64, 2013

Shi L, Feng Y, Sun CC: Roles of granule size in over-granulation during high shear wet granulation. J Pharm Sci 99: 3322-3325, 2010

Shi L, Feng Y, Sun CC: Massing in high shear wet granulation can simultaneously improve powder flow and deteriorate powder compaction: A double-edged sword. Eur J Pharm Sci 43: 50-56, 2011a

Shi L, Feng Y, Sun CC: Origin of profound changes in powder properties during wetting and nucleation stages of high-shear wet granulation of microcrystalline cellulose. Powder Technol 208: 663-668, 2011b

Shiromani PK, Bavitz JF: Studies on a dibasic calcium phosphate - mannitol matrix tablet formulation - a complementary combination. Drug Dev Ind Pharm 14: 1375-1387, 1988

Smook GA: Handbook of pulp & paper terminology: a guide to industrial and technical usage. Angus Wilde Publications, Vancouver 1990

Souihi N, Dumarey M, Wikstrom H, Tajarobi P, Fransson M, Svensson O, Josefson M, Trygg J: A quality by design approach to investigate the effect of mannitol and dicalcium phosphate qualities on roll compaction. Int J Pharm 447: 47-61, 2013

Staniforth J.: Effect of addition of water on the rheological and mechanical properties of microcrystalline celluloses. Int J Pharm 41: 231-236, 1988

Stoyanov E, Beissner B, Durig T: Physical characterization of commonly used pharmaceutical binders for wet and dry granulation. AAPS, T2189 2014a

Stoyanov E, Warnke G, Vago T, Tuglu T, Oren Z, Durig T: The effect of the API's hydrophilicity on the high-shear granulation performance of common tablet binders. AAPS, T2190 2014b

Sun C, Himmelspach MW: Reduced tabletability of roller compacted granules as a result of granule size enlargement. J Pharm Sci 95: 200-206, 2006

Suzuki T, Kikuchi H, Yamamura S, Terada K, Yamamoto K: The change in characteristics of microcrystalline cellulose during wet granulation using a high-shear mixer. J Pharm Pharmacol 53: 609-616, 2001

Takács E, Wojnárovits L, Borsa J, Rácz I: Hydrophilic/hydrophobic character of grafted cellulose. Radiat Phys Chem 79: 467-470, 2010

Tan L, Carella AJ, Ren Y, Lo JB: Process optimization for continuous extrusion wet granulation. Pharm Dev Technol 16: 302, 2011

Thompson MR: Twin screw granulation - review of current progress. Drug Dev Ind Pharm 1, 2014

Thompson MR, Sun J: Wet granulation in a twin-screw extruder: Implications of screw design. J Pharm Sci 99: 2090-2103, 2010

Thompson MR, Weatherley S, Pukadyil RN, Sheskey PJ: Foam granulation: New developments in pharmaceutical solid oral dosage forms using twin screw extrusion machinery. Drug Dev Ind Pharm 38: 771-784, 2012

Thoorens G, Krier F, Leclercq B, Carlin B, Evrard B: Microcrystalline cellulose, a direct compression binder in a quality by design environment - a review. Int J Pharm 473: 64-72, 2014

Van Melkebeke B, Vervaet C, Remon JP: Validation of a continuous granulation process using a twin-screw extruder. Int J Pharm 356: 224-230, 2008

Vanhoorne V, Bekaert B, Peeters E, De Beer T, Remon J, Vervaet C: Improved tabletability after a polymorphic transition of delta-mannitol during twin screw granulation. Int J Pharm 506: 13-24, 2016

Vercruysse J, Burggraeve A, Fonteyne M, Cappuyns P, Delaet U, Van Assche I, De Beer T, Remon JP, Vervaet C: Impact of screw configuration on the particle size distribution of granules produced by twin screw granulation. Int J Pharm 479: 171-180, 2015

Vercruysse J, Córdoba Díaz D, Peeters E, Fonteyne M, Delaet U, Van Assche I, De Beer T, Remon JP, Vervaet C: Continuous twin screw granulation: Influence of process variables on granule and tablet quality. Eur J Pharm Biopharm 82: 205-211, 2012

Vervaet C, Remon JP: Continuous granulation. In book: Handbook of pharmaceutical granulation technology, p. 308-322, 3. Edition. Ed. Parikh DM, Informa Healthcare, USA 2010

Vervaet C, Remon JP: Continuous granulation in the pharmaceutical industry. Chem Eng Sci 60: 3949-3957, 2005

Webb P: Volume and density determinations for particle technologists. Micromeritics Instrument Corp , USA 2001

Weise U: Hornification - mechanisms and terminology. Paperi ja puu 80: 110-115, 1998

Westermarck S, Juppo AM, Kervinen L, Yliruusi J: Pore structure and surface area of mannitol powder, granules and tablets determined with mercury porosimetry and nitrogen adsorption. Eur J Pharm Biopharm 46: 61-68, 1998

Westermarck S, Juppo AM, Kervinen L, Yliruusi J: Microcrystalline cellulose and its microstructure in pharmaceutical processing. Eur J Pharm Biopharm 48: 199-206, 1999

Witt W, Köhler U, List J: Direct imaging of very fast particles opens the application of the powerful (dry) dispersion for size and shape characterization. Partec, Germany 2004 Purchased from internet 29.1.2016: https://www.sympatec.com/docs/ImageAnalysis/publications/IA_2004_Paper_ImageAnalysis_E_2.0_.pdf

Wu CY, Best SM, Bentham AC, Hancock BC, Bonfield W: Predicting the tensile strength of compacted multi-component mixtures of pharmaceutical powders. Pharm Res 23: 1898-1905, 2006

Wu S, Sun C: Insensitivity of compaction properties of brittle granules to size enlargement by roller compaction. J Pharm Sci 96: 1445-1450, 2007

Yu S, Reynolds GK, Huang Z, De Matas M, Salman AD: Granulation of increasingly hydrophobic formulations using a twin screw granulator. Int J Pharm 475: 82-96, 2014

APPENDICES

APPENDIX 1. Masses of the materials in the direct compaction blends.

Batch name	Main excipient (g)	Binder (g)	Lubricant (g)
Mannitol_PVP_MgSt	150.4	8.0	1.6
Mannitol_HPC_MgSt	150.4	8.0	1.6
MCC_PVP_MgSt	188.3	10.0	2.0
MCC_HPC_MgSt	188.2	10.0	2.0
DCPA_PVP_MgSt	188.0	10.1	2.0
DCPA_HPC_MgSt	188.1	10.0	2.0

APPENDIX 2. Batch numbers, expire dates and mean particle sizes of the materials used in DC and granulation blends.

Excipient Name	Grade	Manufacturer	Batch	Expire date	Mean particle size, q50 (μm)
Microcrystalline Cellulose	Avicel PH101	FMC Biopolymer	61201C[1] 61407C[2]	02/2018 02/2018	80 (measured, Appendix 8)
β-mannitol	Pearlitol 160C	Roquette	E663D[1,3] E781E[4]	02/2017 N/A	129 (measured, Appendix 8)
Calcium Phosphate Dibasic Anhydrous	Calipharm A	Univar Innophos	158143[1,6] 342322[5]	09/2015 11/2017	31 (measured, Appendix 8)
Hydroxypropyl cellulose	HPC Klucel	Ashland	40081	06/2015	50 (Ashland Inc 29.7.2016)
Povidone	Kollidon 30	BASF	3745212440	02/2018	107 (Rowe et al. 2012)
Magnesium Stearate	MgSt MF-2-V	Peter Greven	C213758	07/2016	5-20 (Kato et al. 2005; Rowe et al. 2012)

[1]DC blends
[2]MCC granulation runs
[3]Mannitol_PVP dry, Mannitol_HPC dry, Mannitol_PVP prestudy
[4]Mannitol_PVP dry replicate, Mannitol_PVP wet, Mannitol_HPC wet
[5]DCPA_PVP wet 4 ke
[6]Other DCPA runs

APPENDIX 3. Masses of the materials in the granulation blends used with purified water.

Batch	Mass of main excipient (g)	Mass of binder (g)	In total (g)
MCC_PVP_dry (2 runs)	3700.0	196.8	3896.8
MCC_HPC_dry (2 runs)	3700.0	196.8	3896.8
MCC_PVP replicate	2150.0	114.4	2264.4
Mannitol_PVP_dry (2 runs)	3700.0	196.8	3896.8
Mannitol_HPC_dry (2 runs)	3700.0	196.8	3896.8
Mannitol_PVP replicate	2150.0	114.4	2264.4
DCPA_PVP_dry (2 runs)	3700.0	196.8	3896.8
DCPA_HPC_dry (2 runs)	3700.0	196.8	3896.8
DCPA_PVP replicate	2150.0	114.4	2264.4

APPENDIX 4. Calculations for binder solution feed rate and binder concentration in the powder blend.

Feed rate of water (g/min) = F_W
Feed rate of the binder in liquid (g/min) = F_{LB}
Feed rate of the main excipient (g/min) = F_M
Feed rate of the binder in powder blend (g/min) = F_{PB}
Feed rate of the lubricant (g/min) = F_{LU}
Liquid feed rate (g/min) = F_S
Water-to-solid ratio = W/S
Powder feed rate (g/min) $F_P = F_M + F_{PB}$

Table 1. Input data.

Powder feed rate $F_P = F_M + F_{PB}$	250 g/min
Mass fraction of main excipient	94%
Mass fraction of binder	5%
Mass fraction of lubricant	1%
W/S ratio of MCC	1.1
W/S ratio of mannitol	0.09
W/S ratio of DCPA	0.2
Binder solution concentration	0.1

Binder solution feed rate (g/min) of MCC (should have been calculated like this)

$$\frac{W}{S} = \frac{F_W}{F_{MCC} + F_B} = 1.1$$

$$\frac{M_{LB}}{M_{MCC}} = \frac{F_{LB}}{F_{MCC}} = \frac{F_{LB}}{F_P} = \frac{5.05}{94.95}$$

$$F_{LB} = \frac{5.05}{94.95} * \mathrm{F_P}$$

$$F_W = 1.1 * (\mathrm{F_P} + F_{LB})$$

$$F_{S,MCC} = (F_W + F_{LB})$$

Binder solution feed rate (g/min) of mannitol and DCPA

$$\frac{W}{S} = \frac{F_W}{F_M + F_{PB} + F_{LB}}$$

Feed rate of the binder in liquid/solution ($\mathrm{F_{LB}}$) can be solved based on the binder solution concentration

$$\frac{F_{LB}}{F_W + F_{LB}} = 0.1$$

$$F_{LB} = 0.1 * F_W + 0.1 * F_{LB}$$

$$F_{LB} = \frac{0.1}{0.9} F_W$$

$$F_{LB} = 0.111 * F_W$$

$$F_W = \frac{W}{S} * (F_M + F_{PB} + F_{LB})$$

$$F_W = \frac{W}{S} * (F_M + F_{PB}) + \frac{W}{S} * 0.111 * F_W$$

$$F_W = \frac{\frac{W}{S} * (F_M + F_{PB})}{1 - \frac{W}{S} * 0.111}$$

Thus binder solution feed rate is:

$$\boldsymbol{F_S = F_W + F_{LB}}$$

$$\frac{F_{LU}}{F_{PB} + F_{LB}} = \frac{1\%}{5\%} = 0.2$$

$$F_{LU} = 0.2 * (F_{PB} + F_{LB})$$

Feed rate of the binder in powder blend (F_{PB}) is solved based on the binder concentration of the formulation

$$Binder\ concentration = \frac{F_{PB} + F_{LB}}{F_M + F_{PB} + F_{LB} + F_{LU}} = 0.05$$

$$F_{PB} + F_{LB} = 0.05 * (F_M + F_{PB} + F_{LB} + F_{LU})$$

$$F_{PB} + F_{LB} = 0.05 * (F_M + F_{PB} + F_{LB} + 0.2 * (F_{PB} + F_{LB}))$$

$$F_{PB} + F_{LB} = 0.05 * (F_M + F_{PB} + F_{LB} + 0.2 * F_{PB} + 0.2 * F_{LB})$$

$$F_{PB} + F_{LB} = 0.05 * (F_M + F_{PB} + F_{LB}) + 0.01 * F_{PB} + 0.01 * F_{LB}$$

$$F_{PB} - \ 0.01 * F_{PB} = 0.05 * (F_M + F_{PB} + F_{LB}) + 0.01 * F_{LB} - F_{LB}$$

$$F_{PB} = \frac{0.05 * (F_M + F_{PB} + F_{LB}) - 0.99 * F_{LB}}{0.99}$$

$$F_{PB} = \frac{0.05 * (F_M + F_{PB}) + 0.05 * F_{LB} - 0.99 * F_{LB}}{0.99}$$

$$F_{PB} = \frac{0.05 * (F_M + F_{PB}) - 0.94 * F_{LB}}{0.99}$$

$$F_{PB} = \frac{0.05 * (F_P) - 0.94 * F_{LB}}{0.99}$$

Binder concentration in the powder blend (w/w) %

$$\boldsymbol{C_{PB} = \frac{F_{PB}}{F_M + F_{PB}}}$$

$$C_{PB} = \frac{M_{PB}}{M_M + M_{PB}}$$

Amount of binder in the blend (g)

$$\boldsymbol{M_{PB} = \frac{C_{PB} * M_M}{1 - C_{PB}}}$$

Table 2. Binder solution feed rates to be used with mannitol and DCPA and the concentration of the binder in the powder blend.

	MCC	Mannitol	DCPA
Feed rate of the binder in liquid (g/min) (F_{LB})	13.3	2.5	5.7
Feed rate of water (g/min) (F_W)	289.6	22.7	51.1
Binder solution feed rate (g/min) (F_L)	**302.9***	**25.3**	**56.8**
Feed rate of the binder in powder blend (g/min) (F_{PB})	-	10.2	7.2
Binder concentration in the powder blend (w/w) % (C_{PB})	-	**4.1**	**2.9**

*The used binder solution feed rate for MCC was 287.6 g/min (15.3 g/min smaller than it should have been) due to initial incorrect calculation [(L/S + 0.0505) * 250g/min] thus the differences in binder concentration and L/S ratio were 0.24% and 0.05, respectively.

APPENDIX 5. Masses of the materials in the granulation blends used with binder solution.

Batch/Blend	Mass of main excipient (g)	Mass of binder (g)	In total (g)
MCC_PVP_wet (2 runs)	3800.0	-	3800.0
MCC_HPC_wet (2 runs)	3800.0	-	3800.0
Mannitol_PVP_wet (2 runs)	3785.1	161.5	3946.6
Mannitol_HPC_wet (2 runs)	3788.1	161.6	3949.7
DCPA_PVP_wet (2 runs) *	3802.1	113.3	3915.4
DCPA_HPC_wet (2 runs)	3798.0	113.1	3911.1
DCPA_PVP_wet_4ke	2200.0	65.5	2265.5

* DCPA_PVP_wet_4ke batch got ruined due to agglomeration during fluid bed drying.

APPENDIX 6. Masses of the granules and the lubricant (magnesium stearate).

Batch	Mass of granules (g)			Mass of lubricant (g)		
	MCC	Mannitol	DCPA	MCC	Mannitol	DCPA
PVP dry 4 ke	193.4	203.5	193.9	2.0	2.1	2.0
PVP dry 8 ke	208.6	195.4	213.5	2.1	2.0	2.2
PVP dry 4 ke replicate	208.6	187.2	171.7	2.1	1.9	1.7
PVP wet 4 ke	197.8	197.1	198.0	2.0	2.0	2.0
PVP wet 8 ke	206.5	205.0	186.2	2.1	2.1	1.9
HPC dry 4 ke	189.1	198.1	199.7	1.9	2.0	2.0
HPC dry 8 ke	196.3	180.1	196.5	2.0	1.8	2.0
HPC wet 4 ke	211.2	200.7	198.7	2.1	2.0	2.0
HPC wet 8 ke	202.6	204.7	193.8	2.0	2.1	2.0

APPENDIX 7. Results of the granule and tablet characterisation.

	Run	Binder	Binder addition mehtod	Number of kneading	Average bulk density (g/cm^3) (n=2-4)	RSD (%)	Max-min	Average torque (Nm)	STDV (Nm)	RSD (%)	TS at 12% porosity	TS at 25% porosity	TS at 200 MPa pressure	P_{WG} (MPa)	T_{WG} (MPa)	ε_{WG} (%)	T0g - T0dc (MPa)	q10 (µm) milled (n=3)	RSD (%)	q50 (µm) milled (n=3)	RSD (%)	q90 (µm) milled (n=3)	RSD (%)	VMD (µm) milled (n=3)	RSD (%)	SSA (µm^2/µm^3) milled (n=3)	RSD (%)	q10 (µm) unmilled (MCC n=2)	RSD (%)	q50 (µm) unmilled (MCC n=2)	RSD (%)	q90 (µm) unmilled (MCC n=2)	RSD (%)	VMD (µm) unmilled (MCC n=2)	RSD (%)	SSA (µm^2/µm^3) unmilled (MCC	RSD (%)
MCC	1	PVP	Dry	8	0.66	0.46	0.006	5.25	0.46	8.45	N/A	N/A	N/A	N/A	N/A	N/A	N/A	224.67	1.45	762.37	1.83	1264.34	1.00	759.92	1.49	0.01	1.08	406.60	1.92	1562.40	4.82	2772.66	4.60	1572.37	3.84	0.01	2.89
	2	PVP	Dry	4	0.56	0.68	0.007	3.27	0.33	9.49	0.99	N/A	0.83	177.43	3.93	18.93	-3.88	179.69	2.86	718.31	1.68	1225.06	0.91	712.55	0.83	0.02	1.73	376.05	1.63	1785.56	1.67	3068.89	0.28	1745.36	1.09	0.01	1.45
	3	HPC	Dry	4	0.57	2.40	0.024	3.83	0.15	3.67	0.79	N/A	0.72	231.87	6.20	14.96	-9.51	284.04	12.85	813.79	7.62	1254.13	1.76	795.41	5.73	0.01	8.96	684.92	2.29	1939.84	0.78	3629.00	0.55	2060.23	0.59	0.00	1.02
	4	HPC	Dry	8	0.65	1.01	0.012	6.60	0.34	4.96	N/A	N/A	N/A	N/A	N/A	N/A	N/A	304.43	3.08	891.28	1.77	1293.80	1.44	849.33	1.77	0.01	1.97	669.47	1.90	2157.19	1.20	4042.30	0.39	2258.40	1.78	0.00	2.78
	5	PVP	Wet	4	0.57	0.68	0.007	3.96	0.38	9.20	1.11	N/A	0.97	166.44	3.82	20.67	-4.47	91.30	5.69	547.99	8.57	1182.66	2.13	597.47	4.62	0.03	5.78	362.99	7.28	1868.83	1.17	3248.88	2.50	1820.82	2.92	0.01	5.26
	6	PVP	Wet	8	0.64	0.42	0.004	5.57	0.48	8.31	0.76	N/A	0.64	187.01	4.02	15.07	-4.33	186.60	6.36	688.08	7.43	1255.04	3.15	710.33	5.09	0.01	6.11	378.64	6.05	1731.26	5.05	3179.79	2.04	1748.87	3.82	0.01	4.80
	7	HPC	Wet	4	0.55	1.55	0.015	4.41	0.34	7.46	0.90	N/A	0.84	218.98	6.09	16.00	-9.52	131.43	1.86	662.87	2.15	1178.99	1.13	665.45	1.26	0.02	1.26	505.10	0.99	1714.21	3.05	3176.87	5.22	1782.54	3.75	0.01	0.81
	8	HPC	Wet	8	0.63	0.68	0.006	7.52	0.47	6.15	0.57	N/A	0.53	268.93	6.45	12.30	-10.09	263.34	5.75	804.39	0.82	1266.82	0.14	789.74	0.88	0.01	2.78	594.53	1.43	1853.38	1.06	3216.97	4.79	1880.45	1.21	0.01	1.31
rep	9	PVP	Dry	4	0.56	2.25	0.023	2.92	0.20	6.26	0.92	N/A	0.86	177.42	3.93	17.74	-4.43	137.39	6.93	626.93	1.73	1211.69	1.22	657.92	1.58	0.02	4.00	410.80	6.31	1871.46	4.78	3101.74	0.63	1795.40	2.77	0.01	4.92
Mannito	10	HPC	Dry	4	0.55	1.42	0.014	1.35	0.30	19.31	1.60	N/A	2.63	N/A	N/A	N/A	3.44	120.95	1.36	379.68	1.17	936.42	2.36	460.74	1.30	0.02	1.16	221.85	N/A	952.91	N/A	2662.17	N/A	1346.35	N/A	0.01	N/A
	11	HPC	Dry	8	0.54	0.38	0.003	1.89	0.71	33.88	1.75	N/A	2.79	N/A	N/A	N/A	4.46	118.51	6.09	419.38	5.01	992.87	1.53	493.61	2.99	0.02	4.47	251.41	N/A	1127.87	N/A	2498.12	N/A	1379.10	N/A	0.01	N/A
	12	PVP	Dry	4	0.55	1.47	0.018	1.48	0.33	19.43	1.98	N/A	3.18	N/A	N/A	N/A	6.94	103.50	2.37	368.99	1.33	983.28	1.32	463.81	1.19	0.03	1.53	212.09	N/A	1126.26	N/A	2808.07	N/A	1424.22	N/A	0.01	N/A
	13	PVP	Dry	8	0.56	2.51	0.029	1.65	0.70	37.74	2.09	N/A	3.19	N/A	N/A	N/A	7.70	99.12	3.81	336.20	5.28	969.49	3.11	444.16	4.11	0.03	3.50	169.03	N/A	827.21	N/A	2437.74	N/A	1187.58	N/A	0.01	N/A
rep	14	PVP	Dry	4	0.54	0.98	0.007	1.43	0.30	18.65	2.06	N/A	3.00	N/A	N/A	N/A	7.05	99.96	2.26	351.77	3.18	967.78	2.41	452.19	2.48	0.03	2.02	174.92	N/A	620.64	N/A	2343.33	N/A	1096.86	N/A	0.01	N/A
	15	PVP	Wet	4	0.56	0.67	0.005	1.69	0.34	18.05	2.03	N/A	3.06	N/A	N/A	N/A	6.85	111.05	2.68	309.38	5.59	937.17	2.83	423.55	4.29	0.03	3.36	168.35	N/A	658.39	N/A	2132.45	N/A	1052.07	N/A	0.01	N/A
	16	PVP	Wet	8	0.57	0.11	0.001	1.78	0.70	35.17	2.11	N/A	3.17	N/A	N/A	N/A	7.18	108.10	1.82	354.83	2.91	1020.07	2.81	473.82	3.07	0.03	2.03	170.15	N/A	719.54	N/A	2294.62	N/A	1095.14	N/A	0.01	N/A
	17	HPC	Wet	4	0.58	0.98	0.010	1.52	0.36	20.66	1.62	N/A	2.62	N/A	N/A	N/A	4.12	91.41	4.68	359.90	7.00	973.34	5.82	454.23	6.59	0.03	4.71	157.58	N/A	715.02	N/A	2526.00	N/A	1153.60	N/A	0.01	N/A
	18	HPC	Wet	8	0.57	0.42	0.003	1.69	0.72	38.21	1.91	N/A	2.90	N/A	N/A	N/A	4.92	106.44	3.11	427.73	3.02	1030.29	0.80	505.43	1.45	0.03	2.41	183.11	N/A	862.83	N/A	2266.73	N/A	1160.34	N/A	0.01	N/A
DCPA	19	PVP	Wet	8	0.74	0.27	0.003	0.89	0.20	18.43	N/A	3.69	2.43	N/A	N/A	38.32	-115.64	37.61	1.12	271.56	9.75	1025.21	1.06	426.39	3.62	0.06	2.36	71.61	N/A	1018.94	N/A	2368.28	N/A	1213.72	N/A	0.03	N/A
	20	HPC	Dry	4	0.73	1.14	0.016	0.71	0.11	11.53	N/A	3.27	2.31	N/A	N/A	33.97	-86.12	37.29	4.40	297.76	11.93	979.23	4.54	410.26	7.25	0.06	7.10	56.82	N/A	663.55	N/A	2207.31	N/A	1006.90	N/A	0.03	N/A
	21	HPC	Dry	8	0.68	0.24	0.002	0.69	0.17	19.28	N/A	3.21	2.28	N/A	N/A	33.94	-87.54	39.89	1.10	295.41	1.46	970.39	1.11	411.60	0.82	0.05	1.48	57.18	N/A	581.32	N/A	1875.05	N/A	869.72	N/A	0.03	N/A
	22	HPC	Wet	4	0.74	1.40	0.021	0.68	0.10	11.57	N/A	3.12	2.31	N/A	N/A	32.44	-92.18	34.39	2.69	274.23	13.37	955.56	5.54	396.56	7.58	0.06	5.92	45.49	N/A	631.44	N/A	2159.96	N/A	995.97	N/A	0.04	N/A
	23	HPC	Wet	8	0.69	0.06	0.001	0.73	0.16	17.59	N/A	3.16	2.31	N/A	N/A	32.70	-87.22	38.38	0.59	267.04	1.33	948.15	3.17	389.30	3.13	0.06	0.77	47.12	N/A	459.63	N/A	1834.34	N/A	827.82	N/A	0.04	N/A
rep	24	PVP	Dry	4	0.76	1.35	0.019	1.07	0.13	10.19	N/A	3.86	2.49	N/A	N/A	40.25	-98.29	34.41	0.37	216.80	3.18	1002.55	4.12	398.78	3.82	0.07	0.69	55.22	N/A	974.12	N/A	2264.66	N/A	1159.02	N/A	0.03	N/A
	25	PVP	Dry	4	0.77	0.33	0.004	0.75	0.11	12.02	N/A	3.88	2.57	N/A	N/A	40.70	-97.48	33.69	1.68	178.93	14.00	1026.78	1.89	389.57	4.00	0.07	3.51	52.24	N/A	899.64	N/A	2189.72	N/A	1098.71	N/A	0.03	N/A
	26	PVP	Dry	8	0.74	0.45	0.005	0.86	0.21	19.71	N/A	3.91	2.53	N/A	N/A	41.38	-100.42	34.46	0.35	157.97	1.42	979.43	3.05	357.56	2.69	0.07	0.05	80.33	N/A	1203.62	N/A	2338.87	N/A	1293.92	N/A	0.02	N/A
	27	PVP	Wet	4	0.78	0.24	0.003	0.85	0.12	11.72	N/A	3.14	2.23	N/A	N/A	32.14	-119.80	47.27	4.11	452.08	12.07	1122.36	2.35	523.43	4.67	0.04	5.19	141.32	N/A	1246.58	N/A	2540.94	N/A	1429.27	N/A	0.01	N/A

APPENDIX 8. Results of the powder characterisation.

Powder	q10 (µm) (n=2)	RSD (%)	q50 (µm) (n=2)	RSD (%)	q90 (µm) (n=2)	RSD (%)	Width of PSD (n=2)	RSD (%)	VMD (µm) (n=2)	RSD (%)	SSA ($\mu m^2/\mu m^3$) (n=2)	RSD (%)
MCC	40.84	1.07	79.75	2.08	132.20	3.49	1.15	2.49	83.95	2.39	0.09	1.73
Mannitol	49.98	1.76	128.88	0.32	267.36	1.12	1.69	2.10	147.22	0.86	0.06	0.87
DCPA	16.06	0.26	30.67	0.25	47.36	0.44	1.02	0.28	31.72	0.30	0.24	0.27

APPENDIX 9. Results of the regression analysis.

Response is higher with the maximum level of the factor

Response is higher with the minimum level of the factor

Number is the p-value of the factor,
$p < 0.05$ factor significant
N/A Factor not in the model
/ no data for that response/material

Factor not significant or the difference between points not significant

RESPONSES / FACTORS	A - BINDER TYPE (PVP / HPC)			B - BINDER ADDITION METHOD (DRY / WET)			C - NUMBER OF KNEADING ELEMENTS (4 / 8)			AC			AB			BC		
Material	MCC	Mannitol	DCPA	MCC	Mannitol	DCPA	MCC	Mannitol	DCPA	MCC	Mannitol	DCPA	MCC	Mannitol	DCPA	MCC	Mannitol	DCPA
Torque	0.001 (except wet, 4 ke)	N/A	0.018	0.009	N/A	N/A	7.20E-05	0.014	N/A	0.024	N/A	N/A	N/A	N/A	N/A	N/A	N/A	N/A
TS at 12 / 25% porosity	0.004	0.0002	4.00E-06	0.019 (4 ke)	N/A	0.005	0.002	0.019	N/A	N/A	N/A	N/A	N/A	N/A	N/A	N/A	N/A	N/A
TS at 200 Mpa pressure	0.002	0.0002	0.0006	0.003	N/A	N/A	0.0002	0.02	N/A	N/A	N/A	N/A	N/A	N/A	N/A	N/A	N/A	N/A
P_{WG}	0.002	/	/	N/A	/	/	0.041	/	/	N/A	N/A	N/A	N/A	N/A	N/A	N/A	N/A	N/A
T_{WG}	2.97E-06	/	/	N/A	/	/	0.036	/	/	N/A	N/A	N/A	N/A	N/A	N/A	N/A	N/A	N/A
ε_{WG}	0.018 (4 ke)	/	5.23E-07	N/A	/	0.0002	0.019	/	N/A	N/A	N/A	N/A	N/A	N/A	N/A	N/A	N/A	N/A
T0 g - T0 dc	2.46E-06	1.80E-05	1.27E-05	N/A	0.387	0.00008 (exc. 8ke, HPC)	N/A	0.004	0.040	N/A	N/A	N/A	N/A	0.022	0.0002	N/A	N/A	0.003
Bulk density	N/A	0.711	0.0004	N/A	0.0005	N/A	7.19E-06	0.517	0.001	N/A	0.006	N/A	N/A	0.010	N/A	N/A	N/A	N/A
VMD unmilled	0.005 (Dry)	0.1629	0.0006	0.053	0.035	N/A	0.958	N/A	0.639	0.027	N/A	0.007	0.0091	N/A	N/A	N/A	N/A	N/A
Surface area unmilled	7.17E-05	0.185	0.019 (8 ke)	0.013	0.06	0.021 (except PVP, 4ke)	N/A	N/A	0.031 (PVP)	N/A	N/A	0.013	N/A	N/A	N/A	N/A	N/A	N/A
VMD milled	0.005	0.044	0.196	0.006	0.849	0.034 (PVP)	0.004	0.037 (Wet)	0.045 (PVP, dry)	N/A	N/A	0.061	N/A	N/A	0.012	N/A	0.069	N/A
Surface area milled	0.022	0.044 (Dry)	0.028 (Dry)	0.019 (4 ke)	0.086 ((HPC, 4ke) Wet)	0.244((PVP) Dry)	0.006 (Wet)	0.388	N/A	N/A	N/A	N/A	N/A	0.043	0.017	0.072	0.117	N/A

APPENDIX 10. Temperature of the granulation liquid.

Batch	Liquid temperature (ºC)		
	MCC	Mannitol	DCPA
PVP_dry_4	N/A	21.1	21.8
PVP_dry_8	N/A	22.0	21.4
HPC_dry_4	22.1	22.8	23.9
HPC_dry_8	23.1	21.1	23.3
PVP_wet_4	19.2	19.7	20.5
PVP_wet_8	19.4	19.4	20.2
HPC_wet_4	19.4	20.1	20.8
HPC_wet_8	20.0	19.8	20.9
PVP_dry_4_rep	23.5	21.4	22.0

APPENDIX 11. Moisture content after drying and after conditioning.

Batch	Moisture content of the granules after drying (%)			Moisture content of the powder blends and granules after conditioning (%) (before tableting)		
	MCC	Mannitol	DCPA	MCC	Mannitol	DCPA
DC _ PVP	N/A	N/A	N/A	4.76	N/A*	1.21
DC _ HPC	N/A	N/A	N/A	4.90	N/A*	0.55
PVP dry 4 ke	3.48	0.78	0.93	4.52	0.90	1.19
PVP dry 8 ke	4.19	0.90	0.77	4.95	1.01	0.98
PVP dry 4 ke replicate	3.27	0.39	0.74	4.73	0.98	0.96
PVP wet 4 ke	2.59	0.42	0.75	4.53	0.81	0.98
PVP wet 8 ke	3.50	0.57	0.93	4.43	0.82	1.14
HPC dry 4 ke	2.34	0.64	0.65	4.05	0.49	0.51
HPC dry 8 ke	2.69	0.96	0.55	3.55	0.56	0.62
HPC wet 4 ke	2.82	0.63	0.65	4.37	0.59	0.55
HPC wet 8 ke	1.25	0.24	0.48	3.87	0.54	0.71

* Tablets were conditioned before characterisation.